THE UTILIZATION OF FLY ASH AS A FILLER TO STRENGTHEN THE PROPERTIES OF POLYBUTYLENE SUCCINATE

Andiswa Kaleni

Dissertation submitted in fulfilment of the requirements for the Degree

Master of Health Sciences in Environmental Health

in the

Department of Life Sciences

Faculty of Health and Environmental Sciences

at the

Central University of Technology, Free State

Supervisor: Prof M.J. Mochane

Co-supervisor: Dr T. Mokhena

BLOEMFONTEIN

November 2022

DECLARATION OF INDEPENDENT WORK

DECLARATION WITH REGARD TO INDEPENDENT WORK

I, **Andiswa Kaleni**, student number _____, do hereby declare that this research project submitted to the Central University of Technology, Free State for the Master of Health Sciences in Environment, is my own independent work; and complies with the Code of Academic Integrity, as well as other relevant policies, procedures, rules and regulations of the Central University of Technology, Free State; and it has not been submitted before to any institution by myself of any other person in fulfilment (or partial fulfilment) of the requirements for the attainment of any qualification.

_____ _____ 10/11/2022

SIGNATURE OF STUDENT DATE

DEDICATIONS

This thesis is dedicated to myself, and my family. It is a symbol of my hard work and dedication to self-development. I look forward to what the future holds for me in my academic career.

ACKOWLEDGEMENTS

Firstly, I would like to start by extending my eternal gratitude to the Lord God Almighty for empowering me to complete this thesis. It is through the knowledge of His Word that I am able to understand that “I can do all things through Christ who gives me strength - Phillipians 4:13”.

Secondly, I would like to thank my supervisor Prof MJ Mochane, and my co-supervisor Dr T Mokhena and Dr SI Magagula for all the guidance and careful instruction throughout the journey of completing my thesis. May the good Lord bless and protect you and your families.

I would also like to extend my gratitude to my parents: Matilda, and Mbulelo Ndakane, and all my family members for the constant support and encouragement throughout my journey.

Lastly, I would like to thank my research colleagues: Maleshoane Mohapi and Lulama Theys for their continuous support, and motivation. My appreciation also goes to the National Research Fund (NRF) for the financial support. A special gratitude to my amazing husband, Lwazi Magunga for the selfless sacrifices, motivations and always going extra mile to assist me in my research. I look forward to more endeavours and advancements in my academic career because of you.

ABSTRACT

The use of coal as a primary raw material in electrical power generation has been growing exponentially since the 1960s. One of the major drawbacks of concern in electrical power generation through coal utilization is the bulk production of coal fly ash (FA). Fly ash, as a waste product poses a threat to the environment as it contains heavy metals such as aluminium, calcium oxides, potassium, magnesium oxides, silica oxides, and sulphur oxides. When it rains, the heavy metals contained in the fly ash is transferred to nearby water sources through run-off. This can potentially contaminate groundwater and freshwater course posing a threat to humans as well as wildlife and sea-life. Over the recent decade, researchers have been exploring various innovations that can be employed in order to resolve this pollution impediment caused by fly ash. As such, the use of fly ash in various industries ranging from construction, agriculture, and wastewater treatment has gained significant attention. Subsequently, this growing interest has also infiltrated the polymer industries. The excess availability of fly ash (FA) and its high mechanical performance when added to polymer matrices make it an exceptional substitute for commonly used fillers in the industry, thereby enhancing their widespread applications. This study aims to investigate the effect of fly ash at various concentrations *viz* 1, 3 and 5 %, and how they enhance the properties of polybutylene succinate (PBS). In order to further enhance the flammability resistance of the composites, zinc borate has been added to the polymer composite. The synergistic effect of zinc borate is also examined in this study. Characterization techniques such as scanning electron microscopy (SEM), underwriters laboratory testing 94 (UL 94), rheology, thermogravimetric analysis (TGA), Fourier transform infrared spectroscopy (FTIR), and x-ray diffraction (XRD) were utilized to analyse the properties of neat PBS, PBS/FA, and PBS/FA/Zinc Borate (ZB) composites. SEM results revealed a better dispersion of fly ash particles in the PBS matrix at 1%, in addition to silane- treated fly ash. Furthermore, silane-treated fly ash showed an enhancement thermal stability when compared with 1% non-treated FA, however, both of them showed better thermal stability than the neat PBS. The FTIR and EDS results suggested that the type of fly ash used in this study is a silicate class (Class F). The water absorption results also showed a decrease in water absorption with silane-treated fly ash samples.

Key words: Fly ash, polymer composites, silane treatment, zinc borate, flammability, thermal stability, complex viscosity

Research outputs

Published journal articles and chapters:

1. **Kaleni, A.,** Magagula, S.I., Motloung, M.T., Mochane, M.J., & Mokhena, T.C. 2022. Preparation and characterization of coal fly ash reinforced polymer composites: An overview. *Express Polymer Letters*, 16(7).
   DOI: 10.3144/expresspolymlett.2022.54
2. **Kaleni, A.,** Lebelo, K., Mochane, M.J., Mokhena, T.C., & Motloung, M.T. 2022. Recent progress on the morphology and thermal cycle of phase change materials (PCMs)/conductive filler composites: a mini review. *Journal of Polymer Engineering*.
   DOI: 10.1515/polyeng-2022-0020

Book chapter

1. L Magunga, M Mohapi, **A Kaleni,** S Magagula, M.J. Mochane, MT Motloung. Bioplastics and biocomposites in flame-retardant applications. In Book: Handbook of Bioplastics and Biocomposites Engineering Applications. Scrivener Publishing LLC **2023,** 573-593
   https://doi.org/10.1002/9781119160182.ch25

Manuscripts under review:

1. Applications of Polymers in Aerospace: Recent advances in carbon fiber reinforced polymers for aerospace applications (Wiley-Scrivener, Publishing).

Conference attendance:

1. International Online Conference on Reuse, Recycling, Upcycling, Sustainable Waste Management and Circular Economy (ICRSC – 2022) held on September 09, 10 and 11, 2022, and organized by: International Unit on Macromolecular Science and Engineering (IUMSE) Mahatma Gandhi University,P.D Hills P.O, Kottayam, Kerala, India & Wroclaw University of Technology, Wroclaw, Poland & University of Johannesburg, South Africa & IJL, University of Lorraine, Nancy, France.

TABLE OF CONTENTS

LIST OF ABBREVIATIONS

As	Arsenic
Ba	Barium
C	Carbon
CaO	Calcium oxide
$CaCO_3$	Calcium carbonate
CO_2	Carbon dioxide
Cd	Cadmium
Cr	Chromium
DNA	Deoxyribonucleic acid
FTIR	Fourier transform infrared
HCSD	High concentration of slurry disposal
HDPE	High density polyethylene
Hg	Mercury
K	Potassium
LDPE	Low density polyethylene
µm	micron meters
MWCNT	Multi-walled carbon nanotubes
N_2	Nitrogen oxide
Ni	Nickel
nm	nanometers
PBAT	Polybutylene adipate terephthalate

PBS	Polybutylene succinate
PHB	Polyhydroxybutyrate
PLA	Polylactic acid
PVC	Polyvinyl chloride
SEM	Scanning electron microscopy
Se	Selenium
Si	Silica
SiO_2	Silica oxide
SO_2	Sulphur dioxide
TGA	Thermogravemetric analysis
UL-94	Underwriters laboratory testing
XRD	X-ray diffraction
ZB	Zinc Borate

LIST OF TABLES

LIST OF FIGURES

Chapter 1: Introduction

1.1 Background introduction

Coal is one of the most utilized fossil fuels globally for generation of electricity [1]. The excess availability of coal as a fossil fuel as opposed to other natural fuels render it a viable sustainable raw material in the process of electrical power generation [2]. The evidence of coal mining is dated back to the 100-200 AD, but it was not until the Industrial Revolution in the mid-eighteen hundred that the use of coal began to increase exponentially. Coal has been utilized as a direct fuel to power engines and machinery between the eighteen and nineteen hundred. Furthermore, during the same period, coal was employed in steam ships, and as a precursor in the manufacturing of steel as coke in iron blast furnaces. In the latter nineteen hundred, the rapid increase in the urbanization introduced the utilization of coal as a raw material in the production of electrical power [2]. Current statistics reveal that the coal consumption rate has increased dramatically from 1978- 2020 by reaching a global demand of 7 432 million tonnes in the year 2020, and this rate is expected to increase by 2.6% in the year 2023**. Figure 1.1** demonstrates the international coal consumption capacity over 5-year intervals from the year 2000 till 2015. It highlights the top 5 countries namely (1) China, (2) Germany, (3) United Kingdom, (4) Russia, and the (5) United States of America for having the largest coal consumption capacity world-wide. It also illustrates the significant rise in coal consumption and plant capacity between 2010- 2015 in Russia.

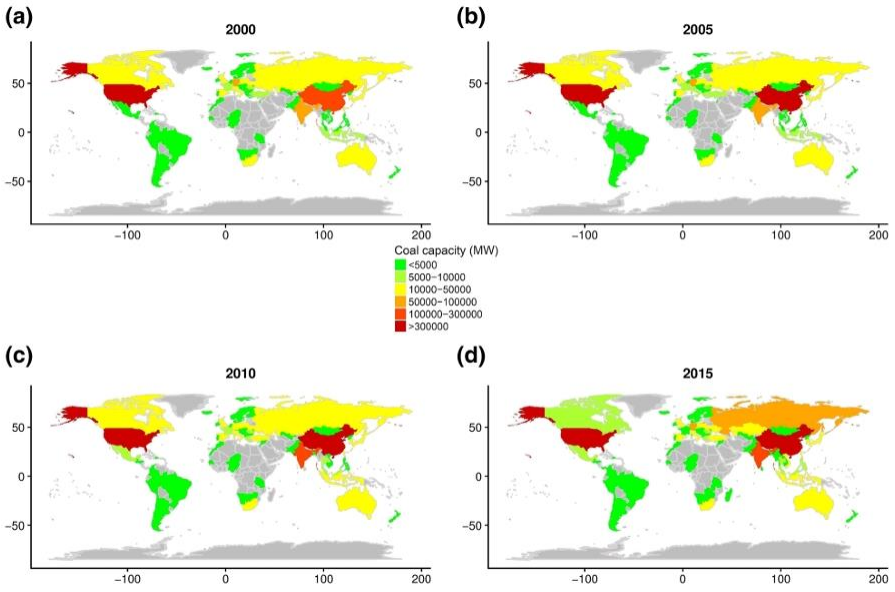

Figure 1.1 The international coal capacity in (a) 2000 (b) 2005 (c) 2010 and (d) 2015 (Lin *et al*., 2019. *Environmental Health*. OPEN ACCESS)

As indispensable as coal has proven to be, it is accompanied by some drawbacks. The process of coal combustion results in obnoxious gases such as nitrogen oxides, sulphur dioxide, mercury, carbon, and particulate matter being emitted into the atmosphere, and thereby contributing to the greenhouse dilemma [1]. For this reason, clean coal technological strategies have been employed in order to reduce the amount of harmful gases emitted into the ambient air. These strategies include: (1) cleaning coal prior to combustion to reduce the amounts of sulphur and nitrogen; (2) regulating pulverization pressures and fluidized bed conditions according to prescribed standards; and (3) flue gas cleaning and desulphurization [2].

Another drawback in the utilization of coal as a primary raw material in electrical power production is coal fly ash. Coal ash is the by-product that is obtained from the coal combustion process. When coal is incinerated in a combustion chamber, small incombustible particles of the coal are collected as dust using electrostatic precipitators, bag-houses, or other dust collection devices, and is referred to as fly ash. Additionally, larger incombustible dust particle that settles at the bottom of the chamber is referred to as bottom ash. Coal ash contains micro-particles of metal oxides, quartz, glass, and clays [4]. The physical appearance of a fly ash particle may range from 0,5µm to 100µm in size, and with a rounded or angular shape, covered by a porous anterior membrane [5]. The chemical composition of the fly ash typically includes Al_2O_3, SiO_2, TiO_2, Fe_2O_3, MnO, MgO, CaO and Na_2O depending on the type of feed-coal from which it was obtained. The chemical composition also affects the colour of the ash, which varies from a tan brown to a dark black [6]. Moreover, Fly ash disposal or recycling follows various steps (i.e., following collection in particulate filtration systems), so, fly ash is transferred using conveyor mechanism under constant pressure into mass tanker trucks to various sites depending on the intended use or disposal method of the ash [7]. **Figure 1.2** outlines the process of electrical power generation from pulverization to disposal or recycling.

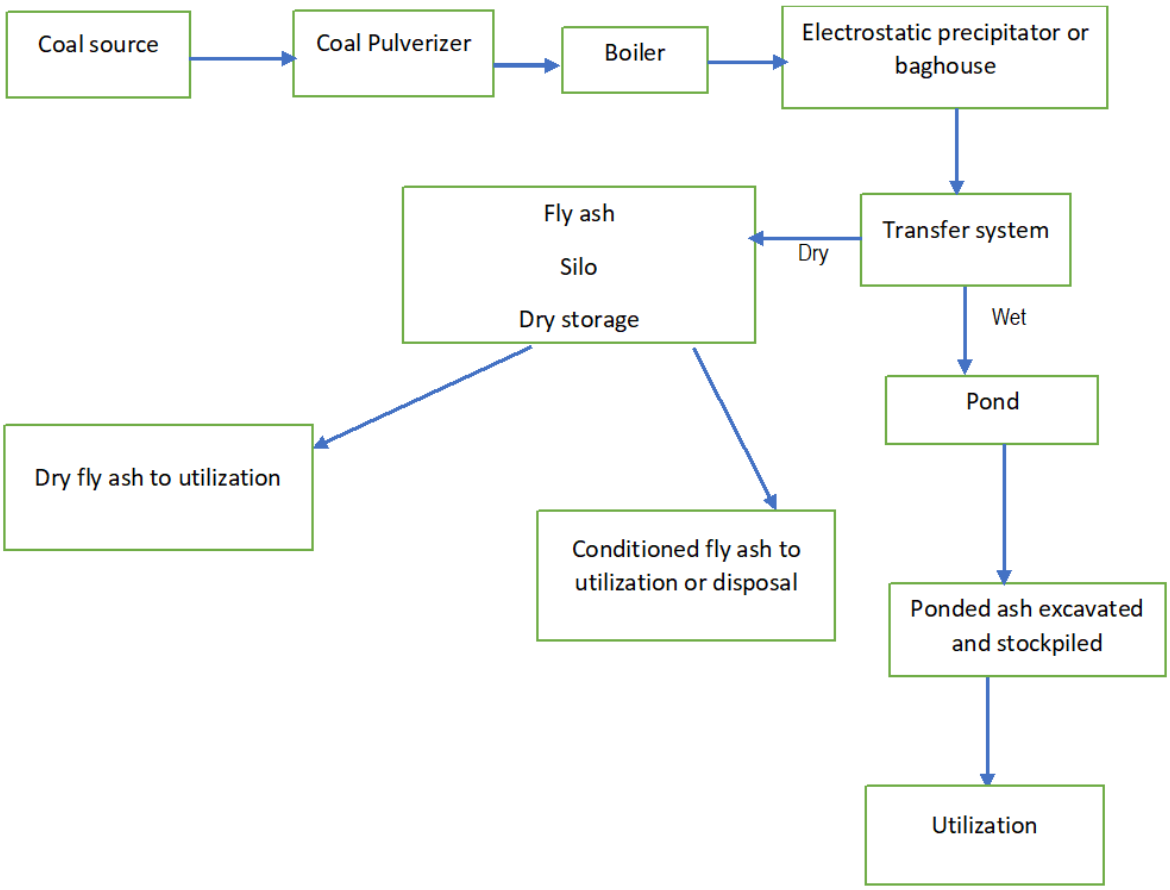

Figure 1.2 The process of coal pulverization and fly ash disposal

There are two classes of fly ash according to the American Society for Testing and Materials (ASTM C618), and they are: Class F and Class C [5]. The differences between the two classes of fly ash are based on the concentration of aluminium, silica, and iron present in the sample. Class F fly ash is a product of anthracite or bituminous coal combustion which is a more mature coal and possess an intense pozzolanic nature with higher concentrations of aluminium oxide. Class C fly ash is therefore a product of sub-bituminous or lignite coal combustion which is a juvenile coal, and it contains a higher lime (CaO) content of more than 20% [5]. Table 1.1 summarizes the differences between Class C and Class F fly ash.

Table 1.1: Summary of differences in Class C and Class F fly ash (Rani & Jain, 2015)

Class C	**Class F**	**Ref**
Greater quantities of Na_2O, SO_3 and CaO as opposed to Class F	Lesser quantities of Na_2O, SO_3 and CaO	[29]
Lime concentration of greater than 20%	Lime concentration of less than 20%	[27]
Produced as a by-product of the combustion of lignite/sub-bituminous coal	Produced as a by-product of the combustion of bituminous and anthracite coal	[28]
Greater sulphate and alkali content	Lesser sulphate and alkali content as compared to Class C	[28]
Exhibits a cementatious behaviour	Exhibits only a pozzolanic behaviour	[30]
Lesser quantities of Fe, Si and K as compared to Class F fly ash	Greater quantities of Fe, Si, and K as compared to Class C fly ash	[29]

As a result of the physical, chemical, and mineralogical composition of fly ash, it poses a major threat to the environment, human, and animal life. Recent research has outlined how long-term exposure to particulate matter in the ambient air can increase the burden of lung cancer and cardiovascular disease [3]. For instance, when fly ash contains particle sizes of 0.5µm or smaller, it means it is still capable of reaching the alveoli region of the thoracic cavity, and is thus referred to as a respirable dust with the potential of having carcinogenic effects. Moreover, trace elements such as barium (Ba), mercury (Hg), cadmium (Cd), arsenic (As), vanadium (V), nickel (Ni), lead (Pb), selenium (Se), Zinc (Zn), and chromium (Cr) found in the fly ash have been proven to be toxic when ingested [11]. Investigations conducted by Lemly (2017) revealed evidence of fly ash and its toxicity to aquatic life, where traces of selenium were found in ash pond water following the High Concentration of Slurry Disposal (HCSD). The HCSD system attempts to minimize the amount of water present in the slurry in order to conserve water as well as reduce landfill space required for ash slurry disposal. However, this conservation mechanism does not lower the concentrations of toxins present in the ash, thus resulting in fatal outcomes to aquatic life as well as the evidence to leaching caused by these ash ponds and the contamination of groundwater that results from such leaching [8].

Over the recent decade, researchers have been exploring various innovations that can be employed to resolve this pollution impediment caused by fly ash. As such, products such as fly ash bricks, concrete, and cement have become increasingly popular because of the pozzolanic and cementitious behaviour of fly ash when incorporated into certain materials [9]. Furthermore, fly ash has been discovered to enhance compressive, flexural strength of foamed cement composites when added at optimum concentrations [10]. Additionally, the agricultural sector has also discovered methods of utilizing fly ash in germination and seedling growth rate enhancements as fly ash contains most plant nutrients except phosphorus, humus, and nitrogen [11]. Other researchers within the sector have also introduced fly ash as a soil stabilizer, and thereby increasing crop growth, and water retention capacities of certain plants [12].

Subsequently, this growing interest has also infiltrated the polymer industries. The polymer industry is growing at a rapid rate, and mass production of plastics and related products has been expanding since the 1940s. In the year 2018, the global production of plastic stood at 360 million metric tons, and it is anticipated to triple by the year 2050 [13]. Polymers are renowned for their remarkable versatility, minimal toxicity, and low cost. Polymers are in two forms namely natural polymers, and synthetic polymers. Natural polymers are those that are extracted from nature such as DNA, silk, protein, and hair [14]; while synthetic polymers are categorized into thermoplastics, thermosets and elastomers and the use thereof ranges from packaging, construction, plumbing, electronics, automotive, and pharmaceutical industries. Nevertheless, the weak mechanical properties and low thermal stability of plastics are of high concern globally as they limit the widespread application of polymers [15]. Consequently, efforts to reinforce polymers have been an intriguing topic amongst researchers.

In an effort to fabricate high performance polymers with enhanced mechanical strength and increased thermal stability, scientists have considered using fly ash as a reinforcing filler in polymer matrices. Reinforcement of polymers using fly ash is a cost-effective alternative to other fillers such as calcium carbonate, carbon nanotubes, and graphene. Research has revealed that the introduction of fly ash to high density polyethylene (HDPE) and low-density polyethylene (LDPE) has significantly improved the shear strength as well as increasing the Young's modulus, and reducing the elongation at break [16][17]. Furthermore, an increased thermal stability was observed with LDPE composites containing fly ash than neat LDPE [16]; and in order to enhance

the properties of the polymers, fly ash is incorporated within the polymer matrices with other nanoparticles. The decision on which nanoparticle requires incorporation into the polymer matrix is based on the desired application. In order to obtain superior flammability resistance, various halogenated, phosphorus as well as antimony trioxide products have been used historically in polymer materials. However, these halogenated products have been suggested to be hazardous when introduced in polymer matrices [25]. As a result, researchers have incorporated eco-friendly nanoparticles in polymer composites to enhance the flammability properties of the polymer matrices. Other particles such as: (i) multi-walled carbon nanotubes (MWCNT); (ii) calcium carbonate; (iii) graphene-oxide; (iv) mica; and (v) glass fibres have since been incorporated with fly ash to form synergy [20- 24]. Moreover, other nanoparticles such as zinc borate have gained significant attention owing to its eco-friendly nature and anti-bacterial properties [25].Zinc borate's flame-retardant properties are predominantly used on commercial furniture as well as in cosmetics and dental materials. In this research, we investigate the synergistic relationship between zinc borate and fly ash in a polymer matrix.

Meanwhile, high demand thermoplastics such as HDPE and LDPE are non-biodegradable taking an average of 100-500 years to fully decompose. In the light of the sustainable development goals 15 (i.e., SDG 15), which speaks to the preservation of life on land with regards to protecting, restoring, and promoting the efficient use of terrestrial ecosystems; commercial packing industries have sought for production of biodegradable plastic on a large-scale capacity. As such, polybutylene succinate has gained the favour of large-scale plastic producers.

Polybutylene succinate is a biodegradable thermoplastic polymer of the polyester family [18]. Renowned for its high thermal and chemical resistance, this polymer has taken centre stage in mega polymer-producing companies in Asia [19]. According to Rudnik (2013), this polymer has characteristics that mimic those of polypropylene and polyethylene which have previously been the most largely produced polymers, and thereby making it an excellent substitute for these polymers. Unlike polypropylene and polyethylene, polybutylene succinate (PBS) is a biodegradable polymer and decomposes naturally to form carbon dioxide and water. Moreover, PBS has a melting point of 114.1ºC, and a heat fusion of 68.4 J/g, thus surpassing that of polyethylene, which is 60.5 ℃ and 52.8 j/g, respectively [18]. The basic building blocks for this polymer is 1-4 butanediol and succinic acid (Polymer database. 2020) synthesized by

polycondensation. The above-mentioned description renders PBS a favourable and cost-effective alternative to other biodegradable polymers such as Polylactic acid (PLA), Polyhydroxybutyrate (PHB), and Polybutylene adipate terephthalate (PBAT). This study aims to utilize fly ash as a reinforcing filler to strengthen the properties of PBS. It is well documented in the literature that there is however poor interaction between the polymer and the fly ash filler due to the presence of silanol, aluminol, and other forms of -OH groups bonded to the fly ash which gives it a surface polarity, and resultantly decreasing effective interaction between fly ash and the polymer matrix [31]. Observably, various methods such as silanization and alkalization have been employed to improve the interaction between the polymer matrices and fly ash. Amongst the above-mentioned methods used to modify fly ash, silane molecules have been preferred due to the formation of a chemical bond the modified fly ash and polymer matrices. Silanes are made up of hydrolyzable groups that can form durable bonds with inorganic fillers, and an organofunctional group that can react with organic polymers [32]. Silane coupling agents work in the interphase to promote adhesion, and thereby enhancing the properties and providing resistance to deterioration of the composite over time [33]. The silane coupling agent additionally functions as a 'bridge' that connects the fly ash particle to the polymer surface as illustrated in **Figure 1.3**. This 'bridging effect' allows the filler (fly ash) to effectively adhere to, and interact with the polymer in the matrix, thus resulting in increased mechanical performance and durability.

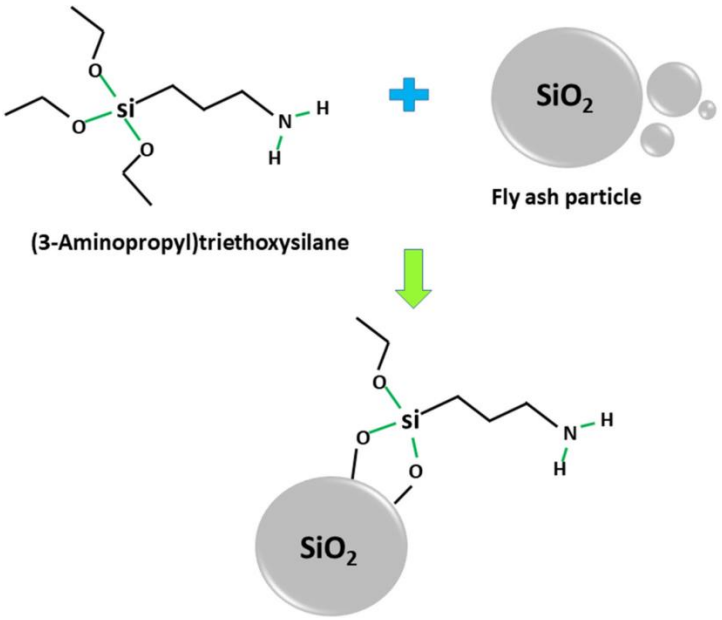

Figure 1.3: Interaction between a silane coupling agent and fly ash particle [34]

This study investigates the effect of non-modified and silane modified fly ash on the properties of PBS matrix. Properties such as morphology, crystallinity, thermal stability, and flammability of the fly ash/PBS composites are reported.

1.2 Research aims

The aim is to investigate the effect of fly ash content, modification, and its synergy with zinc borate on the properties of PBS polymer matrix for advanced applications.

1.3 Research objectives

The objectives of this study are to investigate:

- The effect of 1 %, 3% and 5% of fly ash on the properties of PBS;
- The effect of silane modified fly ash and non-modified fly ash on the properties of PBS;
- The effect of non -modified fly ash and its synergy with zinc borate on the properties of PBS; and
- The effect of silane-modified fly ash and its synergy with zinc borate on the properties of PBS.

1.4 Thesis outline

The outline of this thesis is as follows:

Chapter 1: General introduction

Chapter 2: Literature review (This chapter is published in an international journal, eXpress Polymer Letters)

Chapter 3: Materials and methods

Chapter 4: Results and discussion

Chapter 5: Conclusions

1.5 References

1. Balat, M. 2007. Influence of coal as an energy source on environmental pollution. *Energy Sources, Part A: Recovery, Utilization, and Environmental Effects*, 29(7), pp.581-589.
2. Holuszko, M.E., & de Klerk A. 2014. Coal Processing and Use of Power Generation. *Future Energy*. 53-71.
3. Lin, C.K., Lin R.T., Chen T., Zigler C., Wei Y., & Christiani D.C.2019. A global perspective on coal-fired power plants and the burden of lung cancer. *Environmental Health*, 18:9.
4. Chiang, P.C., & Pan, S.Y. 2017. Fly Ash, Bottom Ash, and Dust. In *Carbon Dioxide Mineralization and Utilization* (pp. 253-264). Springer, Singapore.
5. Dwivedi, A., & Jain, M. 2014. Fly ash- waste management and overview: A review. *Recent Research in Science and Technology*. 6.
6. Upadhyay, A., & Kamal, M. 2007. *Characterization and Utilization of Fly Ash*. (Doctoral dissertation).
7. Khambekar, J., & Barnum, R.A. 2012. Fly ash handling: Challenges and solutions. Power engineering. www.power-eng.com
8. Lemly, A.D., 2018. Environmental hazard assessment of coal ash disposal at the proposed Rampal power plant. *Human and Ecological Risk Assessment: An International Journal*, 24(3), pp.627-641.
9. Prakash, K., & Sridharan, A. 2009. Beneficial properties of coal ashes and effective solid waste management. *Practice Periodical of Hazardous, Toxic and Radioactive Waste Management*. 239-248.
10. Wahab, R., Mohd Noor, M., Jamaludin, S.B., & Nizar, K. 2013. Effects of Fly Ash Addition on Compressive and Flexural Strength of Foamed Cement CompoSites. *Advanced Materials Research*. 796. 664-668.
11. Behera, M.C., Acharya, A.K., Kar, M.R., & Tripathy, M.K. 2020. Impact of fly ash on germination and initial seedling growth performance of Acacia auriculiformis A. Cunn. Ex Benth. *International Journal of Current Microbiology and Applied Science*, 9(7): 2602-2610.
12. Kishor, P., Ghosh, A.K. & Kumar, D., 2010. Use of fly ash in agriculture: A way to improve soil fertility and its productivity. *Asian Journal of Agricultural Research*, 4(1), pp.1-14.
13. Tiseo, I.2021.*Global Plastics Industry—Statistics & Facts*.

14. Evans, A., & Watkins, S. 2017. Polymers: From DNA to rubber ducks. Australian Academy of Science, Retrieved on https://www.science.org.au/curious/everything-else/polymers
15. UKEssays. Polymer use: Advantage and disadvantages and their respective impact on society https://ukessays.com/essays/chemi
16. Porabka, A.; Jurkwoski, K.; & Laska, J. 2015. Fly ash used as a reinforcing and flame-retardant filler in low-density polyethylene. *Polimery*. 60 (4).
17. Hashmi, S.A.R.; Sharma P.; & Chand, N. 2007. Thermal and rheological behavior of ultrafine fly ash filled LDPE composites. *Journal of applied polymer science*, 107 (4): 2196-2202.
18. Rudnik, E. 2013. Compostable Polymer Properties and Packaging Applications. Plastic Films in Food Packaging. *Plastic Design Library*, 217-248.
19. Fujimaki, T. 1998. Processability and properties of aliphatic polyesters, "BIONOLLE", synthesized by polycondensation reaction. *Polymers Degradability and Stability*, 59. 209
20. Chen, P., Wang, Y., Li, J., & Chu, W. 2021. Synergetic effect of fly ash cenospheres and multi-walled carbon nanotubes on mechanical and tribological properties of epoxy resin coatings. *Journal of Applied Polymer Science*, 138(32), p.50789.
21. Atikler, U., Basalp, D. & Tihminlioğlu, F. 2006. Mechanical and morphological properties of recycled high-density polyethylene, filled with calcium carbonate and fly ash. *Journal of applied polymer science*, 102(5), pp.4460-4467.
22. Li, J.C., Zheng, L.F., Sha, X.H., &Chen, P. 2020. Microstructural and mechanical characteristics of graphene oxide-fly ash cenosphere hybrid reinforced epoxy resin composites. *Journal of Applied Polymer Science*, 137(2), p.47173.
23. Sreekanth, M.S., Joseph, S., Mhaske, S.T., Mahanwar, P.A., & Bambole, V.A. 2011. Effects of mica and fly ash concentration on the properties of polyester thermoplastic elastomer composites. *Journal of Thermoplastic Composite Materials*, 24(3), pp.317-331.
24. Chauhan, S.R., Gaur, B., & Dass, K. 2012. Synergistic effects of micro size flyash particulate and glass fiber on friction and wear of vinylester hybrid composites under dry and water lubricated sliding condition. *Intern J Mater Eng*, 2, pp.23-31.
25. Yıldız, B., Seydibeyoğlu, M.Ö., & Güner, F.S. 2009. Polyurethane–zinc borate composites with high oxidative stability and flame retardancy. *Polymer Degradation and Stability*, 94(7), pp.1072-1075.

26. Fang, Y., Wang, Q., Guo, C., Song, Y. & Cooper, P.A. 2013. Effect of zinc borate and wood flour on thermal degradation and fire retardancy of polyvinyl chloride (PVC) composites. *Journal of Analytical and Applied Pyrolysis*, 100, pp.230-236.
27. Obla, K.H. 2008. Specifying fly ash for use in concrete. *Concrete InFocus*, 7(1), pp.60-66.
28. Page, A.L., Elseewi, A.A., & Straughan, I.R. 1979. Physical and chemical properties of fly ash from coal-fired power plants with reference to environmental impacts. In *Residue Reviews* (pp. 83-120). Springer, New York, NY.
29. Murthy, D.S.R., & Narasimha Rao, D.L. 1999. Fly ash and its use in cementitious material in civil engineering.
30. Shetty, M.S. 2005. *Concrete Technology*. S. Chand & Company Ltd., New Delhi.
31. Anandhan, S. 2014. Recent trends in fly ash utilization in polymer composites. *Int. J. Waste Resour*, 4(3), p.1000149.
32. Sroka, J., Rybak, A., Sekula, R., & Sitarz, M. 2016. An investigation into the influence of filler silanization conditions on mechanical and thermal parameters of epoxy resin-fly ash composites. *Journal of Polymers and the Environment*, 24(4), pp.298-308.
33. Pape, P.G., & Plueddemann, E.P. 1991. Methods for improving the performance of silane coupling agents. *Journal of adhesion science and technology*, 5(10), pp.831-842.
34. Gohatre, O.K., Biswal, M., Mohanty, S., & Nayak, S.K. 2021. Effect of silane-treated fly ash on physico-mechanical, morphological, and thermal properties of recycled poly (vinyl chloride) composites. *Journal of Applied Polymer Science*, 138(19), p.50387.

Chapter 2: Literature review

2.1 Preparation and characterization of coal fly ash reinforced polymer composites: an overview

This chapter has been published online:

A. Kaleni, S.I. Magagula, M.T. Motloung, M.J. Mochane, and T.C. Mokhena. Preparation and characterization of coal fly ash reinforced polymer composites: an overview. Express Polymer Letters. (DOI: 10.3144/expresspolymlett.2022.54)

2.1.1 Abstract

Energy and environmental protection are two major problems that are faced by the current generation. Coal has been utilized traditionally as a source of electricity globally. However, more ash is generated from the combustion of coal which is carried by gases and precipitated into fly ash. The main problem with fly ash is that, if it is not properly disposed, it may cause pollution(s) in the water and soil, which in turn disturb ecological cycle, and have negative impact on the environment. Based on the above statement(s), more efforts have been made to recycle fly ash or its utilization for advanced applications. One of the preferred methods for recycling of fly ash is to incorporate it in polymer matrices in order to improve the strength of polymer matrices for advanced applications. Fly ash has been utilized as a reinforcing filler for various polymer matrices due to its high strength and low cost. This paper review discusses different fabrication methods for fly ash/polymer matrices composites. The effect of particle size, modification, synergy of fly ash with other fillers reinforced polymer matrices on the mechanical properties are also discussed. Furthermore, is the review makes an in-depth discussion about the specific applications of fly ash reinforced with different polymer matrices. There is also a discussion based on the fly ash/fiber/polymer hybrid composites in relation to the preparation method and mechanical properties, since hybrid systems are known for better properties than single fillers.

Keywords: Fly ash, coal waste, polymer composites, mechanical properties, hybrid systems

Corresponding author:mochane.jonas@gmail.com

2.1.2 Introduction

Coal is regarded as one of the most abundantly used fossil fuels, following oil, globally [1]. According to the World Energy Council (2016), coal remains the second most important fuel, generating approximately 40% of the world's electrical power, with China accounting for 60% of its demand. Trends analyzed since 1960 have revealed an exponential increase in coal demand annually, and a 64% increase in coal demand was reported from the year 2000 to 2014 [2]. Coal is largely used as the primary raw material in electrical power generation in thermal power plants as well as in the production of steel, gasification, and liquefaction. The fast-growing demand for coal energy can be attributed the rapidly growing population as well as industrialization. Fossil fuel has proven to be an essential material that affords people a decent living environment. It is however also accompanied by a few drawbacks such as carbon emissions into the atmosphere, and the release of fly ash as a waste material. During the process of coal combustion for the purpose of generating electrical power, a by-product referred to as fly ash is produced. Fly ash is made up of incombustible coal particles which are collected during the incineration process using electrostatic precipitators, bag houses, and other particle filtration mechanism; however, some of these particles settle to the bottom of the boiler by reason of its weight; this is then referred to as bottom ash. Collectively, fly ash and bottom ash are called coal ash. Following collection, the ash is transferred to landfill sites where they are disposed in ash lagoons or slurry dams. As a waste product, fly ash poses a major risk to the environment as it contains toxic heavy metals such as aluminium oxide (Al_2O_3), calcium oxide (CaO), sulphur oxide (SO_2), potassium oxide (K_2O), magnesium oxide (MgO), iron oxide (Fe_2O_3), and silicon oxide (SiO_2). Moreover, coal ash that is disposed in slurry dams becomes a major source of groundwater contamination as these heavy metals permeate the soil and percolate out of the soil into the groundwater [3]. Groundwater sources in areas where fly ash is disposed were discovered to have higher than permissible traces of heavy metals and trace elements such as nickel, lead, and zinc [3]. Furthermore, water containing traces of fly ash may potentially leach into various water sources such as dams, rivers, lakes, and seas polluting such water. Researchers have found that water containing fly ash leachate can be absorbed by freshwater fish through the gills. This induces oxidative stress in the fish [4] as well as causing permanent damage to the outer layer of the fish scales, thus preventing the overall functioning and formation of scales on the fish [5]. Typical fly ash sizes from 0.3-250 µm

[6], with the inhalation of smaller fly particles (*viz.*, 2,5µm) lead to a respiratory infection due to deposition in the lung parenchyma [7] as shown in **Figure 2.1**.

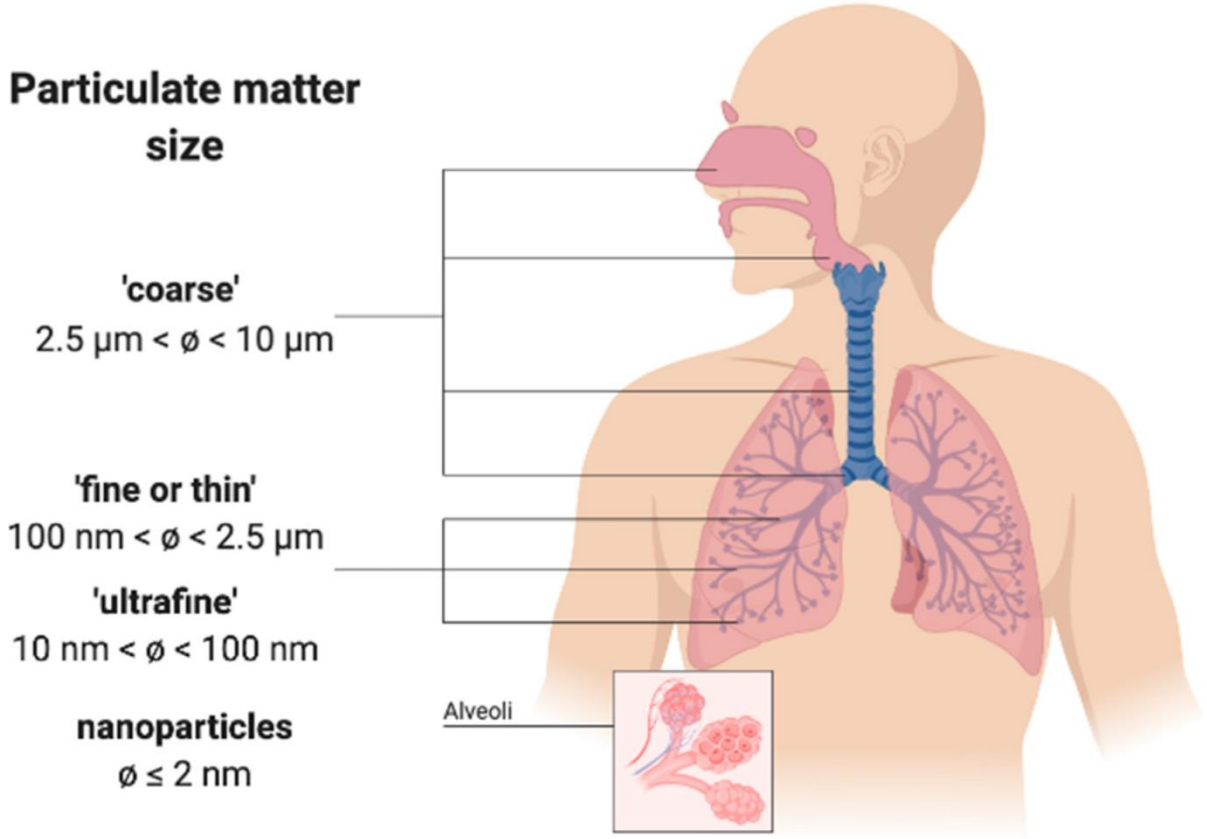

FIGURE 2.1: An illustration of the particle size penetration in lungs [8] (MDPI Open access)

Globally, the People's Republic of China is the leading country in terms of research on coal waste, specifically fly ash **(Figure 2.2)**. This is also correlating with the number of citations obtained globally in the field of fly ash, with the People's Republic of China being the leading country, followed by the United States of America (USA), and Spain being third **(Figure 2.3)**.

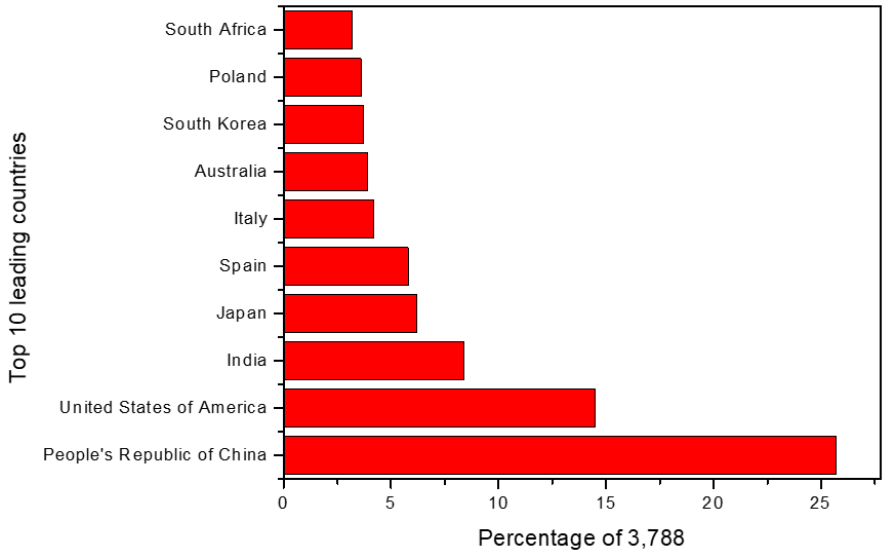

FIGURE 2.2: Top 10 leading countries in terms of coal fly ash research; data captured on the 26/04/2021.

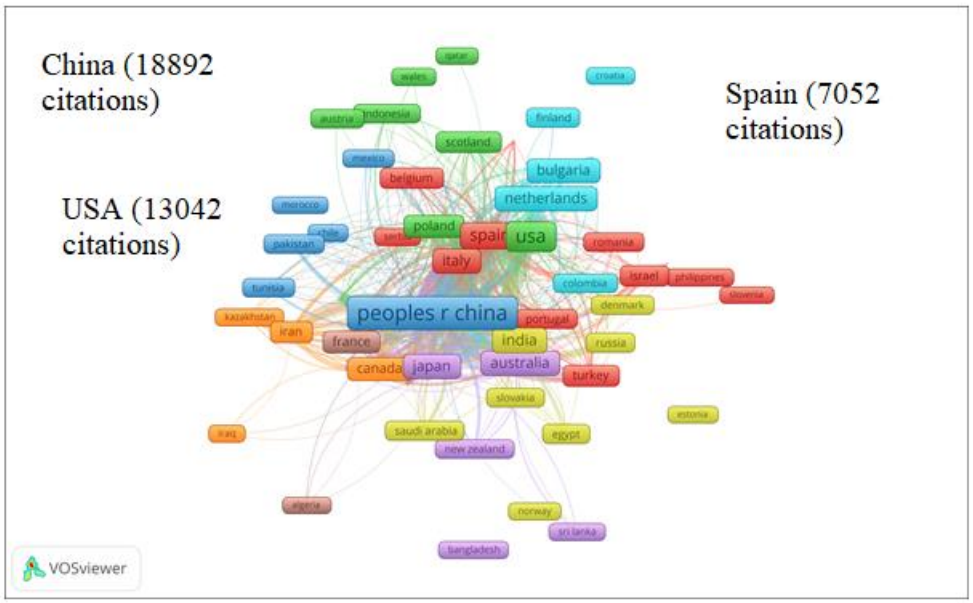

FIGURE 2.3: Network visualization of the leading countries in terms of citations; data captured on the 26/04/2021.

In an effort to combat this environmental hazard and employ sustainable waste management strategies, scientists have studied the physical, chemical, and mechanical characteristics of fly ash. Based on the statement above, it became very clear that most researchers have put enormous efforts

on the research topic of fly ash waste as illustrated by **Figure 2.4**, and such efforts have seen an increase in the number of publications from 2010 to 2021.

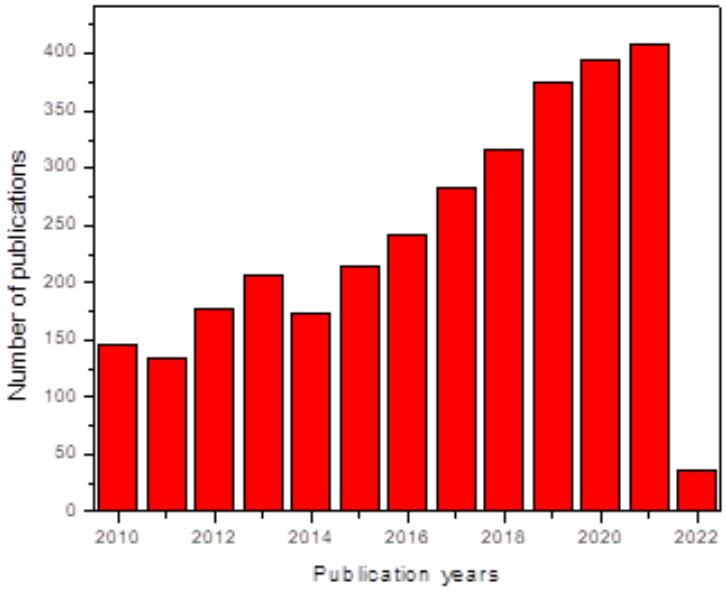

FIGURE 2.4 The number of publications on coal fly ash from 2010 to 2022; data captured on the 22/03/2022.

Based on the research works, different methods were suggested for combating the environmental hazard of fly ash. One of the well-known method is the incorporation of fly ash into polymer matrices in order to improve the properties of polymer(s), as a result enhancing their widespread applications. This review paper discusses the reinforcing of fly ash and its synergy with different nanoparticles in various polymer matrices for advanced applications.

2.1.3 General overview on fly ash

Fly ash can be obtained from various sources including: (i) municipal solid waste, (ii) biomass, (iii) oil, and (iv) coal. Due to a rapid increase in the population over a short period, more municipal solid waste is generated, and the primary waste management protocols such as disposal in landfills have proven to run short of managing the enormous amount of solid waste produced in homes. As

such, incineration of municipal solid waste has been a practiced tradition over many years. A major setback in using incineration as a waste management strategy, or a method for obtaining any type of energy is the production of fly ash and bottom ash [9]. As a result, the use of municipal solid waste fly ash in advanced application has been introduced. Ferreira *et al*. [9] outlines three major factors to be considered when applying municipal solid waste fly ash. These factors are: (i) Physical and chemical characteristics or constituents, (ii) technical applicability, and (iii) the presence of toxic trace elements. The authors further outline possible applications for municipal solid waste fly ash, which includes geotechnical applications such a concrete, cement, brick, pavements, embankments, ceramic and glass as well as applications in agriculture as soil remediation materials [10]. These applications resemble those of coal fly ash, thus suggesting a possible similarity in terms of physical and chemical constituents. Biomass fly ash, on the other hand, is obtained as a result of combustion of plant and animal organic matter [11]. Biomass can be obtained thus: (i) naturally as remains from forests or plantations; (ii) residually from wastes obtained because of agricultural activity; and (iii) as waste from energy crops including: oil seeds/plants (i.e., hempseed, sunflower, coconut, bioethanol producing plants (viz sugar cane, starch among others), and plants containing lignin and cellulose (i.e., wood and grass). Biomass is incinerated for the main purpose of generating electrical power and heat. According to the International Energy Agency in 2012, biomass energy production is expected to increase to 100-300 exajoules (EJ) by the year 2050. Some researchers do not consider biomass combustion as hazardous to the environment but rather neutral in terms of the carbon cycle as it does not temper with the atmospheric carbon concentrations [11]. This phenomenon is illustrated in **Figure 2.5** below.

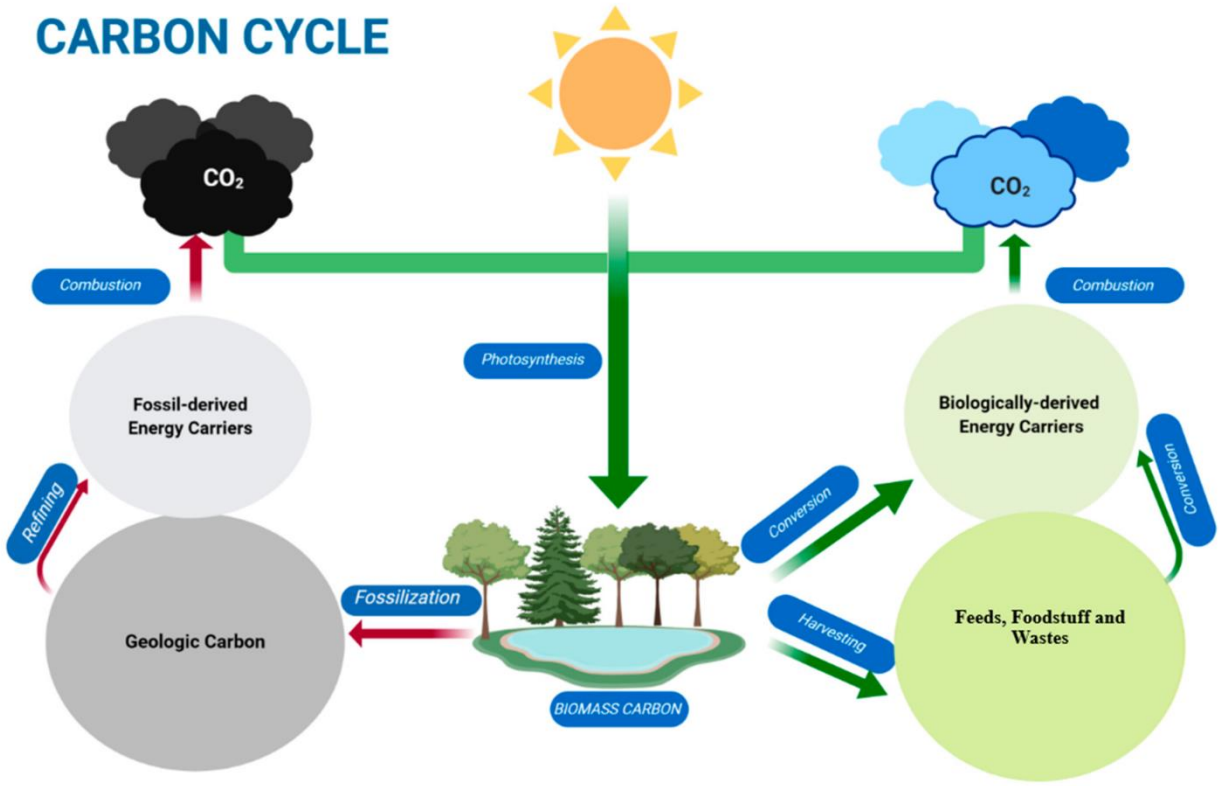

FIGURE 2.5: The carbon cycle of biomass [12] (MDPI Open access)

As is the case with any combustion process, by-products in the form of fly ash and bottom ash are however obtained. In 2013, the annual production of ash from biomass reached 480 million tons [13]. Agrela, *et al*. [11] discussed the properties of biomass fly ash and its potential applications in industry. These applications mentioned by these authors include geopolymers, thermal, and acoustic insulation as well as uses as metal absorbents in wastewater treatment processes.

While oil fly ash can be acquired from sources such as oily plants and seeds as stated above, combustion of heavy oils and crude oils also result in fly ash residues. Notably, incineration of heavy oil results in approximately 3 kg of fly ash per 1000 liters of oil [14]. Literature and research pertaining to heavy and crude oil fly ash is limited because, it contains lesser amounts of silica, thus making it less desirable in geotechnical applications such as is the case with coal fly ash. Nevertheless, industrial applications for heavy and crude oil fly ash remain a great priority since it is produced in major quantities. Mofarrah and Husain [14] explored ways to utilize heavy oil fly

ash as a colouring agent in cement motar. The researchers collected ash produced from a combination of 2% heavy fuel oil and petroleum choke. The results obtained reveal that no potential environmental harm was detected with the use of 2-5% heavy oil fly ash (HOFA). Overall, no improvements to compressive strength were observed although the colour pigmentation was achieved [14]. Dahim [15] also investigated the possible use of crude oil fly ash for road pavement applications. The researcher focused on utilizing the surface capacitance sensor to improve asphalt pavement properties, specifically the dielectric properties. Progressive applications of fly ash from various sources have gained massive attention in the research field. The most common and possibly the highest produced type of fly ash globally, is however coal fly ash, and that will be focused on in this review.

2.1.4 A brief history of coal fly ash and its early applications

Throughout its years of existence, fly ash has mostly been used in concrete mixes for the construction industry, but its use in other fields (i.e. use of fly ash as cement extenders, in polymers, in agriculture, in mining and refractories) outside the construction industry emerged later in the 1980s (between 1980 and 1987 to be specific) [16]. The use of fly ash in concrete mixes was a major breakthrough to the use of high volumes of fly ash for commercial purposes. The use of fly ash in concrete mixtures was inspired by the Romans. In 128 A.D., the Romans used high volumes of volcanic ash in cement mixtures to build the Pantheon temple **(see Figure 2.6)**. Today, after surviving countless storms and earthquakes, the Pantheon still remains in its original form as a result of the quality of concrete materials used to build it. Due to the increasing fly ash waste accumulation, fly ash was later used to replace volcanic ash in concrete mixtures. This is because it was discovered that fly ash has similar properties to those of volcanic ash [17]. Since, fly ash is a form of a naturally occurring pozzolan, thus it possesses similar properties to volcanic. Pozzolans are a group of materials consisting of silica oxide and aluminium oxide. In their natural state, these materials have little or no cementitious properties. In a finely divided form and in the presence of water however, these materials chemically react with calcium hydroxide or lime at ambient temperatures to form compounds with cementitious properties [18].

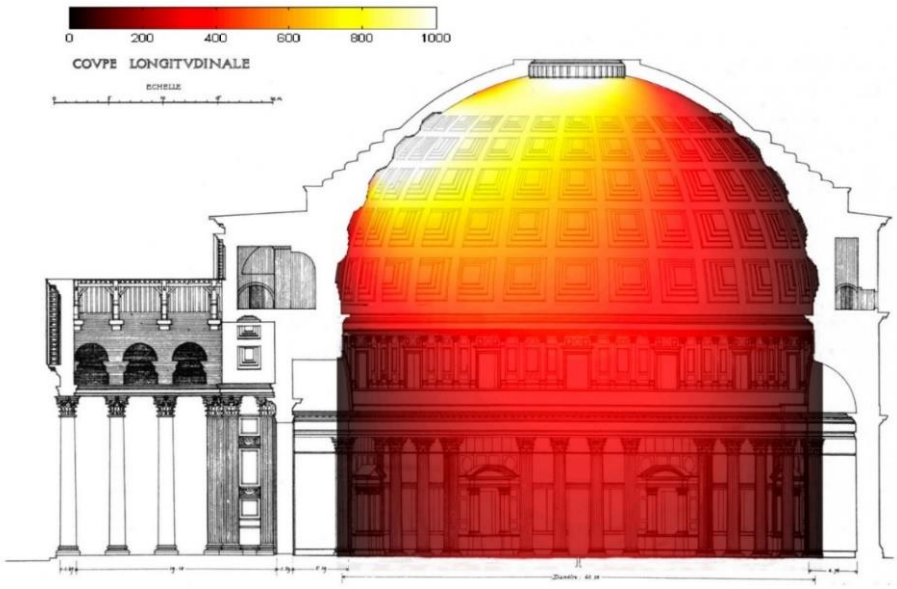

FIGURE 2.6 The Roman Pantheon, lighting simulation conducted and validated by Joseph Cabeza-Laïnez [19] (MDPI open access)

In 1942, the first documentation on the use of fly ash in concrete mixes was carried out by the Bureau of Reclamation in the U.S.A. The documented fly ash concrete mix was used to repair a tunnel spillway for the Hoover dam. Its use in concrete mixtures was later documented between 1948 and 1952 for construction of the Hungry Horse Dam near Glacier National Park in Montana. Till today, the Hungry Horse Dam is still rated amongst the most impressive structures in the U.S.A [17]. In 1983, the U.S.A. Environmental Protection Agency endorsed the use of high volumes of coal fly ash in concrete mixes for projects funded by the federal government. As a result, the Washington D.C. area metro subway system was built using high volumes of fly ash-based concrete. The endorsement also led to the construction of the massive 85,000-seat stadium in Atlanta for the 1996 summer Olympics [17]. This shows that coal fly ash has a rich history in the construction industry, and in order to expand its application scope, it has been reported that coal fly ash can be used for other non-conventional applications outside the construction industry. The use of fly ash in polymers is one of such applications [16], and this application was first discovered in the 1980s. In polymers, fly ash is used in the place of functional fillers like limestone, talc, and other inorganic fillers just to mention a few. The advantages of using fly ash in polymers as compared to other fillers is to improve the polymer processing and compounding. The spherical shape of the fly ash particles, as shown in **Figure 2.7** below improves the flow properties of

materials during extrusion and casting. This imparts physical properties to the resultant fly ash-based polymer materials. For optimum properties, strong compatibility between the fly ash filler and host polymeric matrix is essential; and today, the majority of the commercially available polymer-based materials in South Africa consist of fly ash as filler. These materials include garden hoses, electrical conduits, water pipes, and shoe soles [16].

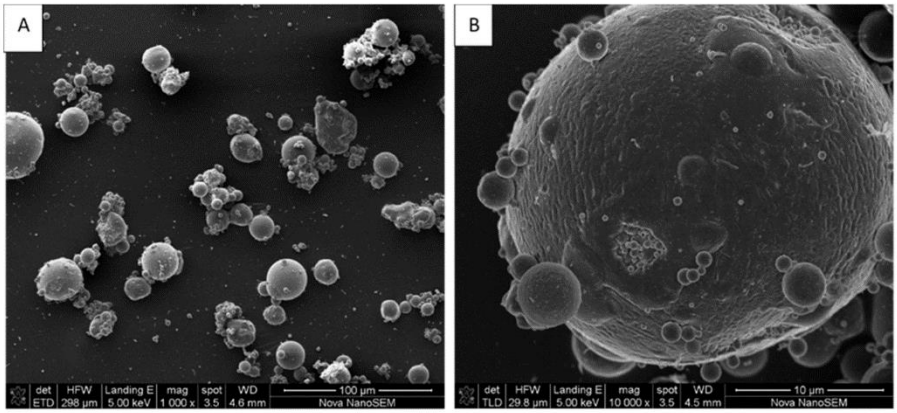

FIGURE 2.7 (A) 1000x and (B) 10,000x magnifications of coal fly as shown by scanning electron microscope images [20] (MDPI open access)

2.1.5 Fly ash waste management protocols, challenges, and regulations for disposal

(i) Fly ash waste management protocols

The process of waste management with reference to fly ash disposal starts when ash is transferred from filter fabric hoppers to bulk storage facilities such as silos or domes where it is kept. The coal ash is conveyed using various forms of conveyors under negative or positive pressure to bulk tanker trucks. These trucks then transport the ash to the final destination either for recycling or disposal [21]. Thereafter, ash intended for recycling is packed into smaller bags or stockpiled for use in concrete. Disposal of ash in lagoons, ponds, and landfills is still the most opted for method of coal ash disposal. Fly ash is therefore regarded a hazardous waste substance in many countries, and the disposal therefore is regulated [22]. In South Africa, coal waste is included in the hazardous waste category pertaining to pyrolytic treatment of coal as well as wastes from thermal processes. Reynolds-Clausen and Singh [23] assessed the coal ash strategy and implementation progress in

South Africa and stated that in order to classify fly ash as a hazardous waste, leachate testing must be undertaken. The toxic nature of fly ash thus makes it imperial to regulate its waste management systems as improper disposal may lead to adverse health and ecological outcomes.

(ii) Challenges regarding improper fly ash storage

Due to high volumes of fly ash production in the developing countries, improper fly ash disposal has become a nation-wide challenge. Poor planning of disposal protocols and an increase in demands for thermal power through coal plants lead to an inevitable socio-medical and environmental problems such as air pollution, water pollution, and soil pollution. The range in sizes of fly ash particles means that they may undoubtedly become airborne when disposed in landfills; and these airborne particles can also lead to pneumoconiosis when inhaled [24]. Hagemeyer *et al*. [25] demonstrated this by examining the respiratory health of adults exposed to coal ash by living near coal storage sites. The results have indicated that individuals who had been exposed to coal ash, experience greater respiratory illnesses than those who were not exposed to the coal ash, thus suggesting that coal ash particles may be present in the ambient air in areas surrounding coal ash storage sites.

Noticeably, fly ash polluted water has an adverse effect on aquatic and plant life. Toxic heavy metals contained in the ash contaminate watercourses may have negative effect on the supply of water intended for potable use. Ankita *et al*. [26] express this as a dual stress, which is exerted on the biological communities as well as aquatic communities present in watercourses. Additionally, the normal pH of fly ash ranges in between 7 and 12 [27], thus rendering it a medium to strong alkaline. When fly ash residues settle on the soil surface, they are able to alter the soil pH levels, thus interfering with the metabolic activity of plants influencing the types animals that are able to thrive in the particular habitat, subsequently affecting the ecosystem of the region [24]. Tiwari *et al*. [28] outline the leachate pollution caused by coal ash and slag as well as the environmental implications thereof. Some present-day health diseases such as anemia and haemochromatosis may be linked to groundwater pollution and soil pollution caused by industrial leachate resulting in access amounts of iron and chromium evident in groundwater.

(iii) Fly ash waste management strategies

There has been a lot of efforts to promote waste utilization of fly ash rather than ash aimless disposal, which includes horticulture as a long-term waste management option [29]; influence on the pH levels of in-vessel compost systems to increase the growth rate of mesophilic and thermophilic microorganisms [30]; incorporation of concrete for building applications [31]; synthesis of zeolites for water purification [32]; and most recently the incorporation of fly in polymer matrices for advanced applications. The incorporation of fly ash into polymer matrices is the preferred method of waste management of fly ash since the fabricated composites has a potential to be applied in various applications.

2.1.6 Morphology

(i) Fly ash/polymer and other nanoparticles hybrid composites

Polymer-filler composites have been an ever-advancing topic amongst researchers for many decades. The demand of polymer composites with advanced performance has given rise to many innovative ideas, including the use of waste products such as fly ash as fillers in polymer composites. When introducing a filler into a polymer matrix, factors such as the mixing and blending processes have a direct influence on whether the desired outcome is achieved. For an effective compounding, a uniform and optimum dispersion of the particles is of upmost importance. This determines the level of interaction between the filler and the host polymer. The morphology of the fly ash reinforced polymer composites was reported to be affected by factors such as: (i) preparation method, (ii) particle size of the fly ash, (iii) content of the fly ash, (iv) surface modification, (v) type of the polymer, and (vi) its synergy with other fillers [33-44]. Morphological studies are conducted using a scanning electron microscope (SEM), transmission electron microscope (TEM), and polarized optical microscopy (POM) in order to indicate the filler dispersion into the polymer matrix. Alghamdi *et al.* [33] reported on the effect of fly ash particle size reinforced high-density polyethylene (HDPE) composites. The particle sizes of fly ash utilized were 50-90 µm denoted FA1, 90-150 µm, which was symbolized as FA2, and finally 150-250 µm, which was denoted FA3. The three types of fly ash (i.e., 10 wt%) were incorporated into the HDPE

matrix using a melt mixer at 220 ℃ for 30 minutes [33] as schematically represented in **Figure 2.8**. Furthermore, the freshly fabricated samples were recycled by utilizing an extrusion and recycling process four times and the samples were "termed" the recycled samples. From SEM images, it was reported that fresh samples showed high interfacial adhesion between the composite' component. It was noticed that, after the first recycling, there was a high delamination of the fly ash in the composites. The lowest debonding was obtained at FA1/HDPE composite after the first recycling **(Figure 2.9A)**. It was further found that fly ash particles of similar sizes kept consistency in terms of the adhesion between the filler/matrix system. It was then concluded that, after the fourth re-cycle, there was no changes on the interfacial adhesion between the components [33].

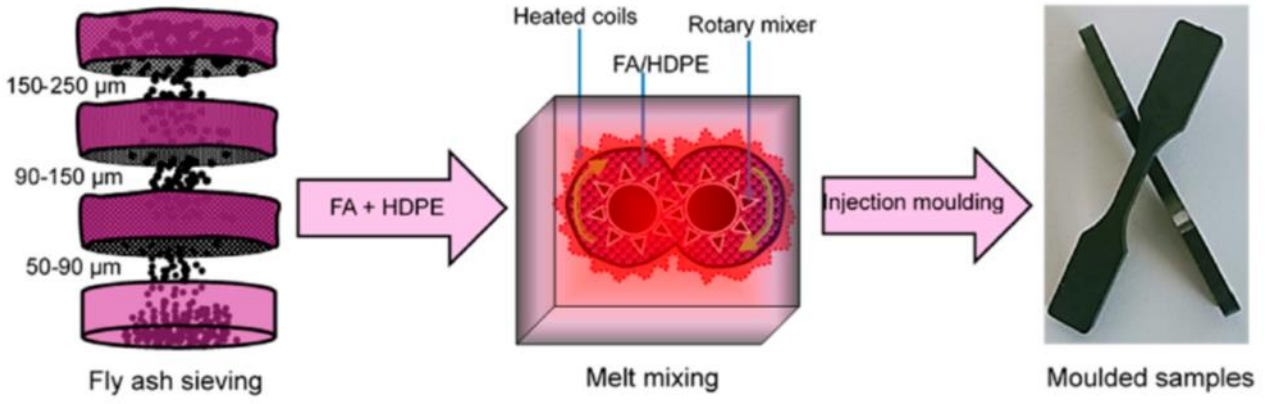

Figure 2.8 Preparation method for HDPE/fly ash composites consisting of various fly ash particle sizes [33] MDPI OPEN ACCESS.

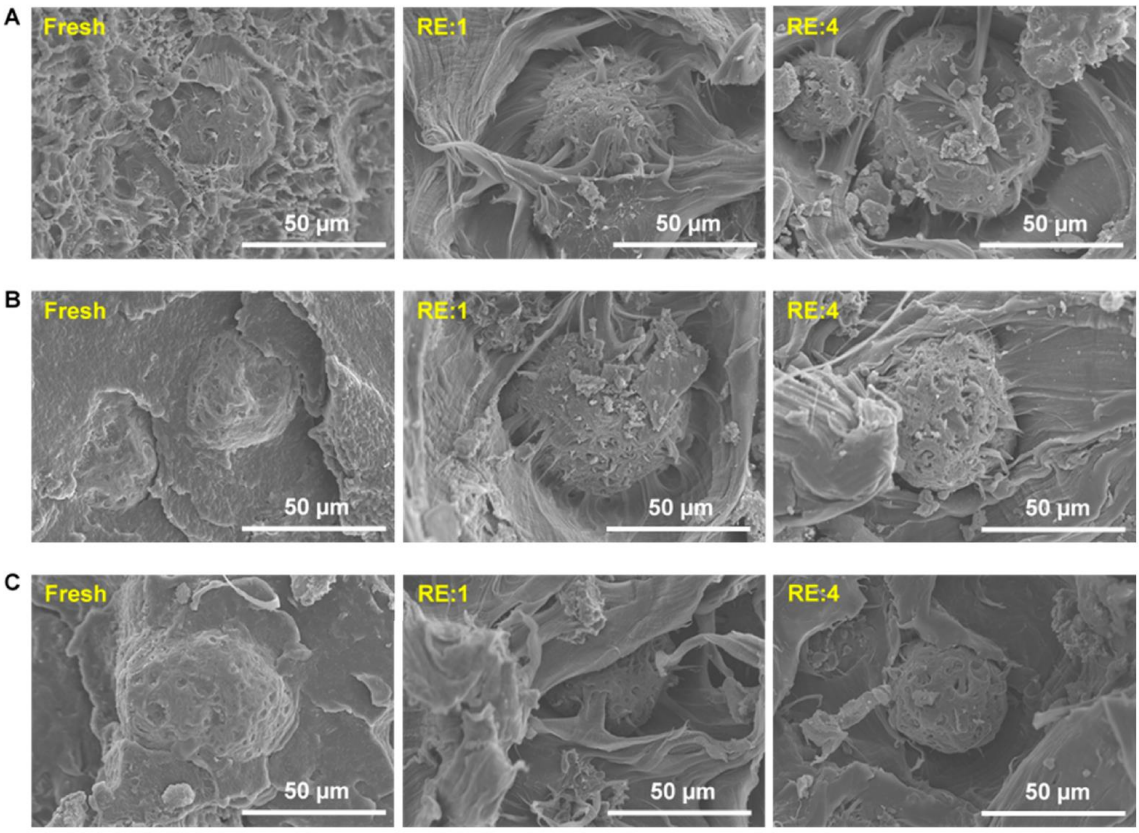

FIGURE 2.9 Cryogenically fractured fresh and recycled SEM images of: (A) FA1/HDPE, (B) FA2/HDPE, and FA3/HDPE composites [33] (MDPI OPEN ACCESS)

The effect of the fly ash content on the morphology of the fly ash/polymer composites was reported by Sim *et al*. [34]. The authors reported that the fly ash/epoxy composites with 10 vol.% fly ash with a size less than 53 µm showed debonding between the matrix, and fly ash due to poor interfacial adhesion between the polymer and fly ash. Furthermore, when the content of fly ash was more than 50 vol.%, there was a significant debonding between the epoxy matrix and fly ash. Several researchers [35-43] have reported on the morphology of polymer reinforced with fly ash together with other fillers. Various particles such mica, carbon nanotubes, calcium carbonate, and clays have been incorporated with fly ash into polymer matrices, as a result, different morphologies were obtained when compared with single fly ash/polymer composites. The synergy of calcium carbonate ($CaCO_3$), and fly ash were incorporated into the epoxy matrix with the composites fabricated by mixing the epoxy, polyamine (curing agent), fly ash (10 wt%), and various content

of calcium carbonate (0, 1,3 and 5) wt% by ultra-sonication for a duration of 30 minutes [35]. There was strong interaction between the epoxy matrix and the nanoparticles, with less agglomerates in the nanocomposites. The inclusion of the second nanoparticles into the system still require more of surface treatment and coating technologies in order to enhance interfacial adhesion, and thus improve the overall properties [36]. Different modifications such as silanization, alkalinization, and addition of compatibilizers were employed into the fly ash/polymer systems in order to enhance the adhesion between fly ash and polymer matrices. Parvaiz *et al.* [37] enhanced the interaction between fly ash and polyetheretherketone (PEEK) through chemical modification by utilizing calcium hydroxide. The unmodified fly ash/PEEK composites showed poor filler/polymer interaction, thus emphasizing a debonding at the interface between the fly ash and PEEK matrix. Contrarily, calcium hydroxide modified fly ash/PEEK composites showed an enhanced interfacial adhesion between composite' components. This was due to the formation of calcium hydroxide coatings on the surface of fly ash, which enhanced fly ash interaction with the PEEK matrix.

Numerous researchers [44-46] have reported on the utilization silane coupling agents for improving the dispersion of fly ash into the organic polymer matrices. Silane as a coupling agent has the amphiphilic functional groups (i.e., silane is able to react with the polymer matrices and inorganic fillers by forming chemical bridges in the polymer/filler composites), and as a result improves the adhesion between the two phases. Qin *et al.* [44] reported on the silane treatment of mesoscopic fly ash (MFA) reinforced polyurethane composites. In this study, 3-glycidoxypropyltrimethoxysilane (GPTMS) was grafted on the surface of MFA to form modified fly ash, and the modified fly ash was mixed polyurethane (PU) as illustrated in **Figure 2.10**. It reported that GPTMS was successfully grafted on the surface on fly ash, with the optimum concentration of GPS/FA being 2.5 wt%. The SEM images of the unmodified PU/MFA composites showed voids at the interface between the fly ash and PU, which is an indication that there was no crosslinking between the two phases **(Figure 2.11B)**. The incorporation of 2.5 wt% of GPTMS into the PU/MFA was observed to eliminate the gaps between the polymer matrix and fly ash filler **(Figure 2.11E)**. The mechanism of chemical crosslinking of PU/MFA in the presence of GPTMS is explained as follows from the literature. It is suggested that the alkoxy group are hydrolyzed into the silanol with the incorporation of silane coupling agent, with the silanol forming a membrane coating on the surface of the mesoscale fly ash particles. Furthermore, it is believed

that the silanol is dehydrated and it undergoes condensation with the hydroxy groups, which are present in the MFA, and as a result, there is a fabrication of chemical crosslinking. **Figure 2.12** (a) and (b) shows the dispersion of modified MFA into the PU matrix and the chemical crosslinking mechanism of the silane coupling in the PU/MFA composite respectively [44].

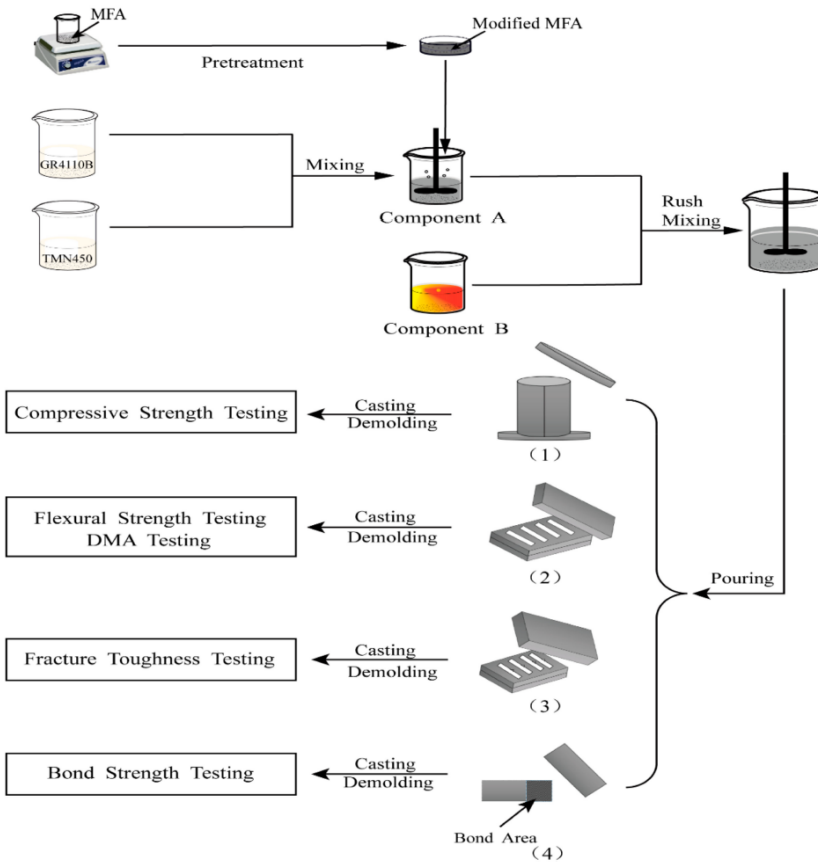

FIGURE 2.10 An illustration of the preparation method for mesoscopic fly ash/polyurethane composites [44] (MDPI OPEN ACCESS)

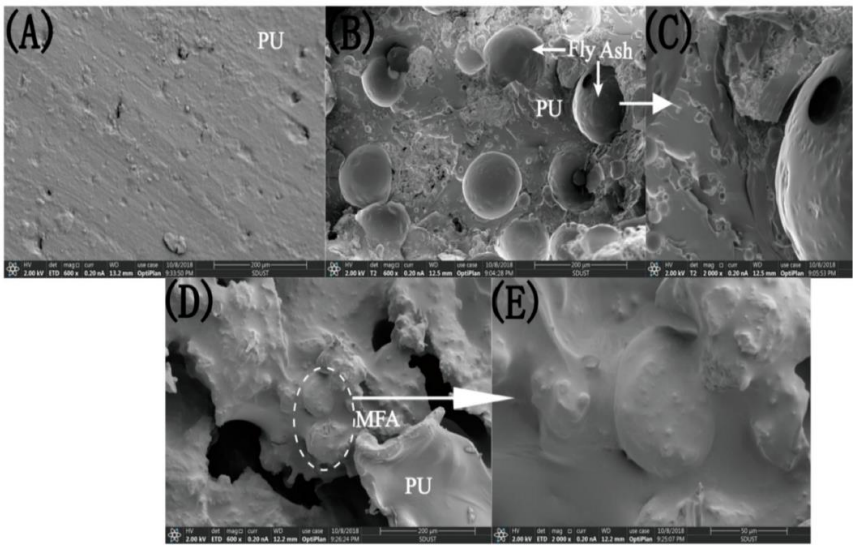

FIGURE 2.11 SEM images of: (A) neat PU, (B) and (C) PU-reinforced with MFA, (D) and (E) PU/MFA -2.5wt% fractured surfaces [44] (MDPI OPEN ACCESS)

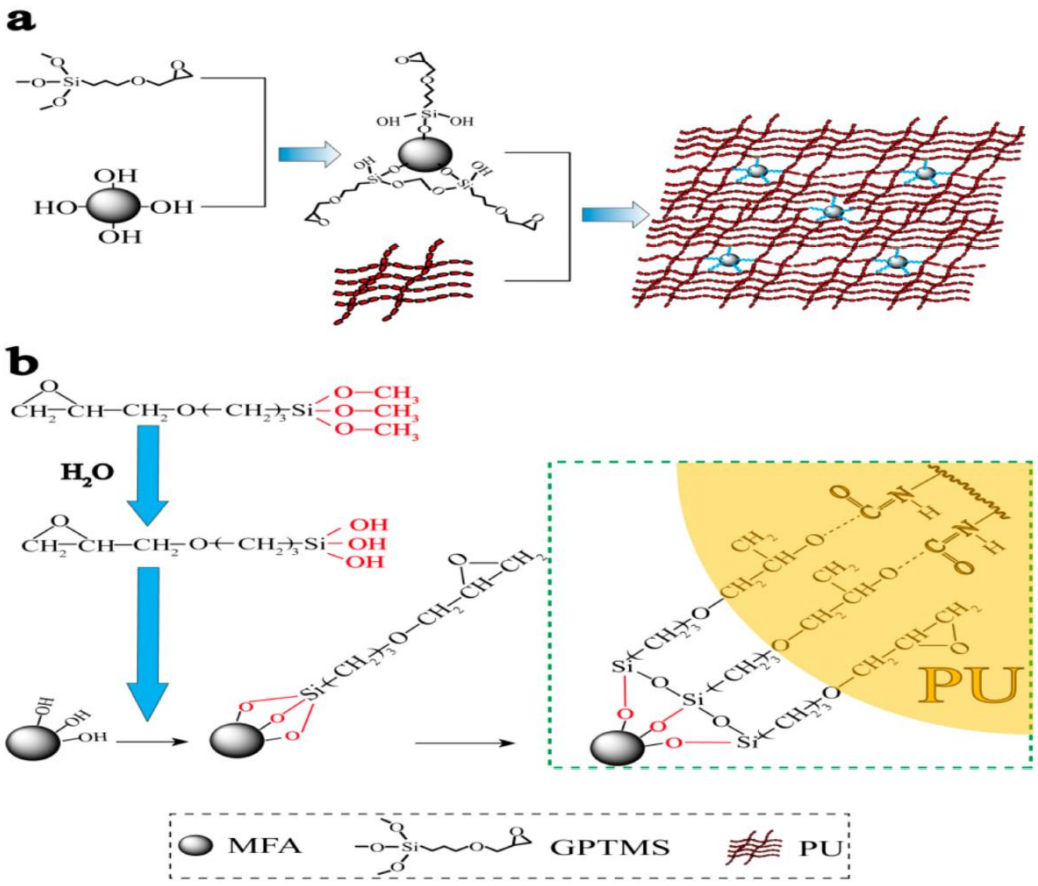

FIGURE 2.12 Possible mechanism for chemical crosslinking of PU/MFA in the presence of silane coupling agent [44] (MDPI OPEN ACCESS)

In general, the incorporation of the fly ash (i.e., 40% and above) have a negative effect on the resulting properties such as mechanical strength and dielectric properties [45]. Based on the above statement, one of the most effective methods that was utilized in order to enhance the overall properties of the polymer/fly ash composites is the incorporation of the second filler [35, 37, 39, 41, 43, 47]. This method is the preferred method because of the improvement in properties (i.e., mechanical, flame retardancy and dielectric properties at lower content of the fly ash) [42,48]. Nguyen *et al.* [45] fabricated a hybrid composites consisting of the fly ash and nanoclay nanoparticles incorporated into the epoxy matrix. In order to find the best possible combinations between the two nanoparticles, various contents of fly ash (*viz.* 10, 20, 30, 40 and 50%) and nano clay (i.e., 1, 3, and 5%) were fabricated by dispersing the fillers into the epoxy matrix and stirring the mixture for 8 hours at 3000 rpm. Furthermore, the nano clays were sonicated for 6 hours in order to break their bundles and improve its dispersion. It was reported that the optimum ratio of the fly ash: nano clay was 40:3, which was evident by a better dispersion of both fillers within the epoxy matrix at this ratio. The same polymer matrix, in the form of epoxy was incorporated with both fly ash and carbon nanotubes in order to fabricate eco-friendly composites with an enhanced flame retardancy and mechanical properties [45]. Various concentrations of fly ash (*viz.*, 30, 40, and 50 wt%) together with carbon nanotubes (CNTs) at different contents (0.03, 0.04, and 0.05 wt%) were dispersed into the epoxy matrix for 8 hours at 3000 rpm. Similar to the previous study on clays, the carbon nanotubes in the form of multi-walled carbon nanotubes (MWCNTs) were dispersed by an ultrasonication for a period of 6 hours in a temperature of 65 ℃. The morphology of the mechanically stirred composites revealed better compatibility of the two nanoparticles (MWCNTs-fly ash) into the epoxy matrix with no visible clusters or agglomerates. Table 2.1 summarizes different studies based on the preparation and morphology of fly ash and its synergy with other nanoparticles.

(ii) Fly ash/fiber/polymer hybrid composites

Researchers [49-53] have reported on the hybrid composites based on the fibers/fly-ash/polymer composites in order to enhance the properties of the resultant hybrid composite. Sathishkumar *et al.* [49] fabricated a jute fiber/lignite fly ash /epoxy hybrid composite by hand layup process

followed by compression molding. The hybrid composites were prepared with various fly ash contents (0.5, 1.0, 1.5, 2.0, and 2.5 wt%), while the content of the jute fiber was kept constant at 10 wt%. The jute fiber was modified by utilizing acetic and sodium hydroxide, which happen to have resulted in roughness in the surface of the composites which enhanced the bonding of jute fiber with both fly ash and polymer matrix. It was reported that the small size of the lignite fly ash (LFA) allowed it to easily penetrate the polymer network and as a result filled up the voids [49]. Moreover, Biswas *et al.* [50] fabricated a hybrid composite system based on alkali-treated fibers (*viz.*, jute, and sisal)/silanized fly ash incorporated in polyester matrix by compression molding. There was a better dispersion as well as compatibility of the silane-treated FA and treated fibers with the polyester matrix when compared with untreated composites [50]. Maurya *et al.* [53] produced a hybrid composite system consisting of mechano-chemically activated fly-ash/sisal fiber/PP. The polymer matrix was made of 85 wt% PP, 10 wt% of SEBS, and 5 wt% of SEBS-g-MA, which was termed the base matrix. In order to enhance its dispersion and reduce agglomeration, fly ash was modified with 2, 4, and 6 wt% modifier in the form of cetyltrimethylammonium bromide (CTAB). It was further noted that the activation of the fly ash was undertaken by using planetary ball milling. The hybrid composites were fabricated by Rheomix and extruded at the temperature of 190 °C at the speed of 50 rpm. The SEM images of the fracture tensile specimen of the hybrid composite showed that the sisal fibers as well as the FA were embedded in the matrix, with the fibers well covered and wetted into the base matrix [53]. Besides the utilization of natural fibers as second fillers for fabrication of polymer hybrid composites, other authors [54] have also reported the preparation of glass fibers for production of such hybrid system. Raghavendra *et al.* [54] used the hand lay-up method for preparation of the jute/glass woven fabric/epoxy hybrid composites reinforced with fly ash. The addition of glass fiber alone into the epoxy matrix revealed a fiber bending, while minor bending was observed in the presence of jute in the epoxy matrix. The incorporation of fly ash in both systems resulted in a decrease in bending in both systems.

Table 2.1 Selective studies on the preparation of fly ash/polymer composites and its hybrid composites

Fly ash/polymer system(s)	Preparation method	Modification(s)	Summary of results	Refs
Fly ash/nylon 6	Twin-screw extruder		• SEM images showed that there was less encapsulation of the fly ash by polymer at 30 wt.%.	**[55]**
Fly ash/polypropylene	Internal mixer at 200 ℃ at 35 rpm	Three silane coupling agents with different functional groups i.e., Vinyl, amine, and vinyl-benzyl-amine.	• SEM images showed that untreated fly ash as well as specimens treated with vinyl-benzylamine exhibited poor adhesion behavior. • Whereas fly ash treated with amine and vinyl exhibited better adhesion and effective interaction between the filler and the matrix.	**[56]**
Fly ash/ epoxy	Thermal and microwave curing	N-2(Aminoethyl)-3-aminopropyltrimethoxysilane (KBM603)	• SEM analysis revealed that samples cured using microwave curing were coarse and ductile. • Samples cured by conventional cure were smoother in texture and more uniform.	**[57]**

Recycled poly (vinyl chloride) resin (r-PVC)/ fly ash	Melt mixing followed by compression molding.		• SEM showed dewetting of fly ash particles with r-PVC polymer matrix at 10 wt%. • Stronger adhesion and uniformity at 20 wt% fly ash with r-PVC. • 40-50 wt% fly ash resulted in agglomeration of fly ash particles in the r-PVC matrix.	**[58]**
Fly ash/ recycled poly (ethylene terephlate)	Samples were Melt blended using a twin-screw extruder.		• SEM images revealed uniform dispersion of filler in the polymer matrix. • Smaller filler particles (below 43 μ) demonstrated an enhanced interaction with PET matrix. • 20 wt% concentration of fly ash resulted in agglomeration and poor filler/matrix adhesion.	**[59]**
Fly ash cenospheres /multi-walled carbon nanotubes/epoxy	FA and MWCNTs were added into epoxy matrix	Silane coupling agent (KH550)	• Flexural fracture of 20 wt% FAC-0.5 wt% MWCNTs/EP displayed the agglomeration of fillers into the matrix.	**[38]**

	solution and mixed for 15 min.			
High density polyethylene/ ultrafine fly ash/ MWCNT	Melt mixing using Brabender followed by compression moulding.	-Acid functionalized multiwalled carbon nanotubes (MWCNTs) - Ultrafine fly ash (UFFA) was modified with aminosilane coupling agent. - Epoxy functionalized HDPE	• TEM revealed that at higher loading of MWCNTs (*viz* 0.4%) in combination with UFFA, there was a clustering of particles and uniform dispersion in the matrix.	**[39]**

2.1.7 Mechanical properties

(i) Fly ash/polymer composites and its nanoparticles hybrid composites

The employment of fly ash in polymer matrices has been suggested to improve the mechanical and tribological properties of polymer materials [60]. Same as the morphology, the following: (i) preparation method, (ii) concentration and particle size of the filler, (iii) surface modification, (iv) viscosity of fly ash composite, and (v) synergy with other fillers and/or fibres have a direct impact on the mechanical properties of the final composite. Sim *et al.* [34] reported on the mechanical properties of fly ash/epoxy composites. The tensile strength of the composite improved with the addition of fly ash into the polymer matrix. However, 30% of fly ash was found to be an optimum concentration whereby enhanced mechanical properties (*viz.*, tensile strength) were obtained **(Figure 2.13)**. In addition, larger fly ash particles (>50 µm) resulted in hollow pores being present in the matrix, and thereby significantly weakening the mechanical properties of the composite [34]. Kumar *et al.* [61] studied the effect of fly ash particle size(s) and content on the mechanical properties of polyester-based composites. In the study, varying sizes of class F fly ash (75 µm and 150 µm) and the filler content ranging from 10- 30 wt% was investigated. The authors employed a basic hand lay-up technique in order to prepare the samples. The results suggested that an increase in filler content led to a reduction in tensile strength irrespective of the fly ash particles size. The decrease in tensile strength with increasing in filler content was due to weak interfacial adhesion between the two phases (i.e., filler and polymer matrix). The flexural strength however increased with an increase in filler content with the smaller particle size fly ash *(viz* 75 microns) displaying a slight increase when compared with larger particle size (i.e., 150 microns) with 30 wt% of fly ash. The compressive strength increased with increasing in filler content with the 30 wt% of fly ash (75 microns) displaying a maximum value of 91.8 MPa when compared with 72 MPa of neat polyester matrix [61]. Alghamdi [33] reported the effect of fly ash particle size on the recyclability of fly ash/HDPE composites by comparing the mechanical properties of the three-particle incorporated into the HDPE matrix. The fly ash samples collected had the following sizes: sample 1 (50-90 µm), sample 2 (90-150 µm), and sample 3 (150-250 µm). The smaller particle size fly ash (50-90 µm) based HDPE composites displayed a higher Young's modulus than the neat HDPE, fly ash (90-150 µm)/HDPE, and fly ash (150-250 µm)/HDPE composites. Both the large fly ash particles-based composites nonetheless had a higher Young's modulus when compared with neat HDPE matrix. This behaviour was ascribed to a uniform dispersion of fly

ash within the polymer matrix with limited agglomerates. The authors further compared the mechanical properties of the recycled system with the unrecycled HDPE/fly ash system. Similarly, with the unrecycled fly ash/HDPE composites, the recycled fly ash/HDPE system with lower particle size (90-150 µm) returned higher mechanical properties (Young's modulus and tensile strength at yield) when compared with large fly ash particles (90-150 µm and 150-250 µm)/HDPE based composites. This behaviour was attributed to a weak filler/polymer interfacial interaction in the presence of large particle sizes [33].

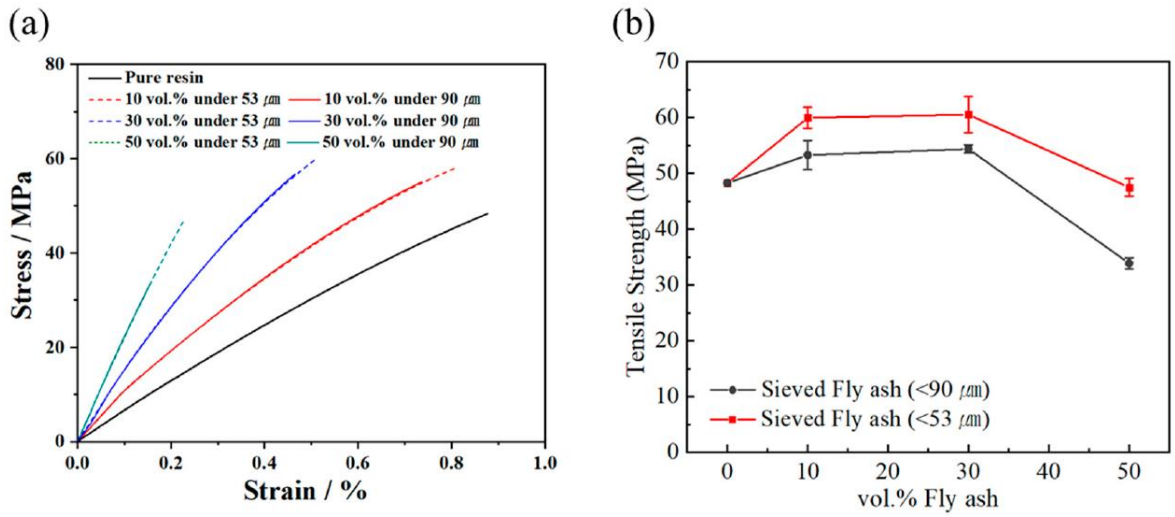

FIGURE 2.13 (a) Stress-strain curves of fly ash/epoxy composites reinforced with less than 90 µm, and 53 µm fly ash particles; and (b) tensile strength graphs of the fly ash /epoxy composites [34] (MDPI OPEN ACCESS)

Surface treatment is continuously employed when fabricating a filler/polymer composites with the aim of enhancing interaction between the two phases in order to have a positive effect on the morphology and mechanical properties [36]. The main aim of surface treatment of fly ash with silane and/or surfactants is to introduce functional groups on the surface of the inorganic filler, and as a result, it enhances its interaction with the polymer matrices. Dharmalingam *et al.* [62] treated fly ash with silane coupling agent and surfactant in the form of sodium lauryl sulfate (SLS). Epoxy matrix was modified with the amine consisting of the liquid silicone (ACS). It was reported that the flexural strength decreased with the increasing in fly ash content (i.e., from 10 to 40%) irrespective of the modification method employed. Despite the fact that the addition of fly ash reduced the flexural strength, the silane-treated samples displayed higher flexural strength when compared with SLS. It was further reported that the highest flexural modulus was attained for 10% fly ash-based composites (*viz.*, 20, 30 and 40%). The decrease in flexural modulus at higher contents was attributed to a poor interaction between the fly ash

and polymer matrix [62]. The effect of two types of silane in the form of vinyl silane as well as aminosilane on the fly ash reinforced waste poly(ethylene terephthalate) (WPET) was also reported [63]. There was an enhancement in mechanical properties (*viz.*, tensile strength) for both silane functionalization fly ash, with the optimum concentration of aminosilane treated system being 1%. The vinyl silane-treated samples displayed different trend. At 0.5% of the coupling agent, there was an increase in tensile strength; however above it, there was not much of improvement in the tensile strength. It was found that the impact strength increased in the presence silane coupling agents. It was further emphasized that 1% of amino silane was the optimum concentration to obtain highest impact strength, which was 280% enhancement when compared with untreated composites [63]. Similar observation was reported by Gohatre *et al.* [47] who investigated the effect of silane treated fly ash reinforced recycled poly(vinyl chloride) composites. The authors showed that the silane treatment at higher concentration (*viz.*, 5%) had a negative impact on the mechanical properties, with the lower silane content (i.e., 1%) revealing higher tensile strength. Besides the utilization of the silanization as a modifier, other authors [64] employed stearic acid for surface modification of fly ash. There was an enhancement in the mechanical properties **(see Figure 2.14)** of the epoxy reinforced with stearic acid treated fly ash. Generally, the modification of fly ash improves the overall mechanical properties. Such improvements in mechanical properties result from strong interfacial adhesion between the polymer matrix and fly ash that enable and facilitate stress transfer between the two phases. It is worth mentioning that there is optimal concentration of the coupling agent in order to achieve preferable mechanical properties.

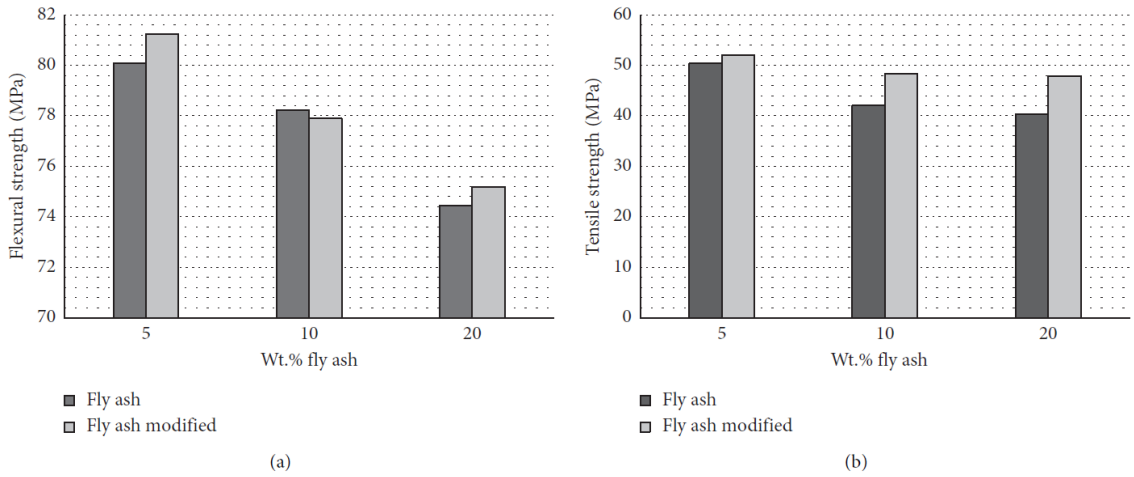

Figure 2.14 Mechanical properties of unmodified and modified fly ash/epoxy composites [64] (HINDAWI OPEN ACCESS)

Mechanical properties of fly ash with other nanoparticles were reported by various researchers, and it became apparent that the synergy between the two nanoparticles showed higher mechanical properties when compared single fly ash reinforced polymer composites. For example, Li *et al.* [65] reported that hybrid composites (GO-FAC/EP) exhibited higher tensile strength values when compared with composites reinforced with GO alone. The optimum filler content in both the GO and GO-FAC hybrid systems was ~0.5 wt.% to achieve superior mechanical performance [65]. Chaturvedi *et al.* [66] reinforced epoxy with both the carbon nanotubes and fly ash through ball milling and compression molding method. Carbon nanotubes and fly ash were mixed at various concentration (i.e., 5, 10, 15, and 20 vol%). Flexural strength was observed to increase with the addition of the carbon nanotubes irrespective of the content when compared with neat polymer, which was attributed to a better dispersion within the epoxy matrix. It was however reported that the optimum concentration was 5 vol%, and above this, the flexural strength was found to decline [66]. Tiwari *et al.* [35] reported that the addition of calcium carbonate into the fly ash reinforced epoxy matrix enhanced the overall mechanical properties. The influence of $CaCO_3$ on the mechanical properties of the fly ash/epoxy was proven by an enhancement in the tensile strength, with 5 wt% resulting in 52.41% improvement in tensile strength. The impact strength and flexural strength enhanced by 43.24% as well as 42.36% with 3 wt% of $CaCO_3$, respectively when compared with fly ash/epoxy composites [35].

(ii) Fly ash/fibers/polymer hybrid composites

Several authors [40, 41, 49, 67-69] have reported on the mechanical properties of the fly ash/fiber reinforced polymer composites. Their reason for incorporating fly ash into fiber(s) based polymer composites was to enhance the mechanical properties of the resultant hybrid composites. It is well-known that the incorporation of the fly ash/fiber synergy as reinforcements for plastics is an attractive method for development of materials for advanced applications. Sathishkumar *et al.* [40] reported on the mechanical properties of the sisal fiber/lignite fly ash/epoxy hybrid composites fabricated by hand layup process. The fabricated epoxy hybrid composite consisted a constant 20 wt% of sisal fiber (SF) together with lignite fly ash (LFA), with the content of LFA varying between 0 to 10 wt.%. The incorporation of 2.5, 5.0, 7.5, and 10 wt.% of the fly ash into the epoxy/sisal fiber composite was found to enhance the tensile strength by 29.54, 29.88, 30.01, and 31.09 MPa, correspondingly when

compared with neat epoxy (*viz* 13.01 MPa), and EP/SF 80/20 (i.e., 26.28). This behaviour was attributed to a uniform distribution of the fly ash within the epoxy matrix, and as a result enhanced the mechanical properties. According to the SEM, it was reported that the spherical fly ash particles were found within the cracks and voids in the hybrid composites, which enhanced the mechanical properties. Similar results were reported by Sathishkumar and co-workers [49], whereby lignite fly ash was incorporated into the epoxy/jute fiber composites. In this study, mechanical strength, which include tensile strength, compressive strength, impact energy and flexural strength were found to improve with the addition of the 2 wt% fly ash content in the epoxy matrix. It became apparent that the addition of the fly ash beyond 2 wt% in other components of the mechanical properties (*viz.*, compressive strength, barcol hardness and impact strength) revealed no significant influence. Jayamani *et al.* [67] reported the mechanical properties fly ash/sugarcane fiber reinforced epoxy matrix. The sugarcane fiber was varied in between 0 to 10 wt.%, with the fly ash incorporated with 2 wt% into the epoxy/sugarcane fiber system. The optimum content of fly ash and sugarcane fiber was reported to be 2 wt% and 4 wt% respectively. This was proved by high mechanical properties at this ratio of the synergy, with samples at 4 wt% sugarcane fiber and 2 wt% fly ash displaying the highest tensile strength. It was noted that the fly ash filled voids in the composites with minimum agglomerates. The addition sugarcane fibers at higher content (i.e., 6, 8, and 10 wt%) showed a reduction in mechanical properties which was ascribed to an inappropriate wetting of the fiber. It was emphasized that the reduction may also be due to a non-uniform distribution of the fly ash at this fiber contents, which may have resulted in voids, and dry spots, which hindered an improvement in mechanical properties [67]. The effect of fiber aspect ratio together with fly ash on the compressive properties of epoxy was investigated in the literature [68]. Generally, there was a reduction in the strengths at higher fiber loading (*viz.*, 15 to 25 vol%) in the absence of fly ash. The behaviour was ascribed to the bunching of glass fibers together with improper wetting between the fibers and epoxy matrix. Therefore, the addition of fly ash into the fiber/epoxy composites resulted in better strength at higher range of the fibers content. Furthermore, the addition of fly ash was also found to have a positive impact on the modulus with a noticeable enhancement in the modulus. Generally, the improvement and/or reduction in the mechanical properties (compressive strength and modulus) was explained by few factors (i.e., bunching of fibers took place in the absence of fly ash *viz.*, lower mechanical properties), and in the presence of smaller fly ash particles there was a better wettability which gave rise to enhanced properties initial, with debonding observed in the presence of larger fly ash particles which may account for reduction in mechanical properties [68]. Kavya *et al.* [69]

investigated the impact of fly ash and TiC nanoparticles on the mechanical properties of the coir fiber/epoxy-based hybrid composites. The tensile strength and modulus of epoxy + 5 wt% coir fibers + 5 wt% fly ash (CFE), epoxy + 5 wt% coir fibers + 5 wt% TiC (CTE), and epoxy + 3 wt% coir + 3 wt% TiC + 4 wt% fly ash (CFTE) enhanced with the addition TiC nanoparticles, fly and a combination of TiC + fly ash synergy. It is well-known that the reinforcement of inorganic ceramic fillers with higher modulus than polymers have the ability to enhance both modulus and tensile strength. Furthermore, the addition of either filler or a combination of fillers in epoxy enhanced both the flexural modulus and strength, with a reduction in strain to break. Besides the enhancement in flexural characteristics, the CFTE system showed lower values when compared with CTE system. The improvement in flexural parameters was ascribed to a stronger bond between the epoxy matrix and the fillers. Furthermore, a good distribution of fillers in the polymer matrix also played a key role in enhancement of the flexural properties [69]. Table 2.2 shows the fly ash content used to achieve optimum mechanical and tribological properties.

Table 2.2 A summary of the mechanical and tribological properties of fly ash/polymer composites

Fly ash/polymer system	**Preparation method**	**Fly ash content**	**Achieved mechanical properties**	**Refs**
Fly ash/polymer composite	Casting	10 vol. % (paraffin oil modified fly ash particles)	Modulus = 58.8 %, compressive strength = 55 %	[70]
Fly ash/epoxy composite	Casting	10 vol. % (silane modified)	Modulus = 100 %, compressive strength = 43.3 %	[70]
Fly ash/epoxy composite	Casting	6.5 vol. %	Toughness = 56.2 %, tensile strength = 8.3 %	[71]
Fly ash/aramid fiber/phenolic hybrid composite	Sequential mixing then curing and post curing	70 vol. %	Coefficient of friction = 0.12, wear depth = 0.25 mm	[72]
Fiber glass/epoxy/fly ash hybrid composite	Hand lay up	10 wt. %	Impact strength = -26.4, tensile stress = -24 %	[73]
Fly ash/E-glass fabric/polyester hybrid composites	Hand lay-up and vacuum bagging techniques	5 wt. %	Impact strength = 186.9 kJ/m^2, tensile strength = 275 MPa, flexural strength = ~ 369 MPa, hardness = 84.9, roughness = 0.33 µm	[74]

Fly ash/carbon fiber/phenolic hybrid composite	Casting on a glass mold	30 % fly ash and 4 laminates of carbon fiber	Flexural strength = 91.42 N/mm	[75]
Fly ash/polyester composite	Curing of liquid polyester resin consisting of fly ash cenospheres	4.9 vol. %	Compressive yield strength = 12 %	[76]
Fly ash/polyester composite	Curing of liquid polyester resin consisting of fly ash cenospheres	29.5 vol %	Compressive yield strength = -19 %	[76]
Fly ash/vinyl ester composite	Sequential mixing then casting in aluminium molds then curing and post curing	60 vol. %	Flexural strength = -73 %, flexural modulus = 47 %, coefficient of thermal expansion = - 67 %	[77]
Fly ash/vinyl ester composite	Sequential mixing then casting in aluminium molds then curing and post curing	40 vol. %	Compressive strength = - 25 %, compressive modulus = 45 %	[77]

Functionally graded fly ash cenosphere/epoxy resin syntactic foams	Mixing then casting in aluminium molds then curing and post curing.	16 wt. %	Compressive modulus = 68 %	[78]
Fly ash/epoxy cast slabs	Casting then curing and post curing	10 vol. %	Modulus = 23.5 %	[79]
Fly ash/epoxy composites	Compression molding	10 wt. %	Flexural strength = -12.37 %, tensile strength = -38 %	[80]
Fly ash/geopolymer composite	Solution mixing	48.2 wt. %	Compressive strength = 63 %	[81]
Fly ash/epoxy composite	Film casting	20 wt. %	Tensile strength = 33.3 %	[82]

2.1.8 Applications of coal fly ash/polymer composites

Due to the increasing worldwide environmental concern on coal fly ash waste accumulation, numerous efforts have been made to find new ways of using it for various applications [83]. Currently, the production rate of coal fly ash waste stands at five million tons per annum. Out of this five million tons, 16 % is recycled, whilst the remaining 84 % is buried in landfills and lagoons [83]. This is not good for the surrounding population and ecosystem. As a result, over the past few decades, researchers have been effortlessly trying to find new applications for coal fly ash waste. The most common use of coal fly ash to date is in building materials as an additive in cement, and concrete [83-86]. Nowadays, coal fly ash is also used in adsorbents for the removal of heavy metals as well as organic and inorganic compounds from aqueous media [87-90]. For example, Darmayanti *et al.* [91] prepared a fly ash based adsorbent for the removal of copper (II) ions from an aqueous solution. Results showed that the adsorption of copper (II) ions by the fly ash-based adsorbents improved with increasing adsorbent dosage, even when two kinds of fly ash (fly ash 1 and fly ash 2) were used. According to their explanation, the improvement in adsorption was due to an increase in surface area and adsorption sites with increasing fly ash content. Malek *et al.* [92] prepared a new magnetic Schiff's base-chitosan-glyoxal/fly ash/Fe_3O_4 (Chi-Gly/FA/Fe_3O_4) biocomposite for the removal of an anionic azo dye. The biocomposite was prepared by using a direct combination of magnetic chitosan and fly ash powder particles followed by a crosslinking reaction of glyoxal with Schiff's base formation. The biocomposite was used to specifically remove the reactive orange 16 (RO16) dye. The surface morphology of the Chi-Gly/FA/Fe_3O_4 biocomposite before RO16 adsorption was rough, porous, consisted of crevices and cracks. The surface morphology of the Chi-Gly/FA/Fe_3O_4 biocomposite after RO16 dye adsorption showed void of crevices, indicating that the RO16 dye molecules were successfully adsorbed onto the Chi-Gly/FA/Fe_3O_4 biocomposite. EDX analysis of the biocomposite after RO16 dye adsorption confirmed the presence of the S element which belonged to the RO16 dye. This was further proof that the RO16 dye was adsorbed by the Chi-Gly/FA/Fe_3O_4 biocomposite [92].

Fly ash is also used in other diverse applications such as zeolite synthesis [93], and in carbon dioxide adsorbents [94,95]. Amongst all the uses of fly ash, its use as a filler in polymer composites is gaining more attention. Fly ash is used to improve the thermal and mechanical properties of polymers. Furthermore, due to its flame retardant properties, fly ash has also been

used to improve the flame retardant properties of polymers. Flame retardant fillers like fly ash are essential for use in applications such as construction, electrical and electronic industries as well as in transportation [96]. The fly ash flame-retardant filler is composed of ceramics such as silica, alumina and calcium oxide and is therefore considered to be inert to fire [48,52, 97-99]. Furthermore, fly ash does not emit any toxic gases and smoke and its use serves as a potential way of fostering economic savings by reusing waste materials [100, 101]. For instance, fly ash has been used by several researchers to improve the flame retardant properties of polymers such as polycarbonate or polyurethane [97, 102], epoxy resins [98, 99], polybutadiene rubber [103, 104], ethylene-propylene-diene rubber [105], and polymer foams such as styrene and urethane foams [99, 106]. Table 2.3 shows more applications and properties of fly ash-based polymer composites.

TABLE 2.3 Summary of fly ash/polymer properties and their applications

Fly ash/polymer composite	**Preparation method**	**Achieved properties**	**Applications**	**Refs**
Fly ash (FA)/recycled polypropylene composites	Twin-screw extrusion	- Composites filled with fly ash exhibited a higher ductility compared with composites filled talc. - Composites with a talc and fly ash hybrid filler system exhibited a higher ductility and a lower impact strength when compared with talc filled composites.	Automotive applications	[107]
Coal fly ash derived mesoporous silica/polysulfone mixed matrix membranes	Solution mixing and solution casting	- Permeability tests confirmed that the membranes can be used to remove CO_2 from CH_4. This was due to unnoticeable differences between real and ideal selectivity. - Membranes exhibited high resistance to CO_2 plasticization. This was due to a decrease in permeability even at a high feed pressure (up to 16 bar).	CO_2/CH_4 separation	[108]
Cationic fly ash/polyepichlorohydrin-dimethylamine adsorbent	Immobilization of poly-epichlorohydrin-dimethylamine (PED) onto raw fly ash	- Immobilization of PED changed the zeta potential of fly ash from negative to positive within a pH range of 3 to 11. The crystal structure of the fly ash was not altered in the process. - Static adsorption results showed that the dye was adsorbed spontaneously, and that the adsorption process was endothermic.	Dye wastewater treatment	[109]

		- The cationic fly ash dye adsorption capability was 1.5 times higher than that of activated commercial carbon. - The synthesized cationic fly ash adsorbent can be reused repeatedly. - To avoid secondary pollution, the disabled cationic fly ash adsorbent can be used in polymer concretes as a functional filler.		
Carbonated fly ash/silicon rubber (SR) composites	Mixing of fly ash and silicon rubber using a twin-roll mill followed by hot press molding.	- Fire resistance of the composites was studied using the gas torch method. The gas torch method confirmed that the carbonation of fly ash increased the penetration time of the composites by 11 %. - Penetration time of carbonated fly ash /silicon rubber composites was 2-3 times higher than that of composites filled with other commercially available fillers.	Fire-proofing applications	[83]
Fly ash and aramid fiber reinforced phenolic hybrid polymer matrix composites	Samples were prepared by following a predefined sequential mixing schedule followed by curing and then compression molding	- Friction-fade behavior followed a consistent decrease with decreasing fly ash content. The friction fluctuations (μ_{max} - μ_{min}) decreased with increasing fly ash content. - A higher friction-recovery response was observed at a fly ash content of 80 wt%. - Material integrity and temperature increase of the disc determined the wear behaviour.	Friction braking applications	[110]

	and then post curing in a standard oven.			
Sulfonated poly(ether ether ketone) (SPEEK)/single walled carbon nanotubes (SWCNTs)/fly ash polymer electrolyte nanocomposite membranes	Solution casting	- SPEEK/SWCNTs/fly ash membranes exhibited proton conductivity values of up to 0.027 Scm^{-1} at 30 °C and 0.034 Scm^{-1} at 90 °C whilst pristine SPEEK membranes exhibited proton conductivity values of up to 0.019 Scm^{-1} at 30 °C and 0.031 Scm^{-1} at 90 °C. - SPEEK/SWCNTs/fly ash membranes also exhibited excellent thermal and mechanical stability when compared to pristine SPEEK membranes.	Electrolyte membranes in fuel cell applications	[111]
Magnetic chitosan-polyvinyl alcohol (m-Cs-PVA)/fly ash (FA) biocomposite blend	Incorporation of fly ash microparticles into a magnetic chitosan-polyvinyl alcohol polymeric matrix	- The highest removal of RO16 dye was found to be 90.3 % at a m-Cs-PVA/FA dosage of 0.06g, solution pH of 4, working temperature of 30 °C and contact time of 17.5 min.	Removing reactive orange 16 (RO16) textile dye from aquatic environments	[112]
Crosslinked sulfonated poly (vinyl alcohol) (SPVA)/ fly ash (FA) composite membranes	Solution casting	- SPVA/FA composite membranes consisting of 20 wt% fly ash exhibited an ionic conductivity of 0.016 Scm^{-1}, whilst pristine SPVA membrane exhibited an ionic conductivity of 0.008 Scm^{-1}.	Polymer electrolyte membrane for fuel cell applications	[113]

Fly ash/ in situ reduced graphene oxide (rGO) geopolymeric composites	Solution mixing of fly ash and in situ reduced graphene oxide	- rGO increased the electrical conductivity of fly ash/ rGO geopolymeric composites from 0.77 Scm^{-1} at 0.00 wt% to 2.38 Scm^{-1} at 0.35 wt%. - rGO also increased the gauge factor of the geopolymeric composites by 112 % and 103 % for samples subjected to tension and compression.	Self-sensing structural materials for civil engineering applications	[114]
Fly ash/octadecane shape-stabilized composite phase change materials (PCMs)	Preparation of fly ash/n-octadecane composites using the vacuum impregnation process followed by dopping the composites with carbon nanotubes, carbon nanofibers and graphene for enhanced thermal conductivity	- Differential scanning calorimetry results showed that the shape-stabilized composite phase change materials exhibited acceptable phase change temperatures (25.01 – 26.43 °C) and reasonable latent heat storage capacities (60.50 – 64.47 J/g) for solar thermal energy storage operations in building applications. - The thermal conductivities of the phase change materials were enhanced by 187.09 %, 135.48 % and 203.22 % with the addition of 8 wt% of carbon nanotubes, carbon nanofibers and graphene.	Thermal energy storage in buildings	[115]
Ultra-lightweight fly ash-based cement (ULFC) foams consisting of ethylene-vinyl acetate	Introduction of EVA emulsion into ULFC slurry and addition of A-3 lab-made	- The dry density, compressive strength and heat conductivity of ULFC after 28 days was 154.7 kg/m^3, 0.57 MPa and 0.0514 w/(m.K).	Ultra-lightweight cement foams in	[116]

(EVA) emulsion and waste-derived calcium silicate hydrate (C-S-H) seeds	hardening acceleration and waste-derived C-S-H seeds.	- The EVA film solidified at the gas-solid interface and well-interwined with hardened cement stone in order to improve the compressive strength when the specimens were cured at a relative humidity of 60-65%. - The foam stability of ULFC was improved by enhanced bubble confinement force with increasing the EVA content.	construction applications	

2.1.9 Conclusion and future recommendations

Generally, the global energy resource is currently commanded by coal due to its usefulness, and applications to many sectors such as energy, construction, and automobile. Coal is employed in many countries as the primary fuel, contributing 36% of the overall fuel utilization in the production of global electricity. During the combustion of coal for production of electricity, a byproduct in the form of fly ash is produced, which is regarded as a waste material. More research works have been done in the utilization for fly ash reinforced polymer matrices for advanced applications. Fly ash reinforced polymer was found to improve various properties of polymer matrices. Different factors were however found to affect the properties of fly ash/polymer composites such as functionalization of the fly ash, its synergy with other fillers, and the particle size of the fly ash. Generally, it can be concluded that the treated fly ash polymer composites showed better properties than the untreated polymer composites. Furthermore, the synergy of fly ash with other fillers were found to enhance the properties of the composites more than fly ash reinforced polymer composites alone. The smaller particle sized fly ash fillers were more dominated than larger particles in terms of improving the properties of the overall composites. Based on the improvements in the polymer composites with the incorporation of fly ash, the fly ash polymer composites have been utilized in various applications such as construction, self-sensing structural materials for civil engineering, automotive, fuel cell, dye wastewater treatment and friction braking applications. It is realized from the literature that fly ash has been utilized as a reinforcing filler for polymers such nylon, polypropylene, epoxy, polysulfone etc., with limited utilization of the biopolymers. There is a need for fabrication of fly ash with biopolymers, since the biopolymers are compatible with the environment.

2.2 Zinc Borate: History, properties, uses, and flammability resistance

Zinc borate is ranked highly in terms of boron-containing industrial chemicals for its wide-spread use and large-scale production [117]. The main constituents of zinc borate are zinc oxide, and boric acid. Zinc oxide is commonly used in dental and cosmetic applications as a topical protectant. Boric acid is commonly used in cosmetics, porcelain, enamels, and insecticides as an antiseptic [118]. In 1967, Lehmann *et al.* [119] outlined the chemical composition of zinc borate by X-ray diffraction analyses as $2ZnO.3B_2O_3.3H_2O$ as it is commercially referred to presently. The author also described then that the chemical composition of zinc borate may be formulated by a 4:1 mole ratio of boric acid and zinc oxide at a temperature of 165°C in a closed vacuum. Nies *et al.* [120] however, challenged this statement in 1970 by suggesting the manufacturing of zinc borate from zinc oxide and stoichiometric excess of boric acid at a temperature of merely 75°C in the presence of water. This method of producing zinc borate has since become popular in industrial manufacturing. **Figure 2.15** illustrates the common structure of industrially produced zinc borate.

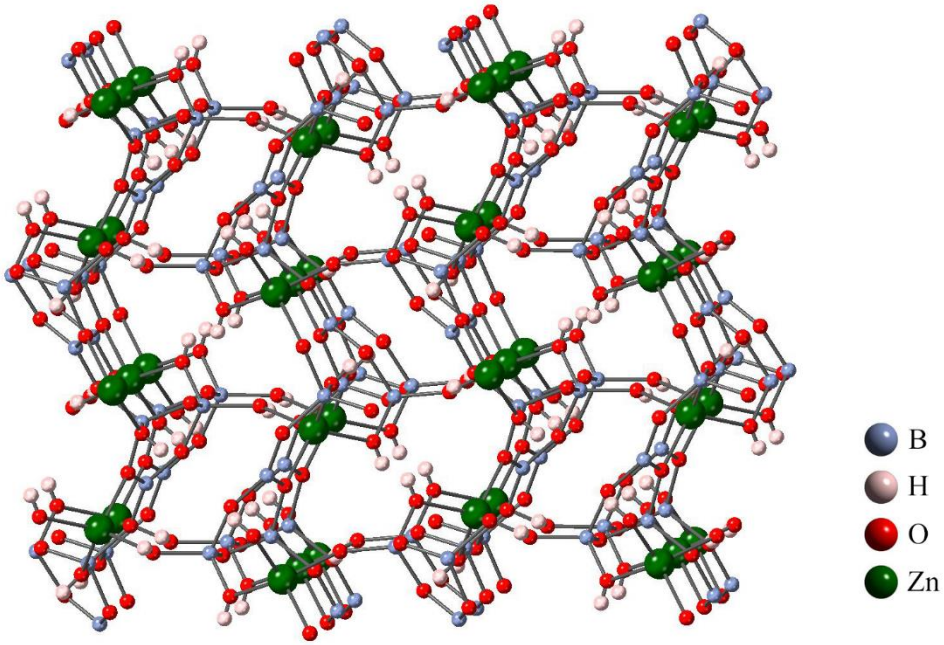

Figure 2.15 Structure of industrial zinc borate Zn $[B_3O_4(OH)_3]$ [1] (MDPI OPEN ACCESS)

The use of zinc borate in the commercial industry dates back to the 1930s as an effective fire retardant in paints, ceramics, automobiles, floor coverings, and selected building materials. In recent times, it has also been utilized in agricultural applications and bio-composites [117].

One of the pressing challenges in the agricultural sector has been plant soil that is deficient of essential nutrients such as zinc, and borate. As such, farmers have included zinc borate as a soil supplement to improve soil performance as well as decrease boron deficiency-related plant diseases [117]. Moreover, zinc borate has also been predominantly used as a preservative for biocomposites such as wood fibers, wafer boards, particle boards, straw boards as well as wood-plastic composites [117]. Subsequently, the prevalent use of zinc borate as a reinforcing material to enhance various composite properties has also infiltrated the polymer industry. The dominating focus when utilizing zinc borate as a reinforcing agent is to enhance flammability and biological resistance of polymers. Tascioglu *et al.* [121] examine the biological effect of zinc borate on various wood plastic composites. Six samples of wood-plastic composites (WPC) were synthesized in a closed mixing blender and compounded into 100x100x40 mm^3 samples at 180°C using wood and polypropylene (PP). Samples were subjected to laboratory testing for termites and decay in a protected above-ground test over a period of 36 months. The research study revealed that an increase in mass loss was associated with increase wood content and the addition of 1% zinc borate resulted in decreased mass loss. All the samples were seen to be resistant to fungal decay; however, termite infestation was observed from 12 months [121]. Chan-Hom *et al.* [122] also studied the effect of zinc borate on the anti-fungicidal and flammability properties of WPC. The composites were synthesized by incorporating wood flour and zinc borate to high density polyethylene (HDPE), and poly (vinyl) chloride (PVC). Samples of silane-treated WPV and WHPE were prepared by dry blending using a high-speed mixer and then melt blended using twin-screw extruder. Zinc borate (ZB) contents of 0,1,3,5, and 7 wt% were incorporated into the samples. The result indicated that the antifungal efficacy against the growth of *Loeweporus sp.* lowered in both WPVC and WHDPE samples, as an increase in weight loss was observed with increased wood loading. The introduction of ZB to wood-plastic composites however led to an increased antifungal efficacy, and ZB was seen to be most effective in protecting the composite against fungal attack at 1% of ZB. Moreover, ZB increased the flame retardancy of WPVC more effectively due to the chemical interaction of HCl in PVC and ZB. The treatment wood flour with silane led to a decrease in flammability resistance of the composites [122]. To further explore the effect of surface treatment of ZB polymer composites, Baltaci *et al.* [123] studied the use of cumene terminated poly(styrene co-maleic anhydride) (PSMA) as a surfactant to reduce the particle size of ZB use in the experiment. The aim of the study was to investigate the role of surfactants in effectively reducing the size of ZB particles in nano size in order to obtained better filler dispersion and increased performance in a PET matrix. The researchers observed that the addition of PSMA

to ZB composites restricted crystal growth but not agglomeration. Furthermore, samples containing PSMA and boron phosphate led to a better particle dispersion in PET, thereby improving flammability resistance and impact strength [123]. Zinc borate is predominantly used in the polymer industry as a smoke suppressant and flame retardant [124]. Moreover, it can be used synergistically with other intumescent flame retardants (IFR's) in order to better enhance flammability resistance of a composite. Gao *et al.* [125] studied the combination of ammonium polyphosphate (APP) and layered double hydroxide (LDH), and its synergy with zinc borate in a polypropylene matrix. The study aimed to investigate the thermal stability and flammability resistance of synthetic APP intercalated LDH and their synergistic behaviour with zinc borate in a PP matrix. A hydrothermal method was used to synthesize Mg_3Al-APP LDH with the aid of acetone to convert the surface of LDH from a hydrophilic nature to a hydrophobic one. PP/APP-LDH and PP/APP-LDH/ZB nanocomposites were synthesized by solvent mixing method. Figure 2.16 shows an illustration of the synthesis of PP/APP-LDH/ZB nanocomposites. The flammability resistance of the various composites was analyzed, and the peak heat release rate is also illustrated in **Figure 2.16**.

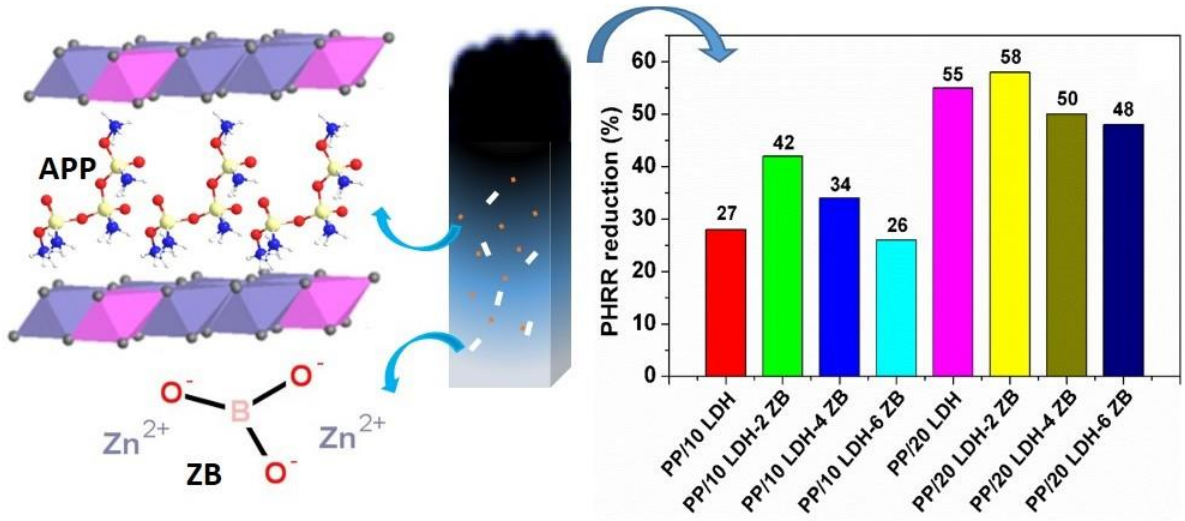

Figure 2.16 Synthesis of PP/APP-LDH and PP/APP-LDH/ZB nanocomposites and the PHRR reduction (%) [123] (MDPI OPEN ACCESS)

Thermogravemetric analysis (TGA) and microscale combustion calorimeter (MCC) results revealed a good thermal stability and fire resistance for PP. The PHRR reduction reached 55% and 27% with the addition of 20 wt% and 10wt% of APP-LDH and elevated the $T_{50\%}$ by 7°C and 52°C respectively. It was also observed that the addition of 2% of ZB increased thermal

stability and flame retardancy. This is due to the enhanced viscosity that seals the carbon layer of the nanocomposites [125]. Table 2.4 shows selective studies of incorporation of zinc borate as a flame retardant additive to polymer composites.

Table 2.4: Selective studies on the flame retardancy of zinc borate/polymer composites

Zinc borate/polymer composite	Preparation method	Modifications/additional of fillers except ZB	Achieved properties	Refs
Ultrafine zinc borate on LDPE/IFR System	Mixed using a two-roll and pressed in vulcanizing press machine	Blends of ammonium polyphosphate (APP) and pentaerythritol (PER)- IFR	• Mass ratios of 4.2 (ZB): 25.8 (IFR) achieved a UL-94 rating of V-0. • LDPE/IFR/ZB showed a char residue at 600°C. • SEM results revealed that a synergy was formed between ZB and IFR's.	[126]
Zinc borate/polyvinyl chloride (PVC)	Dry blending and mixed using a twin-screw and single screw extruder	Wood flour	• Addition of wood flour decreased initial decomposition rate and temperature. • ZB acted as a smoke suppressant for WF-PVC composites.	[127]
Zinc borate/polypropylene	Melt compounding in a two-roll mill	Ammonium polyphosphate and charring-forming agent (CNCA-DA)	• A synergistic effect was achieved between ZB, APP and CNCA-DA • Small amounts of ZB was seen to enhance fire resistance, increase LOI and reduce smoke.	[124]
Zinc borate/polyester	Solution mixing	Ammonium polyphosphate (APP), montmorillonite (MMT),	• Samples composed of 10 wt% DMMP, 17 wt% APP, 1 wt% MMT and 2 wt% ZB had the most superior flammability resistance properties	[128]

		dimethyl methyl phosphonate (DMMP).	having a LOI of 31,3% and obtaining a UL-94 rating of V-0. • One of the significant properties seen in the composite is the formation of a porous char. • SEM analysis confirmed that MMT increased silicon presence thereby improving thermal resistance. • A synergy was formed between MMT, DMMP and ZB in the polyurethane polymer matrix.	
Zinc borate/epoxy	Ultrasonic dispersion and vacuum resin infusion method.	Ammonium polyphosphate	• Composites of 10 wt% APP and 5 wt% ZB showed superior flammability resistance with 0s drip flame time. • The self-extinguishing behavior of the composites were as a result of the synergy between APP and ZB forming an effective char layer as seen in SEM.	[129]
Zinc borate/propylene	Injection molding with a single screw extruder	Aluminum hydroxide (ATH), maleic anhydrate (MAPP)	• The degree of crystallization base increased with the addition of ATH and ZB, but decreased with the addition of MAPP • Addition of ZB to composites containing ATH resulted in increased LOI and fire resistance.	[130]

			However, MAPP addition resulted in decreased LOI.	
Zinc borate/polypropylene	Solution mixing and melt blending	Organo-layered double hydroxides (organo-LDH)	• A decrease in PHRR was seen with PP/organo-LDH and PP/organo-LDH/ZB of 30% and 60%, as well as 16% and 46% respectively. • The nanocomposites showed a slight improvement in LOI which was however, not enough to enhance the flame retardancy. • All system received an HB rating in terms of UL-94 testing.	[131]

2.1.10 References

1. Kholod N., Evans M., Pilcher R.C., Roshchanka V., Ruiz F., Coté M., Collings R.: Global methane emissions from coal mining to continue growing even with declining coal production. Journal of Cleaner Production, **256**, 120489/1-120489/12 (2020). https://doi.org/10.1016/j.clepro.2020.120489
2. Lin J., Fridley D., Lu H., Price L., Zhou N.: Has coal use peaked in China: Near-term trends in China's coal consumption. Energy Policy, **123**, 208-214 (2018). https://doi.org/10.1016/j.enpol.2018.08.058
3. Verma C., Madan S., Hussain A.: Heavy metal contamination of groundwater due to fly ash disposal of coal-fired power plant, Parichha, Jhansi, India. Cogent Engineering, **3**, 1178243/1-1178243/8 (2016). https://doi.org/10.1080/233111916.2016.1179243
4. Ali M., Pandey S., Atif F., Kaur M.: Rehman H., Raisuddin S.: Fly ash leachate induces oxidative stress in freshwater fish Channa punctata (Bloch). Environment International, **30**, 933-938 (2004). https://doi.org/10.1016/j.envint.2004.03.004
5. Shikha S., Sushma D.: Effect of fly ash on fish scales. Research Journal of Chemical Science, **19**, 24-28 (2011).
6. Hui L.: Content and distribution of trace elements and polycyclic aromatic hydrocarbons in fly ash from a coal-fired CHP plant. Aerosol and Air Quality Research, **14**, 1179-1188 (2014). https://doi.org/10.4209/aaqr.2013.06.0216
7. Falcon-Rodriguez C.I., Osornio-Vargas A.R., Sada-Ovalle I., Segura-Medina P.: Aeroparticles, composition and lung disease. Frontiers in Immunology, **7,** 3/1-3/9 (2016) https://doi.org/10.3389/fimmu.2016.00003
8. Sanità di Toppi L., Sanità di Toppi L., Bellini, E.: Novel coronavirus: how atmospheric particulate affects our environment and health. Challenges, **11,** 6/1-6/12 (2020). https://doi.org/10.3390/challe11010006
9. Yao J., Li W.-B., Xia F.-F., Zheng Y.-G., Fang C.-R, Shen D.-S.: Heavy metals and PCDD/Fs in solid waste incinerator fly ash in Zhejiang province, China: chemical and bio-analytical characterization. Environmental Monitoring and Assessment, **184**, 3711-3720 (2011).

https://doi.org/10.1007/s10661-011-2218-0

10. Ferreira C., Ribeiro A., Ottosen L.: Possible applications for municipal solid waste fly ash. Journal of Hazardous Materials, **96**, 2-3 (2003) https://doi.org.10.1016/S0304-3894(02)00201-7
11. Aglera F., Cabrera M., Morales M.M., Zamorano M., Alshaaer M.: Biomass fly ash and biomass bottom ash. New Trends in Eco-efficient and Recycled Concrete, 23-58 (2019). https://doi.org/10.1016/B978-0-08-102480-5.00002-6
12. Ahmed I, Zia MA, Afzal H, Ahmed S, Ahmad M, Akram Z, Sher F, Iqbal H.: Socio-economic and environmental impacts of biomass valorisation: A strategic drive for sustainable bioeconomy. Sustainability, **13,** 4200/1-4200/32 (2021). https://doi.org/10.3390/su13084200
13. Voshell S., Mäkellä M., Dahl O.: A review of biomass ash properties towards treatment and recycling. Renewable and Sustainable Energy Reviews, **96**, 479-486 (2018) https://doi.org/10.1016/j.rser.2018.07.025
14. Mofarrah A., Husain T.: Use of heavy oil fly ash as a color ingredient in cement mortar. International Journal of Concrete Structures and Materials, **7**, 111-117 (2013). https://doi.org/10.1007/s40069-013-0042-3
15. Dahim M.: Crude oil fly ash waste for road pavement application. IOP Conference Series Earth and Environmental Science, **801**, 012006/1-012006/11 (2021) https://doi.org/10.1088/1755-1315/801/1/012006
16. Kruger R., Krueger J.: Historical development of coal ash utilisation in South Africa. International ash utilization symposium and the world coal ash conference, Policy 3, 11-15 (2005).
17. Bajpai S., Dogne N.: An Architectural Study of Fly Ash, Journal of Interior Designing and Regional Planning, **1,** 1-9 (2016).
18. Al-Jumaily I., Kareem Q., Hilal N.: An overview on the Influence of Pozzolanic Materials on Properties of Concrete, International Journal of Enhanced Research in Science Technology and Engineering, **4**,81–92 (2015).
19. Almodovar-Melendo J.-M., Cabeza-Lainez,J.-M., Rodriguez-Cunill I.: Lighting features in historical buildings: Scientific analysis of the church of Saint Louis of the frenchmen in Sevilla. Sustainability, **10**, 3352/1-3352/23 (2018). https://doi.org/10.3390/su10093352

20. Kalombe, R.M., Ojumo V.T., Eze C.P., Nyale S.M., Kevern J., Petrik L.F.: Fly Ash-Based Geopolymer Building Materials for Green and Sustainable Development. Materials, **13**, 5699/1-5699/17 (2020).
https://doi.org/10.3390/ma13245699
21. Khambekar J., Barnum R.A.: Fly ash handling: Challenges and solutions. Power engineering. (2012).
Accessed: www.power-eng.com
22. National Environmental Management Act, Waste Act no 59 of 2008. Government Gazette. Pretoria.
Accessed: April 2021.
23. Reynolds- Clausen K., Singh N.: South Africa's power producer's revised coal ash strategy and implementation progress. World of Coal Ash (2017).
Accessed: www.worldofcoalash.org
24. Prakash K., Sridharan A.: Beneficial properties of coal ashes and effective solid waste management. Practice Periodical of Hazardous, Toxic and Radioactive Waste Management, **13**, 239-248 (2009).
https://doi.org/10.106/(ASCE)HZ.1944-8376.0000014
25. Hagemeyer A.N., Sears C.G., Zierold K.M.: Respiratory health in adults residing near a coal-burning power plant with coal ash storage facilities: a cross-sectional epidemiological study. International Journal of Environmental Research in Public Health, **16**, 3642/1-3642/10 (2019).
https://doi.org/10.3390/ijerph16193642
26. Anikta S.T., Kulkarni G.N., Amin A.: Impact of fly ash on water characteristics in Kharland pond of Ratnagiri (Kokan). Journal of Experimental Zoology India, **19**, 296-301 (2015).
27. Shwartz G.E., Hower J.C., Phillips A.L., Rivera N., Vengosh A., Hsu-Kim H. Ranking coal ash materials for their potential to leach arsenic and selenium: relative importance of ash chemistry and site biogeochemistry. Environmental Engineering Science, **35**, 728-738 (2017).
https://doi.org/10.1089/ees.2017.0347
28. Tiwari M.K., Bajpal S., Dewangen U.K., Tamrakar R.K.: Suitability of leaching test methods for fly ash and slag: A review. Journal of Radiation Research and Applied Science, **8**, 523-537 (2015).
https://doi.org/10.1016/j.jrras.2015.06.033

29. Ansari E.A., Gupta A.K., Yunus M.: Fly-ash coal-fed thermal power plants: bulk utilization in horticulture- a long-term risk management option. International Journal of Environmental Resources, **5**, 101-108 (2010). https://doi.org/10.22059/IJER.2010.295
30. An C. J., Huang G. H., Yao Y., Sun W., An K.: Performance of in-vessel composting of food waste in the presence of coal ash and uric acid. Journal of Hazardous Materials, **203**, 38-45 (2012). https://doi.org/10 1016/j.jhazmat.2011.111.066
31. Sridharan A., Prakash K.: Coal ash utilization for sustainable waste management. In Proceedings of the first US-India workshop on global geoenvironmental engineering challenges, New Dehli, India, 7 (2010).
32. Du Plessis P.W., Ojumu T.V, Petrik L.F. Waste minimization protocols for the process of synthesizing zeolites from south African fly ash. Materials, **6**, 1688-1703 (2013). https://doi.org/10.3390/ma6051688
33. Alghamdi M.N.: Effect of filler particle size on the recyclability of fly ash filled HDPE composites. Polymers, **13**, 2836/1-2836/9 (2021). https://doi.org/10.3390/polym13162836
34. Sim J., Kang Y., Kim B.J., Park Y.H., Lee Y.C.: Preparation of fly ash/epoxy composites and its effects on mechanical properties. Polymers, **12**, 79/1-79/12 (2020). https://doi.org/10.3390/polym12010079
35. Tiwari S., Gehlot C.L., Srivastava D.: Synergistic influence of $CaCO_3$ nanoparticle on the mechanical and thermal of fly ash reinforced epoxy polymer composites. Materials Today: Proceedings, **43**, 3375-3385 (2020). https://doi.org/10.1016/j.matpr.2020.06.205
36. Gilliam M.: Polymer surface treatment and coating technologies. In "Handbook of Manufacturing Engineering and Technology" (ed(s).: Nee A.Y.C.) Springer, London, Edition 1, 99-122 (2015). https://doi.org/10.1007/978-1-4471-4670-4_20
37. Parvaiz M.R., Mohanty S., Nayak S.K., Mahanwar P.A.: Effect of surface modification on the mechanical, thermal, electrical and morphological properties of polyetheretherketone composites. Materials Science and Engineering A, **528**, 4277-4286 (2010). https://doi.org/10.1016/j.msea.2011.01.026

38. Chen P., Wang Y., Li J., Chu W.: Synergetic effect of fly ash cenospheres and multi-walled carbon nanotubes on mechanical and tribological properties of epoxy resin coatings. Journal of Applied Polymer Science, **138**, 50789/1-50789/11 (2021). https://doi.org/10.1002/app.50789
39. Divya V.C., Khan M.A., Rao B.N., Sailaja R.R.N., Vynatheya S., Seetharamu S.: Fire retardancy characteristics and mechanical properties of high-density polyethylene/ultrafine fly ash/MWCNT nanocomposites. Polymer Plastics Technology and Engineering, **56**, 762-776 (2016) https://doi.org/10.1080/03602559.2016.1233253
40. Sathishkumar G.K., Akheel M.M., Ibrahim M., Rajkumar G., Karpagam R., Gopinath B.: Experimental and finite element analysis of lignite fly ash on the mechanical properties of sisal-added polymer matrix composite using ANSYS workbench. Journal of Natural Fibers (2021). https://doi.org/10.1080/15440478.2021.1941487
41. Raghavendra G., Ojha S., Acharya S.K., Pal S.K., Rami I.: Evaluation of mechanical behavior of nanometer and micrometer fly ash particle-filled woven bidirectional jute/glass hybrid composites. Journal of Industrial Textiles, **45**, 1-20 (2014). https://doi.org/10.1177/1528083714557058
42. Atikler U., Basalp D., Tihminlioğlu.: Mechanical and morphological properties of recycled high-density polyethylene, filled with calcium carbonate and fly ash. Journal of Applied Polymer Science, **102**, 4460-4467 (2006). https://doi.org/10.1002/app.24772
43. Sreekanth M.S., Joseph S., Mhaske S.T., Mahanwar P.A.: Effects of mica and fly ash concentration on the properties of polyester thermoplastic elastomer composites. Journal of Thermoplastic Composite Materials, **24**, 317-331 (2011). https://doi.org/10.1177/0892705710389293
44. Qin C., Lu W., He Z., Qi G., Li J., Hu X.: Effect of silane treatment on mechanical properties of polyurethane/mesoscopic fly ash composites. Polymers, **11**,714/1-714/16 (2019). https://doi.org/10.3390/polym11040741
45. Nguyen T.A., Pham T.M.H.: Study on the properties of epoxy composites using fly ash as an additive in the presence of nanoclay: Mechanical properties, flame retardants, and dielectric properties. Journal of Chemistry, **2020**, 1-11, (2020). https://doi.org/10.1155/2020/8854515

46. Nguyen T.A., Nguyen Q.T.: Study on the synergies of fly ash with multiwall carbon nanotube in manufacturing fire retardant epoxy nanocomposites. Journal of Chemistry, **2020**, 1-9 (2019). https://doi.org/101155/2020/6062128
47. Gohatre O.K., Biswal M., Mohanty S., Nayak S.K.: Effect of silane treated fly ash on physico-mechanical, morphological and thermal properties of recycled poly(vinyl choride) composites. Journal of Applied Polymer Science, **138,** 50387/1-50387/14 (2020). https://doi.org/10.1002/app.50387
48. Nguyen T.A., Nguyen Q.T., Nguyen X.C., Nguyen V.H.: Eco-friendly flame retardant additives for epoxy resin nanocomposites. EurAsian Journal of BioSciences, **13,** 323-332 (2019).
49. Sathishkumar G.K., Rajkumar G., Srinivasan K., Umapathy M.J.: Structural analysis and mechanical properties of lignite fly-ash-added jute-epoxy polymer matrix composite. Journal of Reinforced Plastics and Composites, **37**, 90-104, (2017). https://doi.org/10.1177/0731684417735183
50. Biswas B., Hazra B., Chakraborty S., Mukherjee N., Sinha A.: Mechanical behavior of cellulosic fiber-incorporated modified fly ash –dispersed polymeric composites. Journal of Process Mechanical Engineering, **235**, 2201-2208 (2021). https://doi.org/10.1177/09544089211034025
51. Thongsang S., Sombatsompop N.: Effect of NaOH and Si69 treatment on the properties of fly ash/natural rubber composites. Polymer Composites, **27**, 30-40 (2006). https://doi.org/10.1002/pc.20163
52. Paul K.T., Pabi S.K., Chakraborty K.K., Nando G.B.: Nanostructred fly ash-styrene butadiene rubber hybrid nanocomposites. Polymer Composites, **30**, 1647-1656 (2009). https://doi.org/10.1002/pc.20738
53. Maurya A.K., Gogoi R., Manik G.: Mechano-chemically activated fly-ash and sisal fiber reinforced PP hybrid composite with enhanced mechanical properties. Cellulose, **28**, 8493-8508 (2021). https://doi.org/10.1007/s10570-021-03995-4
54. Raghavendra G., Ojha S., Acharya S.K., Pal S.K.: A comparative analysis of woven jute/glass hybrid polymer composite with and without reinforcing of fly ash particles. Polymer Composites, **37**, 658-665 (2014). https://doi.org/10.1002/pc.23222

55. Bose S., Mahanwar P.A.: Effect of fly ash on the mechanical, thermal, dielectric, rheological and morphological properties of filled nylon 6. Journal of Minerals Materials Characterization and Engineering, **3**, 65-89 (2004). https://doi.org/10.4236/jmmce.2004.32007
56. Pardo S.G., Bernal C., Ares A., Abad M.J., Cano J.: Rheological, thermal, and mechanical characterization of fly ash thermoplastic composites with different coupling agents. Polymer Composites, **31**, 1722-1730 (2010). https://doi.org/10.1002/pc.20962
57. Chaowasakoo T., Sombatsompop N.: Mechanical and morphological properties of fly ash/epoxy composites using conventional thermal and microwave curing methods. Composites Science and Technology, **67**, 2282-2291 (2007). https://doi.org/10.1016/j.compscitech.2007.01.016
58. Gohatre O.K., Biswal M., Mohanty S., Nayak S.K.: Study on thermal, mechanical and morphological properties of recycled poly(vinyl chloride)/fly ash composites. Society of Chemical Industry, **69**, 552-563 (2020). https://doi.org/10.1002/pi.5988
59. Sharma A.K., Mahanwar P.A.: Effect of particle size of fly ash on recycled poly(ethylene terephthalate)/fly ash composites. International Journal of Plastic Technology, **14**, 53-64 (2010). https://doi.org/10.1007/s12588-010-00006-2
60. Kasar A.K., Gupta N., Rohatgi P.K., Menezes P.L.: A brief review of fly ash as reinforcement for composites with improved mechanical and tribological properties. JOM: The Journal of the Minerals, Metals and Materials Society, 72, 2340-2351 (2020). https://doi.org/10.1007/s11837-020-04170-z
61. Kumar J., Agrawal A., Mansoor F.: Effect of fly ash and particle size on mechanical properties of polyester-based composites. International Journal of Engineering Research in Current Trends, 3, 120-123 (2021).
62. Dharmalingam U., Dhanasekaran M., Balasubramnian K., Kandasamy R.: Surface treated fly ash filled modified epoxy composites. Polimeros, **25**, 540-546 (2015). https://doi.org/10.1590/0104-1428.2152
63. Joseph S., Bambola V.A., Sherhtukade V.V., Mahanwar P.A.: Effect of fly ash content, particle size of fly ash, and type of silane coupling agents on the properties of recycled poly(ethylene terephthalate)/fly ash composites. Journal of Applied Polymer Science, **119**, 201-208 (2011).

https://doi.org/101002/app.32449

64. Nguyen T.A.: Effect of the amount of fly ash modified by stearic acid compound on mechanical properties, flame retardant ability, and structure of the composites. International Journal of Chemical Engineering, **2020**, 1-6 (2020). https://doi.org/10.10.1155/2020/2079189
65. Li C.-C., Zheng L.-F., Sha X.-H., Chen P.: Microstructural and mechanical characteristics of graphene oxide-fly ash cenosphere hybrid reinforced epoxy resin composites. Journal of Applied Polymer Science, **138**, 47173/1-47173/8 (2018). https://doi.org/10.1002/app.47173
66. Chaturvedi A.K., Gupta M.K., Pappu A.: The role of carbon nanotubes on flexural strength and dielectric properties of water sustainable fly ash polymer nanocomposites. Physics B: Physics of Condensed Matter, **620**, 413283/1-413283/9 (2021). https://doi.org/10.1016/j.physb.2021.413283
67. Jayamani E., Rahman M.R., Benhur D.A., Bakri M.K.B., Kakar A., Khan A.: Comparative study on fly ash/sugarcane fiber reinforced polymer composites properties. BioResources, **15**, 5514-5531 (2020). https://doi.org/10.15376/biores.15.3,5514-5531
68. Kulkarni S.M., Kishore.: Effect of filler-fiber interactions on compressive strength of fly ash and short-fiber epoxy composites. Journal of Applied Polymer Science, **87**, 836-841 (2003). https://doi.org/10.1002/app.11501
69. Kavya H.M., Saravana B., Yogesha B., Sanjay M.R., Suchart S., Sergey G.: Effect of coir fiber and inorganic filler on physical and mechanical properties of epoxy based hybrid composites. Polymer Composites, **42**, 3911-3921 (2021). https://doi.org/10.1002/pc.26103
70. Kulkarni S., Kishore.: Effect of contact at the interface on the compressive properties of fly ash-epoxy composites. The Journal of Adhesion, **78,** 155-166 (2002). https://doi.org/10.1080/00218460210383
71. Srivastava V., Shembekar P.: Tensile and fracture properties of epoxy resin filled with flyash particles. Journal of Materials Science, **25,** 3513-3516 (1990). https://doi.org/10.1007/BF00575379

72. Dadkar N., Tomar B.S., Satapathy B.K.: Evaluation of flyash-filled and aramid fibre reinforced hybrid polymer matrix composites (PMC) for friction braking applications. Materials & Design, **30,** 4369-4376 (2009). https://doi.org/10.1016/j.matdes.2009.04.007
73. Purohit R, Sahu P, Rana RS, Parashar V, Sharma S.: Analysis of mechanical properties of fiber glass-epoxy-fly ash composites. Materials Today: Proceedings, **4,** 3102-3109 (2017). https://doi.org/10.1016/j.matpr.2017.02.193
74. Bekem, A., Birol B., Duygulu N.: Effect of Fly Ash Filler on Mechanical Performance of E-glass/Polyester Composites. In '19th International Metallurgy & Materials Congress'. Istanbul, Turkey, 700-702 (2018).
75. Prasetyo, B.D., Diharjo, K., Ariawan, D., Suharty, N.S. and Masykuri, M.: Flexural and inflammability properties of FA/CF/Phenolic hybrid composite. AIP Conference Proceedings, **2262,** 030006/1-030006/7 (2020). https://doi.org/10.1063/5.0021602
76. Rohatgi, P.K., Matsunaga T., Gupta N.: Compressive and ultrasonic properties of polyester/fly ash composites. Journal of materials science, **44,** 1485-1493 (2009). https://doi.org/10.1007/s10853-008-3165-1
77. Labella, M., Zeltmann, S.E., Shunmugasamy, V.C., Gupta, N. and Rohatgi, P.K.: Mechanical and thermal properties of fly ash/vinyl ester syntactic foams. Fuel, 121, 240-249 (2014). https://doi.org/10.1016/j.fuel.2013.12.038
78. Doddamani, M., Shunmugasamy, V.C., Gupta, N. and Vijayakumar, H.B.: Compressive and flexural properties of functionally graded fly ash cenosphere–epoxy resin syntactic foams. Polymer composites, **36,** 685-693 (2015). https://doi.org/10.1002/pc.22987
79. Kulkarni, S.: Studies on fly ash–filled epoxy-cast slabs under compression. Journal of applied polymer science, **84,** 2404-2410 (2002). https://doi.org/10.1002/app.10507
80. Goh, C.K., Valavan, S.E., Low, T.K., Tang, L.H.: Effects of different surface modification and contents on municipal solid waste incineration fly ash/epoxy composites. Waste management, **58,** 309-315 (2016). https://doi.org/10.1016/j.wasman.2016.05.027

81. Roviello, G., Ricciotti, L., Tarallo, O., Ferone, C., Colangelo, F., Roviello, V. and Cioffi, R.: Innovative fly ash geopolymer-epoxy composites: Preparation, microstructure and mechanical properties. Materials, **9**, 461/1-461/15 (2016). https://doi.org/10.3390/ma9060461
82. Raju, G.M., Madhu, G.M., Khan, M.A., Reddy, P.D.S.: Characterizing and modeling of mechanical properties of epoxy polymer composites reinforced with fly ash. Materials Today: Proceedings, **5,** 27998-28007 (2018). https://doi.org/10.1016/j.matpr.2018.10.040
83. Kim Y., Hwang S., Choi J., Lee J., Yu K., Baeck S-H., Shim S.E., Qian Y.: Valorization of fly ash as a harmless flame retardant via carbonation treatment for enhanced fire-proofing performance and mechanical properties of silicone composites. Journal of Hazardous Materials, **404**, 124202/1-124202/10 (2021). https://doi.org/10.1016/j.jhazmat.2020.124202
84. Rafieizonooz M., Mirza J., Salim M.R., Hussin M., Khankhaje E.: Investigation of coal bottom ash and fly ash in concrete as replacement for sand and cement. Construction and Building Materials, **116**, 15-24 (2016). https://doi.org/10.1016/j.conbuildmat.2016.04.080
85. Pei-Wei G., Lu X., Lin H., Li X., Hou J.: Effects of fly ash on the properties of environmentally friendly dam concrete. Fuel, **86**, 1208-1211 (2007) https://doi.org/10.1016/j.fuel.2006.09.032
86. Xu G., Shi X.: Exploratory investigation into a chemically activated fly ash binder for mortars. Journal of Materials in Civil Engineering, **29**, 06017018/1-06017018/12 (2017). https://doi.org/10.1061/(ASCE)MT.1943-5533.0002075
87. Al-Harahsheh M.S., Alzboon K.K., Al-Makhadmeh L., Hararah M., Mahasneh M.: Fly ash based geopolymer for heavy metal removal: A case study on copper removal. Journal of Environmental Chemical Engineering, **3**, 1669-1677 (2015). https://doi.org/10.1016/j.jece.2015.06.005
88. Zhou Q., Duan Y., Chen M., Liu M., Lu P., Zhao S.: Effect of flue gas component and ash composition on elemental mercury oxidation/adsorption by NH4Br modified fly ash. Chemical Engineering Journal, **345**, 578-585 (2018). https://doi.org/10.1016/j.cej.2018.02.033
89. Yildiz E., Phosphate removal from water by fly ash using crossflow microfiltration. Separation and Purification Technology, **35**, 241-252 (2004). https://doi.org/10.1016/S1383-5866(03)00145-X

90. Nemade P.D., Rao A.V., Alappat B.J.: Removal of fluorides from water using low cost adsorbents. Water Science and Technology: Water Supply, **2**, 311-317 (2002). https://doi.org/10.2166/ws.2002.0037
91. Darmayanti L., Notodarmodjo S., Damanhuri E.: Removal of Copper (II) Ions in Aqueous Solutions by Sorption onto Fly Ash. Journal of Engineering and Technological Sciences, **49**, 546-559 (2017). https://doi.org/10.5614/j.eng.technol.sci.2017.49.4.9
92. Malek N.N.A, Jawad A.H., Abdulhameed A.S., Ismail K., Hameed B.H.: New magnetic Schiff's base-chitosan-glyoxal/fly ash/Fe3O4 biocomposite for the removal of anionic azo dye: An optimized process. International journal of biological macromolecules, **146**, 530-539 (2020). https://doi.org/10.1016/j.ijbiomac.2020.01.020
93. Belviso C.: State-of-the-art applications of fly ash from coal and biomass: A focus on zeolite synthesis processes and issues. Progress in Energy and Combustion Science, **65**, 109-135 (2018). https://doi.org/10.1016/j.pecs.2017.10.004
94. Montes-Hernandez G., Pérez-Lopéz R., Renard F., Nieto J.M., Charlet L.: Mineral sequestration of CO2 by aqueous carbonation of coal combustion fly-ash. Journal of hazardous Materials, **161**, 1347-1354 (2009). https://doi.org/10.1016/j.jhazmat.2008.04.104
95. Chen H., Khalili N., Li J.: Development of stabilized Ca-based CO2 sorbents supported by fly ash. Chemical Engineering Journal, **345**, 312-319 (2018). https://doi.org/10.1016/j.cej.2018.03.162
96. Lu S.-Y., Hamerton I.: Recent developments in the chemistry of halogen-free flame retardant polymers. Progress in polymer science, **27**, 1661-1712 (2002). https://doi.org/10.1016/S0079-6700(02)00018-7
97. Jiao C., Wang H., Chen X.: Preparation of modified fly ash hollow glass microspheres using ionic liquids and its flame retardancy in thermoplastic polyurethane. Journal of Thermal Analysis and Calorimetry, **133**, 1471-1480 (2018). https://doi.org/10.1007/s10973-018-7190-2
98. Nguyen T.A., Nguyen Q.T., Nguyen X.C., Nguyen V.H.: Study on fire resistance ability and mechanical properties of composites based on Epikote 240 epoxy resin and thermoelectric fly ash: an ecofriendly additive. Journal of Chemistry, **2019**, 1-8 (2019).

https://doi.org/10.115/2019/2635231

99. Wang L., Wang C., Liu P., Jing Z., Ge X., Jiang Y.: The flame resistance properties of expandable polystyrene foams coated with a cheap and effective barrier layer. Construction and Building Materials, **176**, 403-414 (2018). https://10.1016/j.conbuildmat.2018.05.023

100. Tarakcılar A.R.: The effects of intumescent flame retardant including ammonium polyphosphate/pentaerythritol and fly ash fillers on the physicomechanical properties of rigid polyurethane foams. Journal of Applied Polymer Science, **120**, 2095-2102 (2011). https://doi.org/10.1002/app.33377

101. Surtiyeni N., Rahmadani R., Kurniasih N., Kairurrijal K., Abdullah M.: A fire-retardant composite made from domestic waste and PVA. Advances in Materials Science and Engineering, **2016**, 1-10 (2016). https://10.10.1155/2016/7516278

102. Soyam, M., Inoue K., Iji M.: Flame retardancy of polycarbonate enhanced by adding fly ash. Polymers for Advanced Technologies, **18**, 386-391 (2007). https://doi.org/10.1002/pat.900

103. Mishra S., Sonawane S., Badgujar N., Gurav K., Patil D.: Comparative study of the mechanical and flame-retarding properties of polybutadiene rubber filled with nanoparticles and fly ash. Journal of applied polymer science, **96**, 6-9 (2005). https://10.1002/app.21114

104. Mishra S., Shimpi N.: Studies on mechanical, thermal, and flame retarding properties of polybutadiene rubber (PBR) nanocomposites. Polymer-Plastics Technology and Engineering, **47**, 72-81 (2007). https://doi.org/10.1080/03602550701580987

105. Mishra S., Patil U., Shimpi N.: Synthesis of mineral nanofiller using solution spray method and its influence on mechanical and thermal properties of EPDM nanocomposites. Polymer-Plastics Technology and Engineering, **48**, 1078-1083 (2009). https://doi.org/10.1080/03602550903092492

106. Usta N.: Investigation of fire behavior of rigid polyurethane foams containing fly ash and intumescent flame retardant by using a cone calorimeter. Journal of Applied Polymer Science, **124**, 3372-3382 (2012). https://doi.org/10.1002/app.35352

107. Ajorloo M., Ghodrat M., Kang W.-H.: Incorporation of recycled polypropylene and fly ash in polypropylene-based composites for automotive applications. Journal of Polymers and the Environment, **29**, 1298-1309 (2021). https://doi.org/10.1007/s10924-020-01961-y

108. Miricioiu M.G., Niculescu V.-C., Filote C., Raboaca S., Nechifor G.: Coal Fly Ash Derived Silica Nanomaterial for MMMs—Application in CO2/CH4 Separation. Membranes, **11**, 78/1-78/18 (2021). https://10.3390/membranes11020078

109. Zhou J., Xia K., Fang L., Du H., Zhang X.: Utilization of cationic polymer-modified fly ash for dye wastewater treatment. Clean Technologies and Environmental Policy, **23**, 1273-1282 (2021). https://10.1007/s10098-020-02019-2

110. Dadkar N., Tomar B.S., Satapathy B.K.: Evaluation of fly ash-filled and aramid fibre reinforced hybrid polymer matrix composites (PMC) for friction braking applications. Materials and Design, **30**, 4369-4376 (2009). https://doi.org/10.1016/j.matdes.2009.04.007

111. Sivasubramanian G., Krishnan H., Paradesi D., Jeyalakshmi R.: High-performance SPEEK/SWCNT/fly ash polymer electrolyte nanocomposite membranes for fuel cell applications. Polymer Journal, **49**, 703-709 (2017). https://10.1038.p.j.2017.38

112. Abd Malek, N.N., Jawad, A.H., Ismail, K., Razuan, R., ALOthman, Z.A.: Fly ash modified magnetic chitosan-polyvinyl alcohol blend for reactive orange 16 dye removal: Adsorption parametric optimization. International Journal of Biological Macromolecules, **189**, 464-476 (2021). https://doi.org/10.1016/j.ijbiomac.2021.08.160

113. Punniakotti G., Sivasubramanian G., Thangavelu S.A.G., Deivanayagam P.: Sulfonated Poly (Vinyl Alcohol)/Fly Ash Composite Membranes for Polymer Electrolyte Membrane Fuel Cell Applications. Polymer-Plastics Technology and Materials, **60**, 571-578 (2021). https://doi.org/10.1080/25740881.2020.1850782

114. Saafi M., Tang L., Fung J., Rahman M., Sillars F., Liggat J., Zhou X.: Graphene/fly ash geopolymeric composites as self-sensing structural materials. Smart materials and structures, **23**, 065006/1-0650061/11 (2014). https://doi.org/10.1088/0964-1726/23/6/065006

115. Hekimoğlu G., Sarı A.: Fly Ash/Octadecane Shape-Stabilized Composite PCMs Doped with Carbon-Based Nanoadditives for Thermal Regulation Applications. Energy and Fuels, **35**, 1786-1795 (2021). https://doi.org/10.1021/acs.energyfuels.0c03369

116. Zhang J., Pan G., Zheng X., Chen C.: Preparation and characterization of ultra-lightweight fly ash-based cement foams incorporating ethylene-vinyl acetate emulsion and waste-derived C-S-H seeds. Construction and Building Materials, **274**, 122027/1-122027/11 (2021). https://doi.org/10.1016/j.conbuildmat.2020.122027

117. Schubert, D.M. 2019. Hydrated zinc borates and their industrial use. *Molecules*, 24(13), p.2419.

118. Shen, K.K., Kochesfahani, S., & Jouffret, F. 2008. Zinc borates as multifunctional polymer additives. *Polymers for Advanced Technologies*, 19(6), pp.469-474.

119. Lehmann, H.A., Sperschneider, K., & Kessler, G., 1967. Zur Chemie und Konstitution borsaurer Salze. XVIII. *Über wasserhaltige Zinkborate. Zeitschrift für anorganische und allgemeine Chemie*, 354(1-2), pp.37-43.

120. Nies, N.P., & Hulbert, R.W., United States Borax and Chemical Corp, 1970. Zinc borate of low hydration and method for preparing same. *U.S. Patent* 3,549,316.

121. Tascioglu, C., Yoshimura, T., & Tsunoda, K. 2013. Biological performance of wood–plastic composites containing zinc borate: Laboratory and 3-year field test results. *Composites Part B: Engineering*, 51, pp.185-190.

122. Chan-Hom, T., Yamsaengsung, W., Prapagdee, B., Markpin, T,.& Sombatsompop, N. 2017. Flame retardancy, antifungal efficacies, and physical–mechanical properties for wood/polymer composites containing zinc borate. *Fire and Materials*, 41(6), pp.675-687.

123. Baltaci, B., Çakal, G.Ö., Bayram, G., Eroglu, I., & Özkar, S. (2013). Surfactant modified zinc borate synthesis and its effect on the properties of PET. *Powder technology*, 244, pp.38-44.

124. Feng, C., Zhang, Y., Liang, D., Liu, S., Chi, Z., & Xu, J. 2015. Influence of zinc borate on the flame retardancy and thermal stability of intumescent flame retardant polypropylene composites. *Journal of Analytical and Applied Pyrolysis*, 115, pp.224-232.

125. Gao, Y., Wang, Q., & Lin, W., 2018. Ammonium polyphosphate intercalated layered double hydroxide and zinc borate as highly efficient flame retardant nanofillers for polypropylene. *Polymers*, 10(10), p.1114.

126. Wu, Z., Shu, W., & Hu, Y. 2007. Synergist flame retarding effect of ultrafine zinc borate on LDPE/IFR system. *Journal of Applied Polymer Science*, 103(6), pp.3667-3674.

127. Fang, Y., Wang, Q., Guo, C., Song, Y., & Cooper, P.A. 2013. Effect of zinc borate and wood flour on thermal degradation and fire retardancy of polyvinyl chloride (PVC) composites. *Journal of Analytical and Applied Pyrolysis*, 100, pp.230-236.

128. Jiang, M., Zhang, Y., Yu, Y., Zhang, Q., Huang, B., Chen, Z., Chen, T., & Jiang, J. 2019. Flame retardancy of unsaturated polyester composites with modified ammonium polyphosphate, montmorillonite, and zinc borate. *Journal of applied polymer science*, 136(11), p.47180.

129. Khalili, P., Liu, X., Tshai, K.Y., Rudd, C., & Yi, X. 2019. Development of fire retardancy of natural fiber composite encouraged by a synergy between zinc borate and ammonium polyphosphate. *Composites Part B: Engineering*, 159, pp.165-172.

130. Ramazani, S.A., Rahimi, A., Frounchi, M., & Radman, S., 2008. Investigation of flame retardancy and physical–mechanical properties of zinc borate and aluminum hydroxide propylene composites. *Materials & Design*, 29(5), pp.1051-1056.

131. Wang, L., He, X., Lu, H., Feng, J., Xie, X., Su, S., & Wilkie, C.A. 2011. Flame retardancy of polypropylene (nano) composites containing LDH and zinc borate. *Polymers for advanced technologies*, 22(7), pp.1131-1138.

Chapter 3: Experimental section

3.1 Materials

3.1.1 Polybutylene succinate (PBS)

Polybutylene succinate (PBS) was supplied in pellet form by 2 MBIO- Engineering Polymers, India. It has an MFI of 190℃ 2.16kg/10min.), heat combustion of 23.6 KJ/g, melting temperature of 90 ~ 120℃, and a density of 1.25 g/cm^3.

3.1.2 Fly ash (FA)

Fly ash (FA) was obtained from a coal producing power station in Mpumalanga, South Africa.

3.1.3 Zinc Borate (ZnB)

Zinc Borate (ZnB) was supplied in powder form by Sigma-Aldrich, South Africa. It is a technical light inorganic filler containing ≥ 45% ZnO basis, and ≥36% B2O3 basis.

3.14 Trimethoxymethylsilane

Trimethoxymethylsilane was supplied in liquid form by Sigma-Aldrich, South Africa. It was used to treat fly ash and has a molecular weight of 136.22 g/mol, a boiling point of 102 - 104℃ (lit), a freezing point of 16℃ and a density of 0.955 g/mL at 25℃ (lit). It has a chemical formula of $C_4H_{12}O_3Si$.

3.2 Methods

3.2.2 Treatment of fly ash

Fly ash was chemically treated using trimethoxymethylsilane. The treatment was followed by dissolving 100g of fly ash in 0.2 ml of trimethoxymethylsilane and 100 ml of ethanol. The solution was mixed by hand for 5 minutes, and mechanically stirred for another 5 minutes. A

vacuum pump was used to remove some of the moisture from the slurry. The slurry was further dried at 50℃ for 12 hours in a vacuum oven.

3.2.2 Preparation of PBS/Fly ash composites

Before preparation, PBS and fly ash were dried at 40 °C in a vacuum oven for a period of 48 hours. To prepare the polymer composites, PBS and fly ash were physically mixed in a beaker, and then the mixture was extruded using a co-rotating twin-screw extruder with an L/D ratio of 40 (L=720 mm). The extruder was operated at various temperature profile set at 135, 140, 145, 150, 155 °C (i.e., for different zones from hopper to die). **Figure 3.1** illustrates the type of extruder utilized in this study.

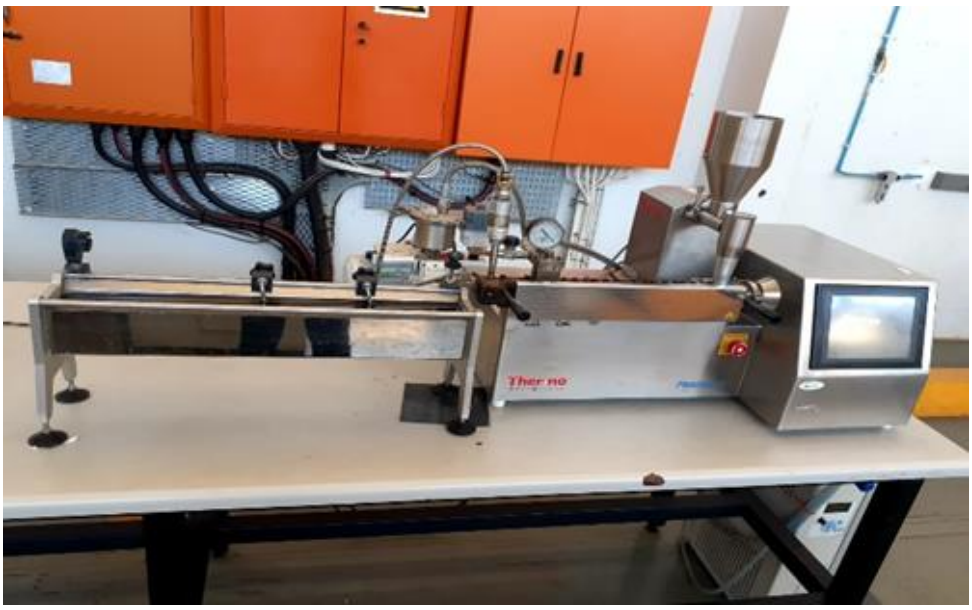

Figure 3.1 A co-rotating twin-screw extruder used for fabrication of PBS/fly ash composites

The samples were cooled in an ice-bath immediately after each processing, and then dried in an oven for 24 hours. In order to characterize various properties for different techniques, the samples were compressed molded at 155 °C at the pressure of 20 MPa under nitrogen atmosphere. Table 3.1 shows the sample ratios of all the investigated samples.

Table 3.1: A summary of all the investigated samples in this study

Polymer composite	**Sample ratios**
PBS	100
PBS/Fly ash	99/1
PBS/Fly ash	97/3
PBS/Fly ash	95/5
PBS/Fly ash_silane	99/1
PBS/Fly ash_silane	97/3
PBS/Fly ash_silane	95/5
PBS/Zinc Borate	97/3
PBS/Zinc Borate	99/1
PBS/Fly ash/Zinc Borate	96/1/3
PBS/Fly ash/Zinc Borate	94/3/3
PBS/Fly ash/Zinc Borate	92/5/3
PBS/Fly ash_silane/Zinc Borate	96/1/3
PBS/Fly ash_silane/Zinc Borate	94/3/3
PBS/Fly ash_silane/Zinc Borate	92/5/3

3.3 Characterization and sample analysis

3.3.1 Scanning electron microscopy (SEM)

Scanning electron microscopy (SEM) is an intricate technique with various strands that have grown over the last 8 decades. In SEM, the electron beam is concentrated on a single point and scanned through the material in a sequence. Signals are released by the specimen and captured by detectors at each place. The location of the beam and the detector signal operate in sync to modulate the image pixel [1]. Typical electron energies may reach 40 keV [2]. In addition,

signals obtained from the specimen when analysing SEM are scattered primary electrons, X-rays and SEs [1]. The majority of commercially available SEMs are equipped with an energy-dispersive spectrometer (EDS) system and the current software for data analysis. The EDS provides the benefit of using a computer software to evaluate the composition of various elements in a sample; thus, speeding up the entire process by converting the x-ray intensity ratio to chemical compositions in a matter of seconds as well as improving quantitative analysis performance [3]. To determine the morphology of the fractured surfaces in this study, a Shimadzu ZU SSX550 Superscan scanning electron microscopy was used, and the analysis was done at room temperature. The samples were fractured by freezing them in liquid nitrogen, and simply breaking the specimen into appropriate size to fit the specimen chamber. The fractured samples were gold coated by sputtering to produce conductive coatings onto the samples. The fracturing of samples by liquid nitrogen was done only Fly/PBS composites, however since neat fly ash was in powder form there was no need for fracturing, but the samples were gold coated by sputtering before recording the SEM micrographs.

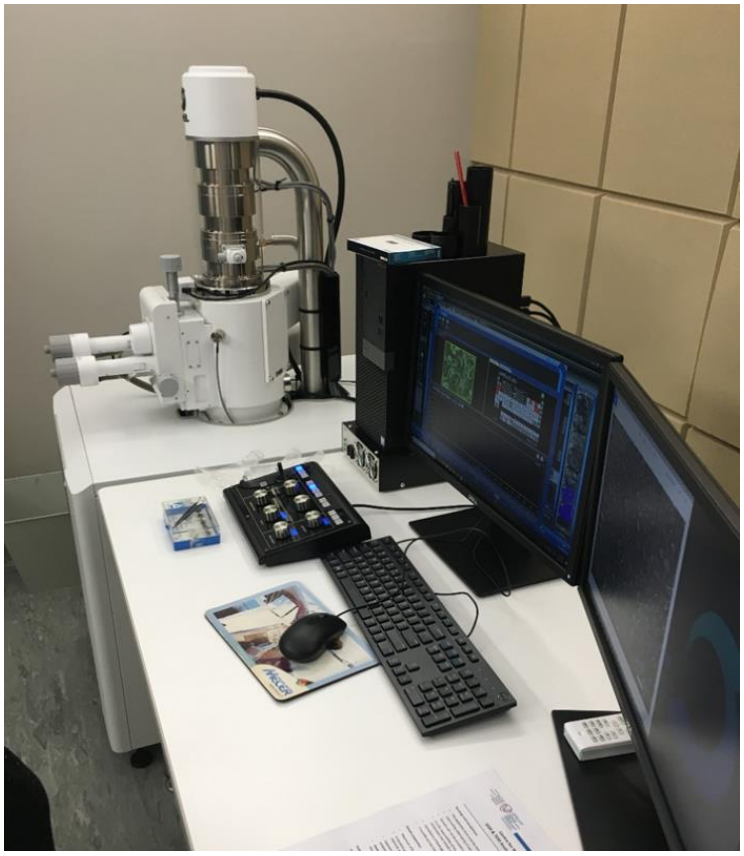

Figure 3.2 Scanning electron microscopy employed in this study to investigate the surface morphology.

3.3.2 X-ray diffraction (XRD)

X-rays are high-energy electromagnetic waves with a wavelength ranging from 10^{-3} to 10^{1} nm. They are typically synthesized by utilizing synchrotron radiation, seal tubes, or rotating anodes. The incident electrons cause two “effects” that lead to the creation of X-rays, and the first is electron deceleration, which causes the emission of X-ray photons with a broad continuous wavelength distribution, commonly known as Bremsstrahlung. The second ‘effect’ involves ejecting electrons from the inner shells of the impinged atoms, thus resulting in ionization [4]. Various interactions occur when X-ray photons reach the specimen such as scattering or absorption. X-ray diffraction involves constructive or destructive scattering X-ray photons. The constructive interference of a monochromatic beam of X-rays dispersed at certain angles from each pair of lattice planes in a sample produces X-ray diffraction peaks. The distribution of atoms within the lattice determines the peak intensities. The technique of X-ray diffraction (XRD) is a strong tool for the characterization of crystalline materials. It contains data on structures, phases, preferred crystal orientations (texture), and other structural factors like average grain size, crystallinity, strain, and crystal defects [5].

Figure 3.3 X-ray diffraction analysis utilized in this study.

3.3.3 Thermogravimetric analysis (TGA)

Thermogravimetric analysis is a useful for determining how much a sample's mass changes over time when it is subjected to a temperature program. TGA is primarily used to assess the breakdown and thermal stability of materials under a variety of settings as well as to investigate the kinetics of physico-chemical processes in the sample [6]. The TGA analyses in this study were carried out in a Perkin Elmer TGA7 thermogravimetric analyzer. Samples ranging between 5 and 10 mg were heated from 30 to 600 °C at a heating rate of 10 °C min^{-1} under nitrogen (flow rate 20 mL min^{-1}). TGA is mainly used to characterize the decomposition and thermal stability of materials.

Figure 3.4 TGA technique used for investigating the thermal stability of all investigated samples

3.3.4 Underwriters Laboratories test standard (UL 94)

The UL94 vertical burning test for industrial polymeric materials and products is a frequently used fire test. To perform this test, a Bunsen flame is applied to a small-size specimen, and the flame is removed after 10 seconds. The specimen is given time to extinguish the flame, thereafter, the Bunsen flame is applied for an additional 10 seconds [8]. The UL-rating is based on 3 concepts, i.e. (i) how long the specimen takes to self-extinguish, (ii) whether the specimen

drips, and (iii) whether the dripping ignites the cotton placed under the test specimen. In order for a sample specimen to be regarded as flame-retardant, it has to obtain a UL-rating of V0. This means that the sample does the following: (i) self-extinguishes within 10 seconds, (ii) exhibits no flaming drips and (iii) flaming drips do not ignite the cotton placed under the sample specimen. The vertical burning test (UL-94) was utilized through the Bunsen burner method according to the ASTM D 3801 testing procedure with the dimensions of 120 mm x 13mm x 3 mm.

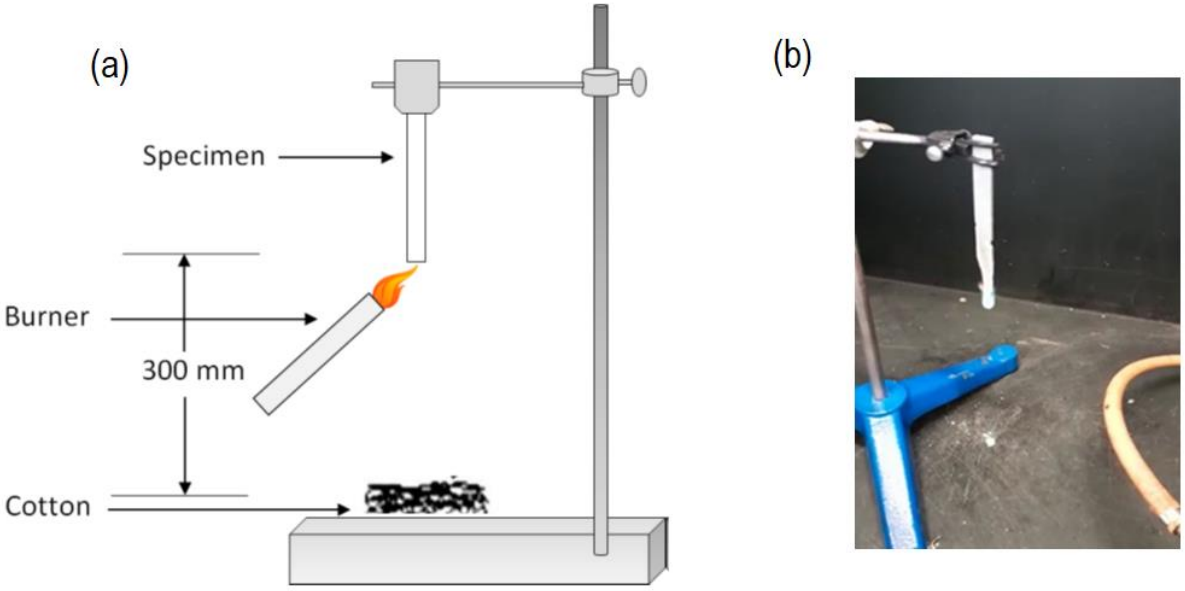

Figure 3.5 (a) A diagram illustrating a vertical burning setup [R], and (b) an example of sample used in this study for UL-94.

3.3.5 Fourier-transform infrared (FTIR) spectroscopy

FTIR involves infrared radiation is being transmitted through a sample. The sample absorbs some of the IR radiation and some of it passes through. The resulting spectrum depicts the sample's molecular absorption and transmission, thus resulting in a molecular fingerprint. IR spectroscopy reveals a qualitative analysis of a how much material is present in a sample through peaks in the spectrum [9]. Perkin Elmer Spectrum 100 infrared spectrometer was utilized for analysis the samples on FTIR. These samples were analysed by attenuated (ATR) detector over 400-4000 cm $^{-1}$ wavenumber range with a resolution of 4 cm $^{-1}$.

3.3.6 Rheology

Rheology involves the study of the flow of matter and deformation. The concept of a complex modulus and a phase angle are used to elaborate on the viscoelastic properties of a material. The complex modulus depicts the behaviour of a material under dynamic loading at a particular strain level. The phase angle is the time difference between the elastic (storage) modulus and viscous (loss) modulus responses [10]. Additionally, effective dispersion of particles can be influenced by flow conditions (viscosity). Rheological properties of a material likewise aids in assessing the state of dispersion of a filler in a polymer composite [11]. The rheological measurements were done at 190 °C under atmospheric conditions.

Figure 3.6 The equipment that was utilized to determine the dynamic rheological measurements.

3.3.7 Water absorption

Water absorption test are done to determine the amount of water that can be absorbed by a polymer over time. The tests are done in accordance with ASTM D570-81 test standard whereby samples are dried and weighed prior to immersion in distilled water at room temperature or 23°C. Afterward, the samples are removed from the water to be weighed at

intervals of 14 hours. The weights of the samples are recorded and the following formula is used to calculate the water absorption [12]:

Water absorption (W_a) %= $\frac{Wwet-Wdry}{Wdry}$ X 100

Where W_a is the % of water absorbed, W_{wet} is the weight of the sample after immersion and W_{dry} is the weight prior to immersion.

3.4 References

1. Inkson, B.J. 2016. Scanning electron microscopy (SEM) and transmission electron microscopy (TEM) for materials characterization. In *Materials characterization using nondestructive evaluation (NDE) methods* (pp. 17-43). Woodhead Publishing.
2. Bogner, A., Jouneau, P.H., Thollet, G., Basset, D., & Gauthier, C. 2007. A history of scanning electron microscopy developments: Towards "wet-STEM" imaging. *Micron*, 38(4), pp.390-401.
3. Mohammed, A., & Abdullah, A., 2018, November. Scanning electron microscopy (SEM): A review. In *Proceedings of the 2018 International Conference on Hydraulics and Pneumatics—HERVEX, Băile Govora, Romania* (pp. 7-9).
4. Epp, J. 2016. X-ray diffraction (XRD) techniques for materials characterization. In *Materials characterization using nondestructive evaluation (NDE) methods* (pp. 81-124). Woodhead Publishing.
5. Bunaciu, A.A., UdriŞTioiu, E.G., & Aboul-Enein, H.Y. 2015. X-ray diffraction: instrumentation and applications. *Critical reviews in analytical chemistry*, 45(4), pp.289-299.
6. Bottom, R. 2008. Thermogravimetric analysis. *Principles and applications of thermal analysis*, 1, pp.87-118.
7. McKenna, G.B., & Simon, S.L., 2002. The glass transition: Its measurement and underlying physics. *Handbook of thermal analysis and calorimetry*, 3, pp.49-109.
8. Wang, Y., Zhang, F., Chen, X., Jin, Y., & Zhang, J. 2010. Burning and dripping behaviours of polymers under the UL94 vertical burning test conditions. *Fire and Materials: An International Journal*, 34(4), pp.203-215.
9. Dutta, A. 2017. Fourier transform infrared spectroscopy. *Spectroscopic methods for nanomaterials characterization*, pp.73-93.
10. Widyatmoko I. Sustainability of bituminous materials, Editor(s): Jamal M. Khatib, In *Woodhead Publishing Series in Civil and Structural Engineering, Sustainability of Construction Materials* (Second Edition), Woodhead Publishing, 2016, Pages 343-370.
11. Abraham, J., Sharika, T., Mishra, R.K.,& Thomas, S. 2017. Rheological characteristics of nanomaterials and nanocomposites. In *Micro and nano fibrillar composites (MFCs and NFCs) from polymer blends* (pp. 327-350). Woodhead Publishing.

12. Gohatre, O.K., Biswal, M., Mohanty, S., & Nayak, S.K., 2021. Effect of silane treated fly ash on physico-mechanical, morphological, and thermal properties of recycled poly (vinyl chloride) composites. *Journal of Applied Polymer Science*, 138(19), p.50387.

Chapter 4: Results and discussion

4.1 Scanning electron microscopy (SEM)

Figures 4.1(a) and (b) show the SEM images of the untreated fly ash particles (5%) and silane-treated fly ash particles (5%) incorporated in the PBS matrix, respectively. In this study, 2% of silane was utilized to modify the fly ash nanoparticles. It is observed in **Figure 4.1 (a)** that the fly ash nanoparticles show agglomerated and irregular spherical shapes within the PBS matrix. The average particle size of the untreated fly ash was estimated to be 37.9 µm. The fact that there are agglomerations of fly ash within the biopolymer matrix (Figure Symbol A) is an indication of poor adhesion between the fly ash and the PBS polymer matrix. It is well known that in order to obtain a better interfacial interaction between different materials blended or mixed together, must have similar properties (i.e., hydrophilic fillers and hydrophilic matrices or hydrophobic fillers and hydrophobic matrices) [1-3]. In our case, there is a hydrophilic filler and hydrophobic matrix; as a result, there is a poor interfacial interaction between the two phases. A careful inspection of the image in **Figure 4.1(a)** shows that the fly ash nanoparticles are slightly embedded within the polymer matrix. Furthermore, within the same system it seems as if the polymer matrix loses its holding capacity in other cases, which allows the fly ash to isolate itself within the matrix with little interaction between the two phases. As much as there is an isolation between the two phases, there is an embedding of the fly ash filler within the polymer matrix is more dominant.

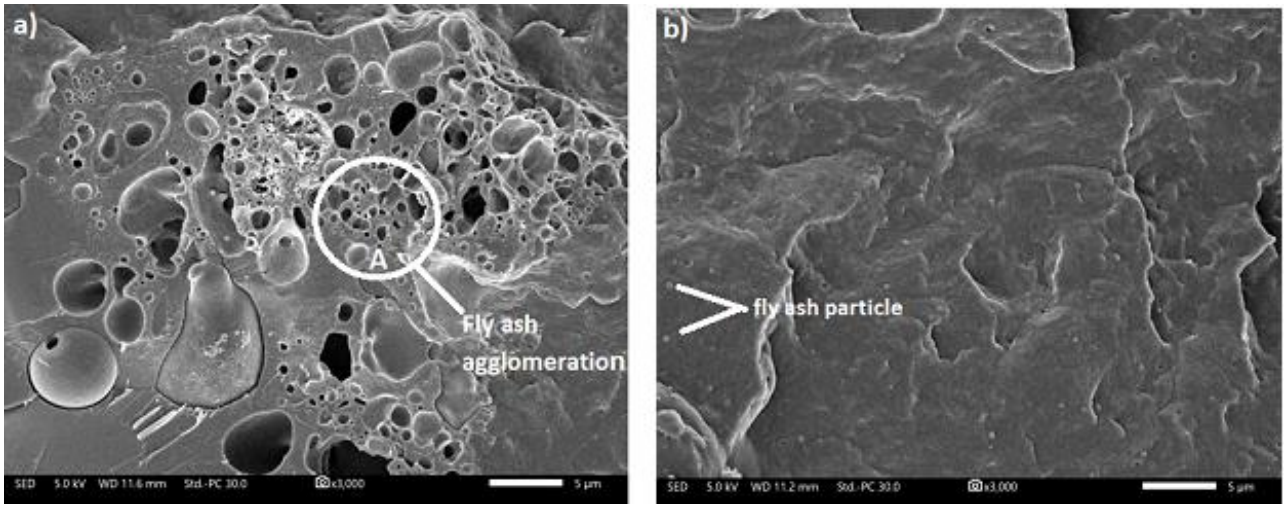

Figure 4.1 SEM micrographs of 95/5: (a) untreated PBS/fly ash composite, and (b) silane-treated PBS/fly ash composite

Figure 4.2 (b) reveals that the fly ash particles were uniformly dispersed within the polymer matrix with an average particle size of 0.8 µm. This is attributed to the effect of silane treatment, which allows the fly ash particles to sufficiently interact with the polymer matrix. Comparing the average particle sizes of the untreated and treated fly ash, it clear that the silane-treated fly ash appears to have smaller size with less agglomerates. Sim *et al*.[4] have also reported that composites with smaller particle sizes of fly ash revealed better mechanical properties due to better particle dispersion in the matrix. Ares *et al* [5] who studied the effect of aminomethoxy silane on fly ash-filled polypropylene composites also observed that the introduction of silane modified the surface and reduced the size of fly ash particles, and thereby improving particle flow and subsequently leading to a uniform dispersion of particles and lessening the chances of agglomeration. **Figures 4.2 (a) and (b)** show the SEM images of untreated fly and silane-treated fly ash at 1% of the filler reinforced PBS matrix. The untreated fly ash particles at 1% seems to be uniformly dispersed in the biopolymer matrix **(Figure 4.2(a)),** especially when compared with the 5% fly ash composite **(Figure 4.1(a)).** This may be attributed to the low filler content as opposed to the higher filler content. **Figure 4.2 (b)** shows silane-treated fly ash at 1% within a PBS polymer matrix. The image shows no clear visibility of fly ash particle in the matrix. This indicates that the fly ash is completely covered with silane and incorporated within the polymer matrix. It is known that the surface treatment (silane) of a filler (in this case fly ash) acts at the interface between an organic and inorganic substrate leading to enhanced interfacial interaction, and improved morphological behaviour.

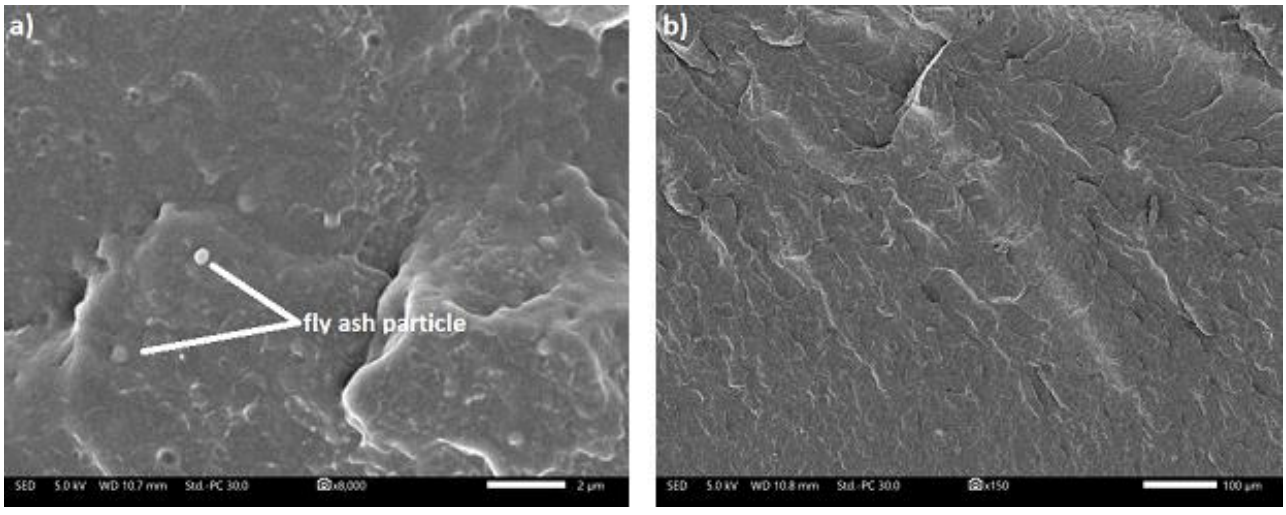

Figure 4.2 SEM micrographs of 99/1: (a) untreated PBS/fly ash composite, and (b) silane-treated PBS/fly ash composite

Figures 4.3 (a) and (b) show the SEM images of the 96/1/3 PBS/fly ash/zinc borate and (b) 92/5/3 PBS/fly ash/zinc borate. There is a clear agglomeration of the zinc borate (3%) (symbol A and B) in

the presence of the 1% of fly ash in the PBS matrix. There seems to be less interaction between the inorganic fillers at lower fly ash nanoparticles and high zinc borate content (3%). There seems to be a better interaction between the inorganic fillers at high content of fly ash (5%) however; the particles interacted better at this content of fly ash with fewer agglomerates Figure 4.3 (symbol C and D).

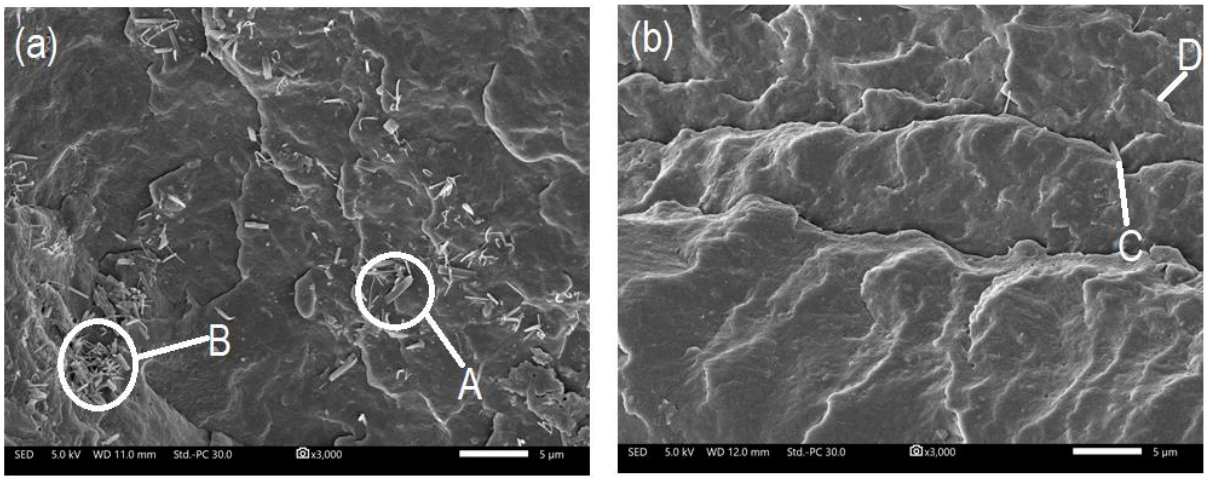

Figure 4.3 SEM images of (a) 96/1/3 PBS/fly ash/zinc borate, and (b) 92/5/3 PBS/fly ash/zinc borate

Figures 4.4(a) and (b) reveal the EDS graphs of the 99/1: (a) untreated PBS/fly ash composite, and (b) silane-treated PBS/fly ash composite. Generally, the fly ash consists of SiO_2 (52.3%), Al_2O_3 (27.4%), K_2O (4.1%), Fe_2O_3 (7.9%), CaO (2.9%), MgO (1.4%), and TiO_2 (1.4%) [6]. Meanwhile, our fly ash belongs to the silicate type of fly ash due to a large amount of SiO_2 (Figure 4.4), and according to the ASTM C 618, it is classified as group F type of fly ash. The presence of silane resulted in higher peaks of silica observed in **Figure 4.4 (b)**. This may be attributed to the direct interaction between the fly ash and silane –Si-OH groups of silica thereby forming –Si-O-Si- bonds. Typical silane coupling agents exhibit a chemical structure of R-Si-(R^1X), where R is alkoxy and X is an organofunctional component both linked to a silicon atom [7]. Therefore, the result of silane treatment on class F fly ash is high levels of silica as seen in **Figure 4.4 (b)** which is one of the reasons why trimethoxysilane was preferred as a method of treatment.

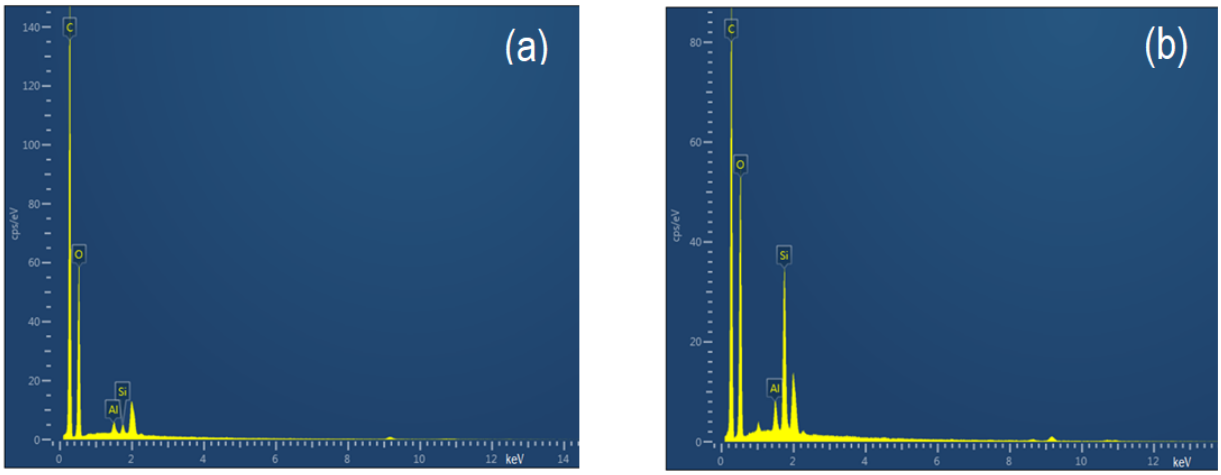

Figure 4.4 EDS graphs of the 99/1: (a) untreated PBS/fly ash composite, and (b) silane-treated PBS/fly ash composite

In summary, one can realize that the addition of 1% of fly ash dispersed better in the PBS matrix when compared with 5% of fly ash. The dispersion was further enhanced in the presence of silane. Furthermore, it is very interesting to observe that there seems to be an interaction some extent between fly ash and ZB at 5% with no interaction at all at 1% fly ash. This enhanced interaction between fly ash and ZB does not necessarily guarantee a better improvement in the properties. One realized that the improvement in results was composition dependent in the overall study.

4.2 Fourier transform infrared (FTIR)

Figure 4.5 depicts the FTIR spectrum of the unmodified fly ash and silane treated fly ash. **Figure 4.5 (b)** is the enlargement of **Figure 4.5(a)**, to provide more visibility in the major peaks. **Figure 4.5 (a)** indicates a clear asymmetric stretching vibration as well as asymmetric vibrations at 1033 and 865 cm^{-1}, respectively. Similar peaks were reported by Gohatre et al [3], with the asymmetric stretching vibration and asymmetric vibrations being reported at 1068 and 772 cm^{-1}. The absorption peak at 2900-3000 cm^{-1} is associated with the Si-O-Si, CH_2, and Si-O (**see Figure 4.5 (b)**). The broad peak at 3404 (**Figure 4.5 (b)**) is attributed to the OH groups associated with water molecules. This peak suggests that there is an amorphous silicate material or probably hydrated aluminum silicates [8]. This observation is well supported by the EDS spectra, whereby the dominating elements in this fly ash are aluminum and silica, as a result the type of fly ash herein is class F. One can realize that there is a high affinity between the fly ash and silane as a modifier due to a common functional group (i.e., Si-O-Si), as a result

most of the functional groups of the modifier interacted with the fly ash. The SEM in section 4.1 however proved that there a high affinity between the filler in the form of fly ash and modifier (*viz.* silane), with better dispersion of the fly ash and lower particle size observed for modified fly ash.

Figure 4.6 (a) depicts the peak intensities for neat PBS compared to PBS/fly ash composites at 95/5. PBS reveal a peak at 945 cm^{-1} which is attributed to the -C-OH bending in the carboxylic group of PBS. The bands in the range 1050-1064 were ascribed to the O-C-C- stretching vibrations within PBS matrix. The peaks around 1330 and 2925 cm^{-1} are assigned to the symmetric and asymmetric deformational vibrations of $-CH_2-$, respectively. It can be seen that the addition of fly ash at 5% resulted in lower intensities at 1750 cm^{-1} and between 1000 cm^{-1} and 1250 cm^{-1}. This may be associated with the structural changes within the composites. All the peaks for fly ash and ZB seems not to be visible in the PBS composites FTIR spectra (Figure 4.6 (a-c)), with the dominating peaks being the one for PBS. There is no clear explanation for such a behaviour.

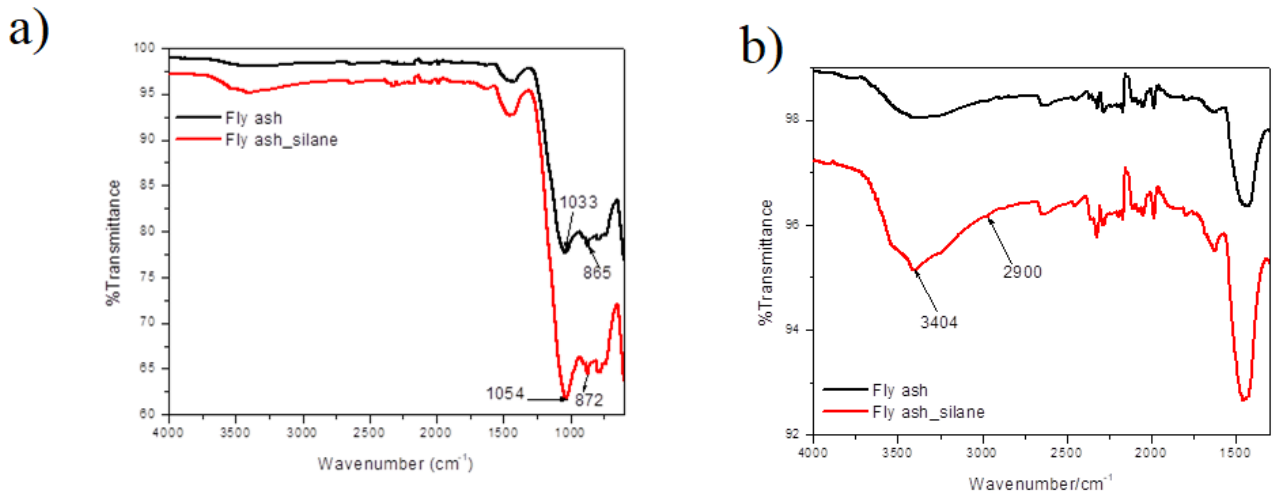

Figure 4.5 FTIR spectra of: (a) Fly ash and modified fly ash (in the range of 500-4000 cm^{-1}), and (b) Fly ash and modified fly ash (in the range of 1500-4000 cm^{-1}**)**

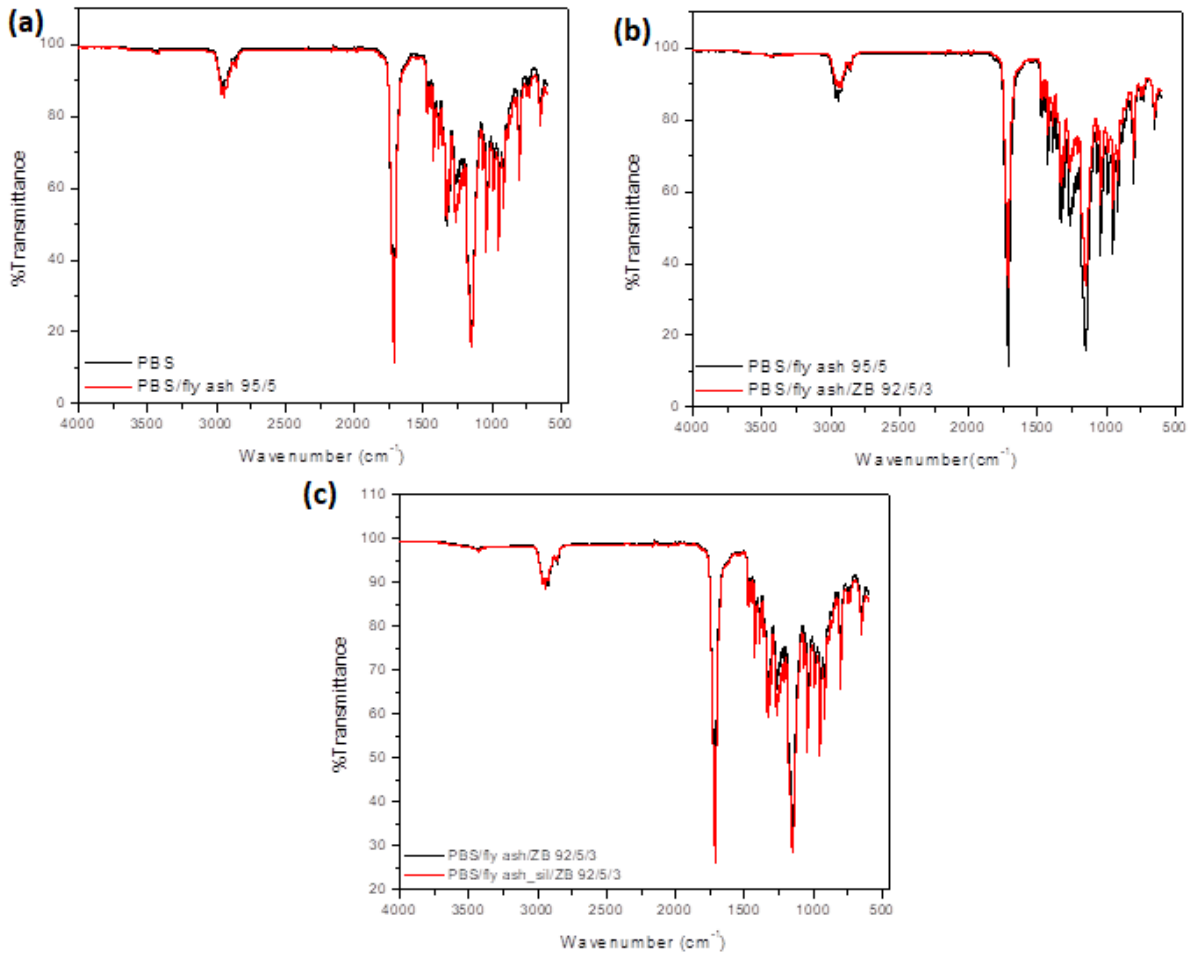

Figure 4.6 FTIR spectra of: (a) Neat PBS and PBS/fly ash 95/5 (in the range of 500-4000 cm-^{1}), (b) PBS/fly ash 95/5 and PBS/fly ash/ ZB 92/5/3 (in the range of 500-4000 cm^{-1}), and PBS/fly ash/ZB 92/5/3 and PBS/fly ash_silane/ZB 92/5/3 (in the range 500-4000 cm^{-1})

4.3. Thermogravimetric analysis (TGA)

Figure 4.7 depicts the TGA graphs of PBS, PBS/FA and PBS/ZB composites. It is observed in **Figure 4.7** and Table 4.1 that the thermal stability of PBS/FA (97/3), PBS/FA (95/5) and PBS/ZB (97/3) is low than the thermal stability of neat PBS. This may be attributed to the agglomeration of FA particles in the PBS matrix as seen in **Figure 4.1 (a)** of SEM analysis at a fly ash content of higher than 1%. Due to the agglomeration and poor particle dispersion at 3 and 5 wt%, there is an ease of access of heat into the system thus decreasing the thermal stability. This is an indication that at 3 and 5% of FA, there is a formation poor char, which is inhomogeneous, discontinuous, and brittle. It is evident that this type of char provides poor protection against the entrance of heat and the release flammable volatiles, leading to a slight

reduction in thermal stability. The lower thermal stability of PBS/ZB composite may be as a result of the dehydration reaction of zinc borate that occurs at ±290°C [9] which can be the catalytic effect that accelerates the degradation of the polymer matrix. Qin *et al* [10] have also reported the thermal degradation of zinc borate in the region of 250-450 °C, which is attributed dehydration of zinc borate. Unlike in our case whereby the thermal stability decreased throughout the investigated temperature range (i.e.,550), the study by Qin *et al.* [10] however reported a gradual increase in the initial decomposition temperature (T_i) and a reduction in the peak temperature (T_m) due to the fabrication of more stable carbon residue. The PBS/FA (99/1) sample appeared to have the highest thermal stability compared to other samples. This may be attributed to a more uniform dispersion of smaller FA particles in the matrix, which limits the amount of heat that is able to transfer in and out of the matrix into the surrounding, thus enhancing the thermal stability. The type of char or heat barrier formed in this system is a typical stable compact char which delays the accumulation of heat into the system and prevents any further degradations. Similarly, Prusty *et al.* [11] observed higher thermal stability which was associated with a good dispersion of graphite within the copolymer matrix. Elsewhere in the literature [12], it was observed that the incorporation of 0.25 wt% of GO showed higher degradation temperatures when compared with the composite with 0.5 wt% of GO. The reason for such an observation was associated with a well-dispersed platelet in low GO content, and as a result formed an effective protective barrier against gases and enhances the overall thermal stability.

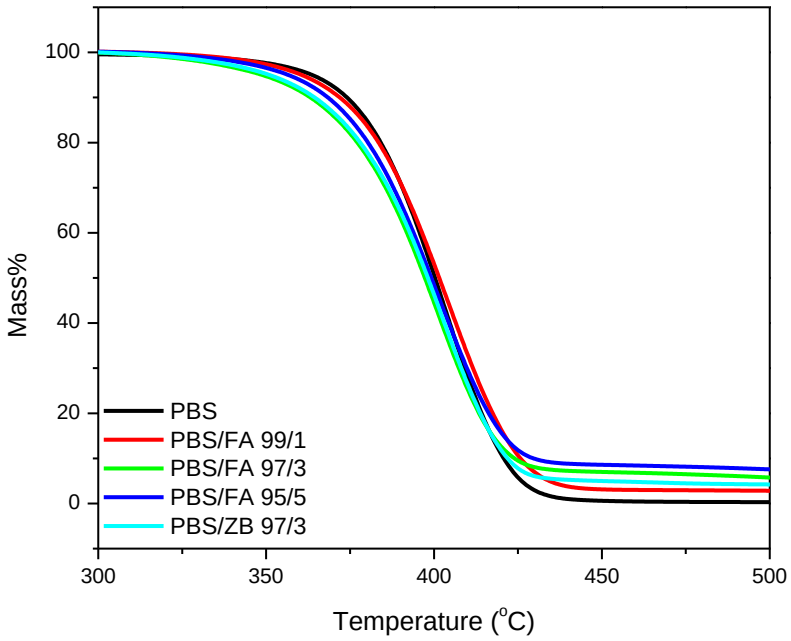

Figure 4.7 TGA graphs of neat PBS, PBS/FA and PBS/ZB composites

Table 4.1: Char residual of PBS, PBS/FA and PBS/FA/ZB composites

Sample(s)	**$T_{20\%}$ (°C)**	**$T_{80\%}$ (°C)**	**Residual (%)**
Neat PBS	383.10	413.14	0.13
PBS/FA 99/1	385.06	416.84	2.75
PBS/FA 97/3	375.71	413.14	5.41
PBS/FA 95/5	379.40	416.84	7.47
PBS/ZB 97/3	377.66	413.14	4.22
PBS/FA_silane 99/1	385.06	418.78	3.30
PBS/FA_silane 97/3	385.06	420.76	4.22
PBS/FA_silane 95/5	381.36	415.76	7.19
PBS/ZB/FA 96/3/1	377.66	415.16	4.22
PBS/ZB/FA 94/3/3	377.67	416.84	6.88
PBS/ZB/FA 92/3/5	377.66	411.40	8.35

$T_{20\%}$ and $T_{80\%}$ are degradation temperatures at 20% and 80% mass loss respectively

According to **Figure 4.7 and 4.8**, there seems to be little differences between the silane-treated samples and non-silane-treated samples. There seems to be a similar trend between the treated

and untreated samples, whereby the 1% (FA_silane and non-silane FA) in both cases is showing a better thermal stability. It became clear that even at 2wt% treatment of silane, 3 and 5 % of fly ash were unable to enhance the thermal stability of the PBS in the temperature range as shown by symbol A. This is very interesting because one would expect an enhancement in thermal stability since there was a good interaction between the fillers (*viz* fly ash and zinc borate) at this content. One possible reason for such a decrease might be associated with low thermal stability of the traditional flame retardant fillers.

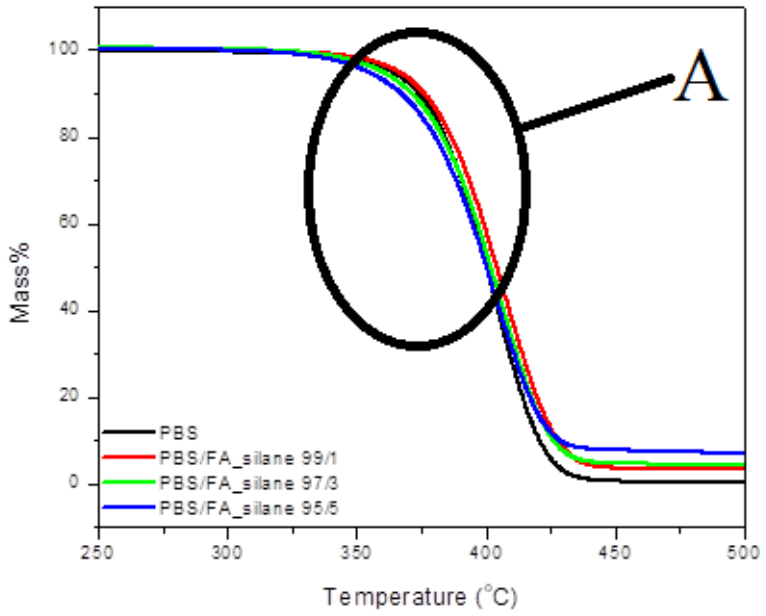

Figure 4.8 TGA graphs of neat PBS, and silane-treated PBS/FA composites at 1, 3, and 5 wt% of FA

A careful inspection of the **Figure 4.9** and Table 4.1, however shows that the silane-treated samples showed slight enhancement in the thermal stability of PBS/FA composites. For an example, 1% of silane treatment showed 2 °C enhancement when compared with 1% non-treated FA; however, both of them showed better thermal stability than the neat PBS. Research has revealed how the incorporation of a silane coupling agent can enhance the thermal stability and char residual of a composite as a result of improved filler-matrix interaction [13]. Lee *et al.* [14] reports on the effect of silane-treated basalt fiber on the properties of epoxy composites. The authors observed how silane-treated basalt fiber contributed to the high thermal performance of the basalt fiber/epoxy composite. It was noted that incorporation of basalt fiber

resulted in a 15% increase in Tg than neat epoxy. Although, there was no significant difference between the thermal stability of silane-treated and untreated basalt fibers, silane-treated basalt fiber resulted in high char yield gains at 800°C. In a similar study, Gohatre *et al.* [3] investigated the effect of silane-treated fly ash reinforced recycled poly (vinyl chloride) (r-PVC/FA) composites on thermal stability of the composite. The authors reported that at maximum degradation, silane-treated r-PVC/FA composites showed higher thermal stability than untreated r-PVC/FA and r-PVC composites. It was also observed that silane-treated composites displayed a char content of ±50 wt% at 800°C, which is higher than r-PVC by 105%. The author(s) further suggested that this was due to a barrier layer created by silane, which protected the PVC thereby improving its flame retardancy.

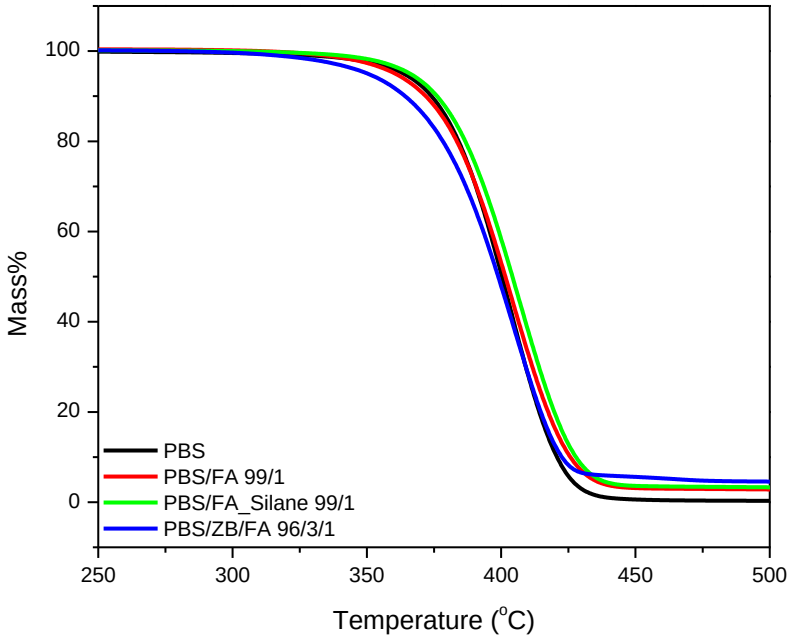

Figure 4.9 TGA graphs of neat PBS, PBS/FA, and PBS/ZB composites at 1 wt% of FA

Figure 4.10 illustrates the TGA curves of the neat PBS, PBS/FA, PBS/FA_silane and PBS/ZB/FA all at 3% of the filler(s) (i.e., ZB and FA). There is a reduction in the thermal stability of the composites in the investigated temperature range. The synergy of ZB and FA however shows an enhanced thermal stability (symbol B) in the temperatures between 400 to 500 °C. It is clear that the reduction at lower temperature may be ascribed to the dehydration of zinc borate, which accelerated the degradation of the PBS. At high temperatures nonetheless,

there is formation of synergy between the nanofillers (*viz* FA and ZB) with the fabrication of the ceramic-carbonized char, which is able to protect the substrate against heat. At 5% of the FA and 3% of ZB, there seems to be no enhancement in the thermal stability of the composites **(Figure 4.11)** when compared with neat PBS and other composites. One may suggest that the ZB may have acted as a degradation catalyst which enhanced the degradation of the whole composite as a result decreasing the thermal stability. This is very interesting since there is better interaction at this content when compared with 1% of fly ash and 3% of ZB. However, it was mentioned that a better interaction in some compositions did not enhance the properties thereof.

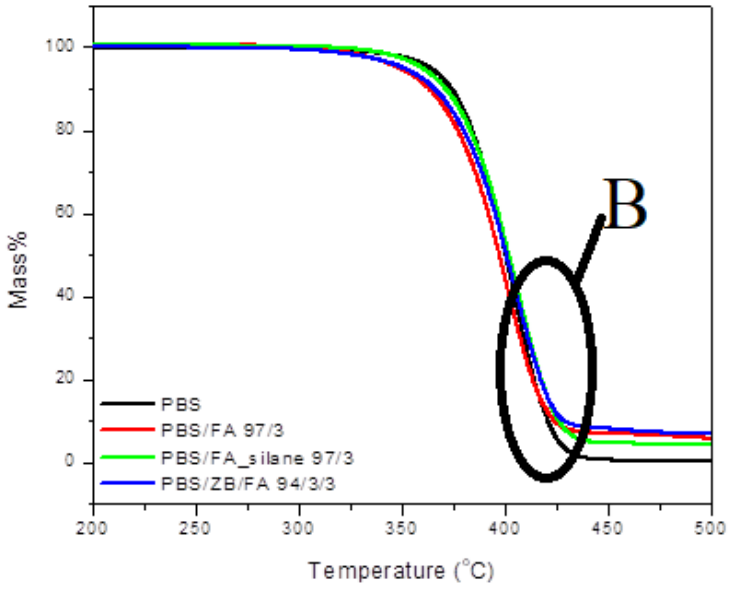

Figure 4.10 TGA graphs of neat PBS, PBS/FA, and PBS/ZB composites at 3 wt% of FA

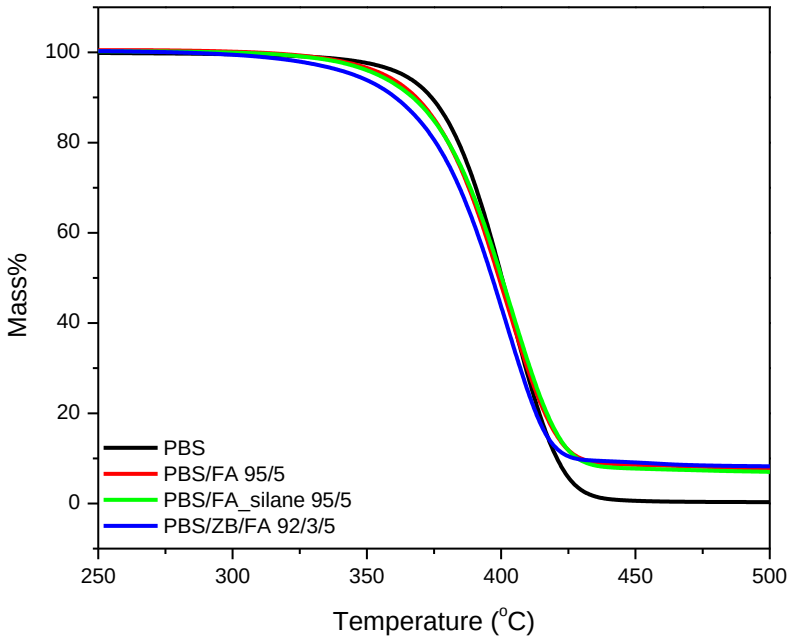

Figure 4.11 TGA graphs of neat PBS, PBS/FA, and PBS/ZB composites at 5 wt% of FA

Figure 4.12 summarizes all the thermal stability of the synergistic contents of the FA, and ZB incorporated into the PBS matrix. There seems to be a low thermal stability of the composites at 5% and 3% of FA and ZB, respectively **(Figure 4.12)**. The reduction might be associated with the catalytic effect of ZB at lower temperatures which results in decreased thermal stability of the composite. Furthermore, this might have resulted in an inhomogeneous char layer formation. Obviously, this type of chars has been proven to be brittle and discontinuous, and thereby provides poor protection against heat and volatiles as a result decreases the thermal stability.

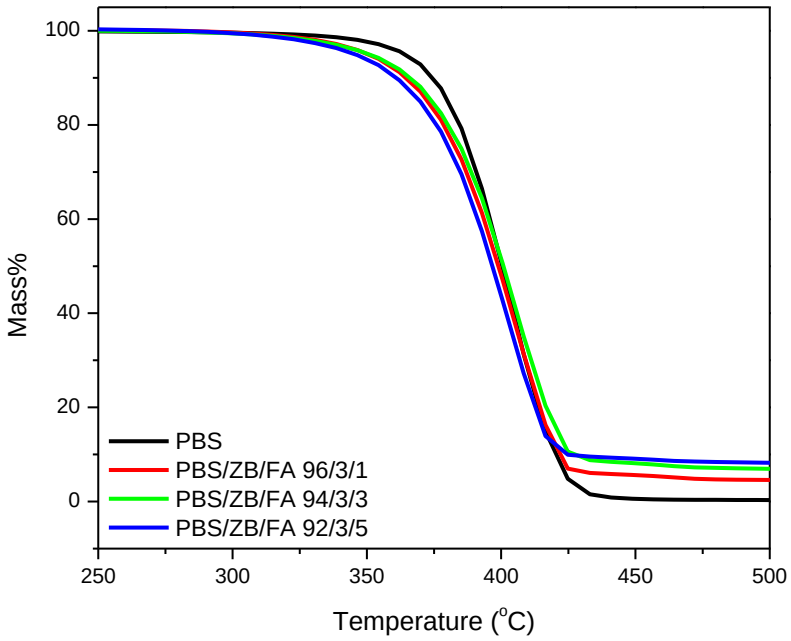

Figure 4.12 TGA graphs of neat PBS, and PB/ZB/FA composites

4.4 X-ray diffraction (XRD) analysis

Figure 4.13 depicts the crystalline phases of neat fly ash. The major crystalline phases observed contained quartz and mullites, and the minor crystalline phases consisted of haematites and calcium oxide. The presence of quartz implies an indication of SiO_2 and the mullites indicate Al_2O_3. Additionally, the mullite (aluminium oxide) intensities appear at 12° and 27-28°, while the high intensities of quartz appearing at 21° and 28°. The presence of a highly intense quartz peak **(see Figure 4.13)** is an indication of high silica content in the fly ash. Similar results were observed in **Figure 4.4** when analyzing SEM EDS samples, whereby the EDS peaks of SiO_2 were found to be more intense than the Al_2O_3 peaks. The results support the conclusion reached in section 4.1, that the type of fly ash used in this study can be classified as class F fly ash or silicate fly ash. The minor peaks between 50-70° are associated with haematites peaks, and they are an indication of Fe_2O_3 and calcium oxide which are found in lesser amounts in this fly ash. Similar observations were reported by Musapatika *et al.* [15] when investigating coal fly ash and its ability to neutralize wastewater and remove heavy metals. The researchers also observed SiO_2 and Al_2O_3 peaks in the coal fly ash with an

amorphous phase at ± 24° leading to the suggestion that the type of fly ash used in their study was of an amorphous aluminosilicate nature.

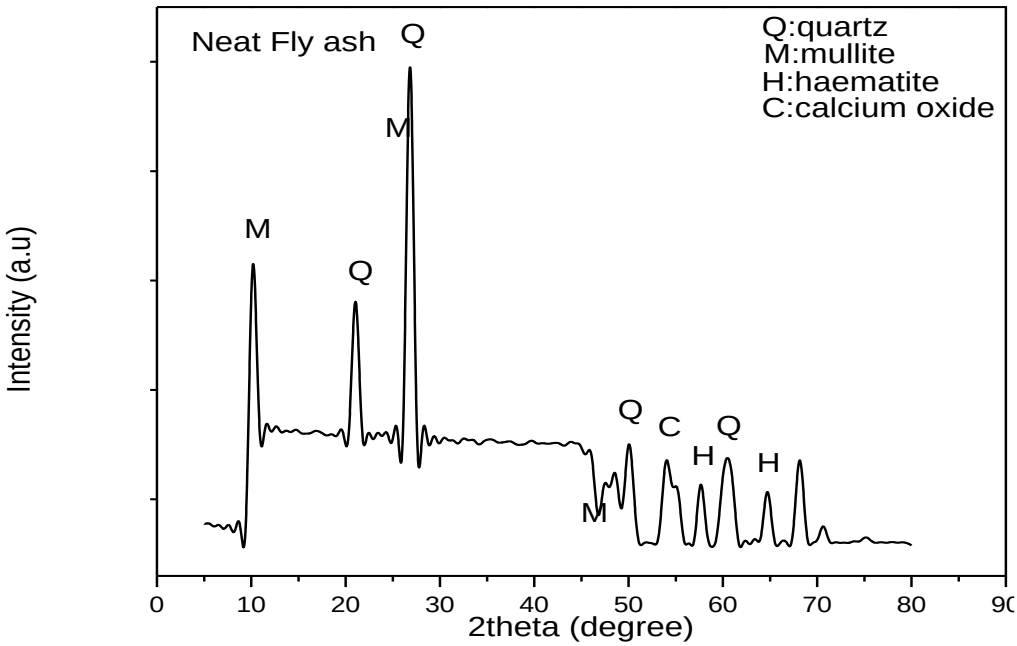

Figure 4.13 XRD graph of the crystalline and amorphous phases of pristine fly ash

The incorporation of silane to fly ash affected the crystalline structure of the fly ash (i.e., quartz) **(Figure 4.14)**. For an example, there is a reduction in the crystalline peaks of the fly ash in the presence of silane. This might be due to the formation of polysiloxane network which might have reduced the mobility of the fly ash and also limits its ability to pack into the crystalline phases. On contrary, the study by Rahmatulloh reported that the presence of silane into the fly ash enhanced the intensity of the fly ash crystalline peaks [16]. **Figure 4.15** illustrates the Figure XRD pattern for neat PBS and peaks were observed at 2 theta = 20.0˚, 23.12˚, 27.4˚, 29.2˚, 34.3˚.

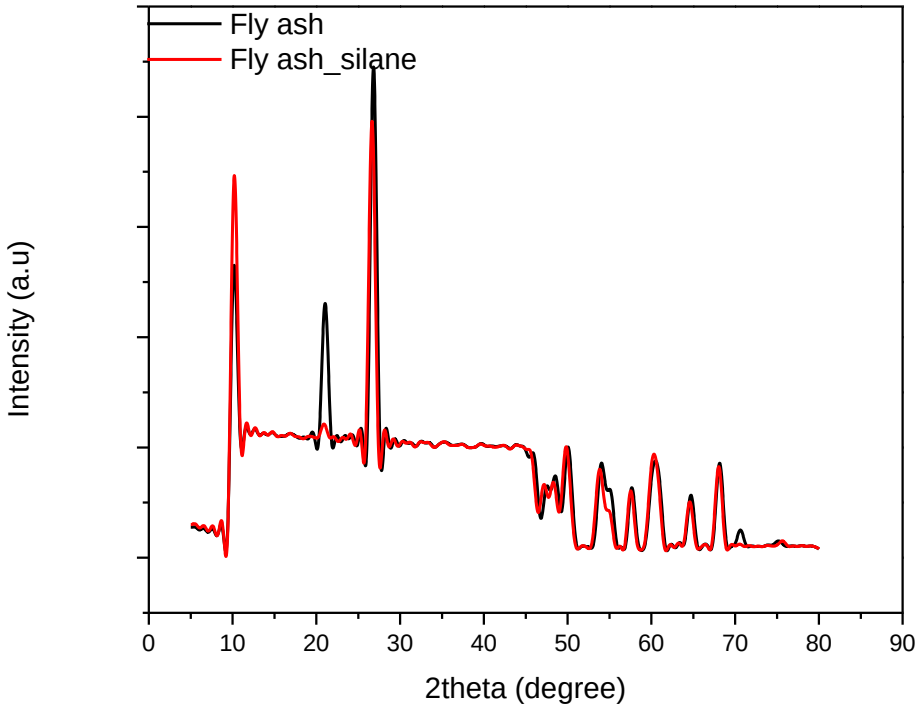

Figure 4.13 XRD patterns of neat fly ash and silane treated fly ash.

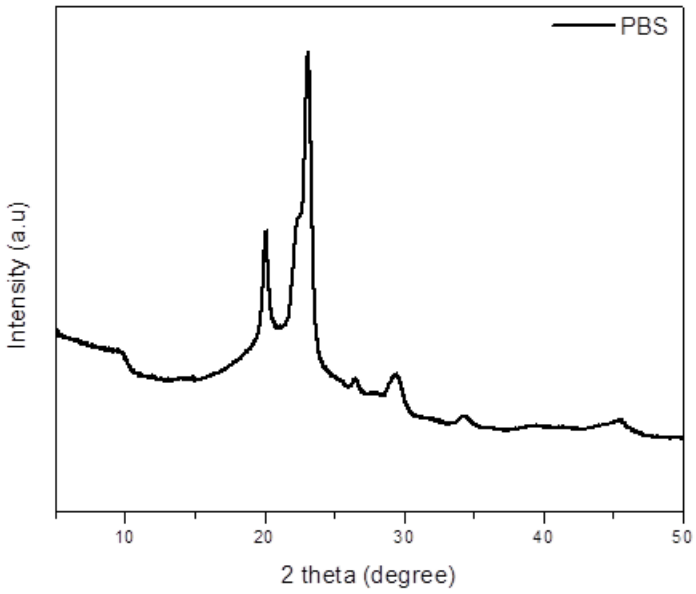

Figure 4.15 XRD pattern of neat PBS

Figure 4.16 indicates a clear increase in the peak intensities of PBS matrix with the introduction of fly ash. This is an indication that fly ash acts as a nucleating agent thus increasing the crystallinity of the PBS matrix. It is also clear that the addition of 1% of fly ash resulted in the highest peak intensities and crystallization. This is attributed to an enhanced filler dispersion of smaller fly ash particles in the PBS matrix as explained in section 4.1. The addition of 5% fly ash led to a reduced intensity of peaks as compared to 1%. This was as a result of poor particle dispersion of fly ash at higher concentrations resulting in the formation of agglomerates within the PBS matrix. Moreover, the rigidity of fly ash at high concentrations hinders the movement of polymer chains therefore impeding the crystallization of PBS. Similar results were reported for the XRD patterns of PBS/grafted nanocellulose fabricated by *In situ* polymerization [17]. The authors reported an effective improvement in the crystallinity of PBS matrix with 3 wt.% of nanocellulose. There was a decrease nonetheless in the peak intensity of the PBS at higher content of the nanocellulose. This behaviour was ascribed to the agglomerates at higher content(s) of the nanocellulose with less homogeneity as a result more reduction in crystallinity of the PBS matrix [17]. Similarly, there was a reduction in the intensity of the main peak of the PBS with the addition of ZB at 3 and 5%. As it was the case with the fly ash, ZB at lower content (1%) in this case showed better enhancement in crystallinity when compared with 5% fly ash. This behaviour is very interesting since the SEM showed that there was little interaction between the PBS and ZB with the majority of the ZB agglomerating with the PBS matrix.

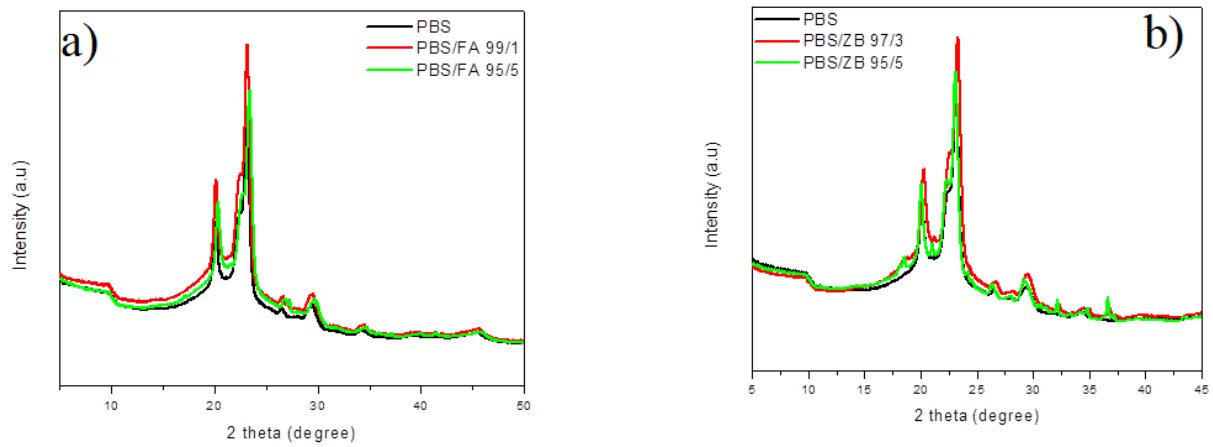

Figure 4.16 XRD patterns for (a) PBS, PBS/FA 99/1, and PBS/FA 95/5; and (b) PBS, PBS/ZB 97/3, PBS/ZB 95/5.

Figure 4.16 (a) depicts the XRD patterns of the PBS, PBS/FA 99/1, PBS/FA_silane 99/1, and PBS/FA/ZB composites. The 1% fly ash and 1% treated fly ash showed higher intensities when compared with PBS and PBS/FA/ZB 96/1/3 composites. The 1% treated fly ash indicated a slight enhancement in the intensity when compared with 1% untreated fly ash. This may be ascribed to a better dispersion of the fly ash in the presence of silane, which enhanced the crystallinity of the PBS matrix. The addition of ZB into the system however reduced the crystallinity of the PBS matrix, which may be ascribed to a poor interaction between ZB and FA, and as a result reducing the crystallinity of the matrix. Interestingly, the untreated 5% fly ash reinforced PBS matrix seems to show a better crystallinity when compared with other 5% composites (viz FA 5%_silane, FA/ZB@5%, FA_silane/ZB@5) **(Figure 4.11(b))**. This behavior is very interesting since it was observed in the SEM discussion that the 5% fly ash showed poor dispersion with the PBS matrix.

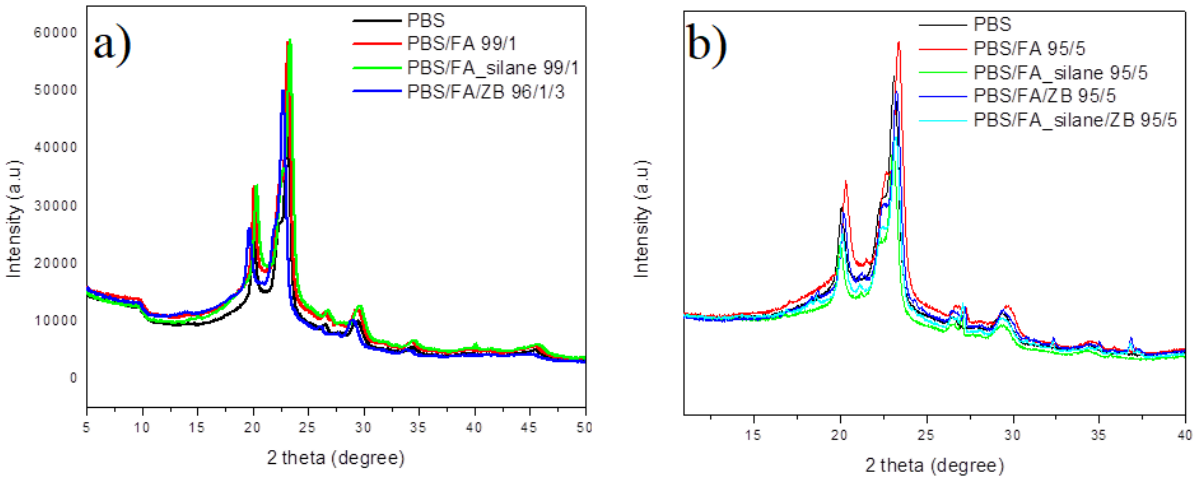

Figure 4.17 XRD patterns for (a) PBS, PBS/FA 99/1, PBS/FA_silane 99/1, PBS/FA/ZB 96/1/3; and (b) PBS, PBS/FA 95/5, PBS/FA_silane 95/5, PBS/FA/ZB 95/5 and PBS/FA_silane/ZB 95/5

4.5 Rheological properties

The addition of fillers to pristine polymer changes their rheology, thus affecting both the melt process and final properties of the product overall. The addition of fly ash and silane-treated fly ash showed higher complex viscosities when compared with neat PBS, PBS/fly ash, PBS/fly ash_silane, PBS/ZB, and PBS/ (ZB/fly ash_silane) composites **(Figure 4.18)**. There are several factors that are affecting the rheological properties, and they include but not limited to filler size, rigidity of the filler, filler content, synergy of fillers and extent of interactions between the filler(s) and polymer matrix. The addition of rigid or stiff material like fly ash immobilizes the chains of PBS matrix, and as a result reduces the flexible part of the polymer and enhances the complex viscosity of the system. The silane-treated fly ash also heightens the viscosity of the polymer matrix by improving the interaction between the filler component and the polymer matrix; immobilizing the polymer chains, and thereby enhancing the complex viscosity of the system. Huang and Zhang [18] observed similar results when examining the effect of poplar wood flour and maleic anhydride- modified polyethylene as compatibilizers on high density polyethylene (HDPE) with various melt indexes. The researchers discovered that the incorporation 50 wt% of wood flour and a compatibilizer increased the storage modulus and complex viscosity of the composite at lower frequency regions. It was further established that the incorporation of higher wood flour loading led to an agglomeration of wood particles. This agglomeration together with increased polymer-filler interaction caused by the compatibilizer resulted in hindered mobility of polymer chains, which resulted in an increased complex viscosity.

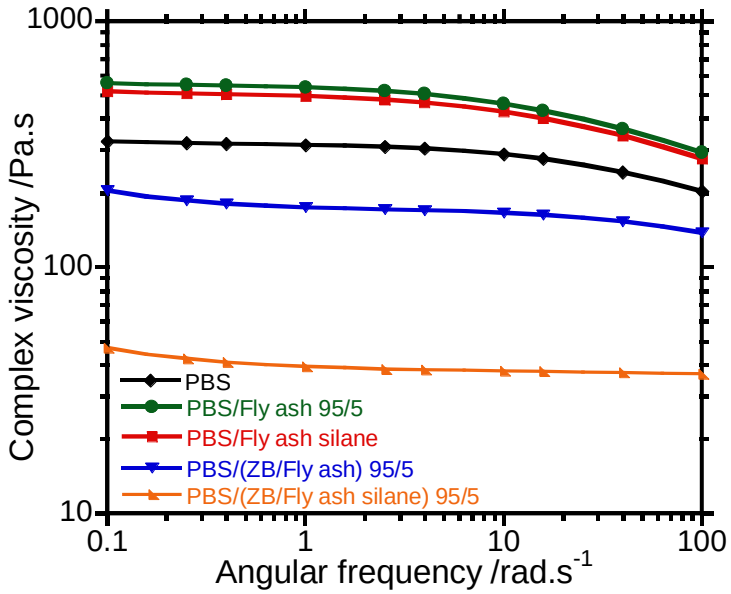

Figure 4.18 Complex viscosity vs angular frequency of PBS, PBS/fly ash, PBS/fly ash_silane, PBS/ZB, and PBS/ (ZB/fly ash_silane)

Based on **Figure 4.18**, it is apparent that the addition of ZB into the system reduces the complex viscosity of the overall systems. For instance, the complex viscosity of the PBS/fly ash/ZB and PBS/ (ZB/fly ash_silane) showed lower complex viscosities when compared with PBS and PBS/fly ash composites. The behaviour may be ascribed to a poor dispersion between fly and ZB, which might contribute to a low complex viscosity of the system. Based on Scheme 1, it is clear that a poor dispersion allows a movement of polymer chains due to lack of immobilization in some polymer chains, and resultantly, the complex viscosity is decreased. Another possibility might be due to a lower viscosity of the ZB as seen from flammability section, which played a significant role in terms of reducing the complex viscosities. Somehow, as seen from the PBS/ (ZB/fly ash_silane) complex viscosities, the effect of treatment in the form silane seems to have played no role in this system in terms of the complex viscosities with ZB playing a significant role in terms of reduction in complex viscosity, more specifically in the PBS/ (ZB/fly ash_silane). Ikuta *et al.* [19] studied the effects of silane coupling agents on the magnetic particles in resin composites and its effectiveness in depressing the content of void yielding. The authors used various types of silane coupling agents *viz.* vinyl, amino, alkyl ammonium cationic, epoxy and methacryl silanes. Some silanes

were mixed into Fe-Si-Al metal alloy powder by hydrolyzation and others by chemical bonding process. The results showed that organic groups of silane do have an effect on the void yield of the composite. The authors conceived that introduction of silane into polymer composites resulted in higher composite density thereby lowering void fractions. Physiosorbed silane was however seen to lower composite viscosity over time and decreasing void fractions through weak bonding strength. Clearly, the incompatibility of ZB/ fly ash and polymer allowed ease of movement in the PBS chains and as a result reduced the complex viscosity. Thongsang *et al.* [20] investigated the effect of fly ash silica and precipitated silica fillers on the viscosity, cure and viscoelastic properties of natural rubber. Both fillers were treated with Si69 coupling agent and the effect of treatment was analyzed. The results revealed that composites reinforced with fly ash silica (FASi) exhibited a lower viscosity in comparison to the precipitated silica (Psi) reinforced composite. It was believed to be due to the larger particle sizes of FASi which were observed in TEM micrographs as well as a smaller surface area. Moreover, it was suggested that surface treatment of the fillers with Si69 had minimal to no effect of the viscosity of the composites.

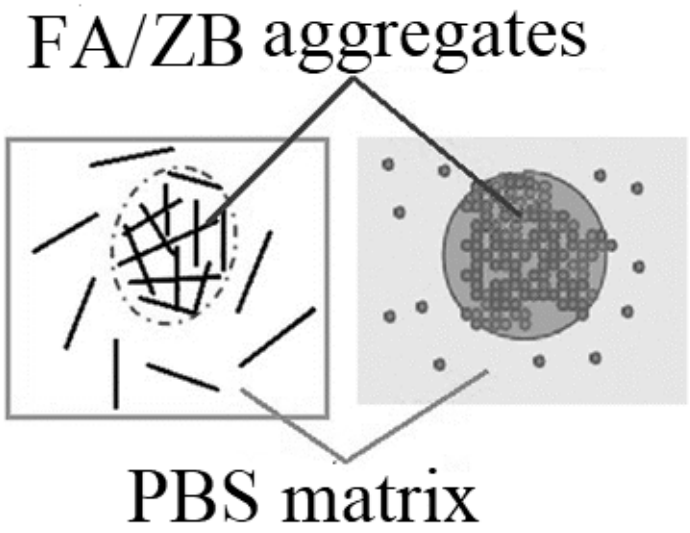

Scheme 1 Schematic representation of the PBS/ZB composites.

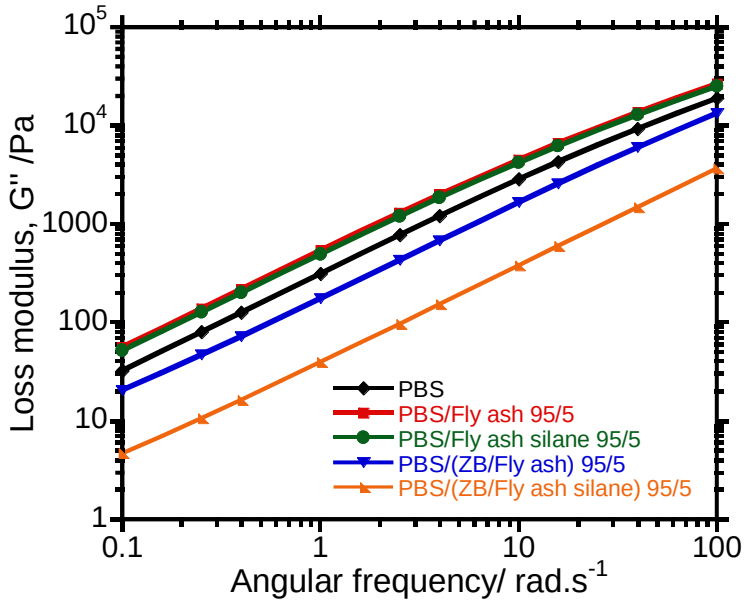

Figure 4.19 Complex viscosity vs angular frequency of PBS, PBS/fly ash, PBS/fly ash_silane, PBS/ZB and PBS/ (ZB/fly ash_silane)

In the presence of poorly dispersed ZB nanoparticles, there seems to be a high free volume (i.e. unoccupied spaces between the PLA chains), which in turn enhances flexibility in the system which reduces the complex viscosity. Similar behaviour has been also observed in the loss modulus of the investigated samples **(Figure 4.19)**. The loss modulus is known as the energy that is lost during a process of deformation. In short it is the viscous response of the investigated material; and as a result, it is related to the molecular movements. There is an enhancement in loss modulus in the presence of fly ash and fly ash_silane-treated composites when compared with neat PBS matrix and PBS/(ZB/fly ash) as well as PBS/(ZB/fly ash_silane). This behaviour can be explained by the immobilization of the segmental motion in the polymer resulting in high loss modulus. In the presence of ZB however, there seems to be a poor dispersion which resulted in low loss modulus as it was the case for complex viscosity.

4.6 UL-94 PBS based fly ash composites

Table 4.2 depicts the UL-94 of the PBS and PBS/fly ash composites. The PBS matrix was found to have a smoke and dripped easily in the absence of the fly ash. This is due to an absence of a flame retardant in the system; therefore, there is ease of heat penetration into the PBS and

the movement of volatiles out of the PBS system as a result decreasing the flammability properties of the PBS. The addition of 1% of fly ash presents a pass UL 94 with a rating of V-0 with no dripping. There are various factors that are associated with the behaviour above, and which include the dispersion of the filler and viscosity of the system. A better dispersion of the fly ash in the PBS matrix enhanced the stability of the char layer fabricated; and as a result, it was more difficult for the heat to reach the PBS matrix. According to rheology, the PBS/fly 99/1 composite was found to have a higher complex viscosity. The viscosity was sufficient enough to restrain gaseous products from the degradation of the material; and as a result, enhancing flammability resistance. **Figure 4.20** illustrates a possible flame retardant mechanism in the presence of fly ash. Three key steps are seen from **Figure 4.20 (**i.e., barrier system, whereby there is a smoldering as well as the flaming combustions). At this stage, the flame retardants together with a better dispersion enhance the formation of a good charring to protect the substrate against volatiles, oxygen, and heat. The second step is the free radical inhibition. This step includes the release of inhibitors from the flame retardants materials in order to inhibit flame propagating radicals [21]. The silane-treated fly ash (1% of fly ash) also enhanced the flammability of the PBS matrix with the UL rating of V-0. In addition, the viscosity and better dispersion at fly ash at lower content (i.e., 1% and the presence of the modifier) played a key role in V-0 rating without dripping. Meanwhile, a viscous and well dispersed fly ash resulted in the formation of a homogenous and compact char layer. It is well known that this type char layer is able to prevent heat from entering the system and preventing the volatiles from leaving the system, and a result enhances the flame resistance. Similar findings were reported by Wang *et al.* [22] when comparing the flammability resistance of retardants and non-silane microencapsulated intumescent flame retardants (ammonium polyphosphate (APP) and pentaerythritol (PER)) silane precursor microencapsulated intumescent flame (MCAPP and MCPER). Their results indicated that the addition MAPP and MPER to ethylene-vinyl acetate (EVA) copolymer cable exhibited better flammability resistance compared to APP and PER systems. The EVA/MCAPP/MCPER system obtained a UL 94 rating of V-0 at a ratio of 4:1 and 2:1 with 35 wt% loading. This was attributed to the formation of silica shell that enhanced char formation. The addition of 5% fly ash in the PBS resulted in the V-1 rating with dripping. The reason for V-1 rating might be associated high viscous PBS/fly ash 95/5 composite and poor dispersion of the fly ash within the system. A poor dispersion in this case seems to be the major factor in terms of the dripping that was observed in this system. This type of the chars tends to form an inhomogeneous and discontinuous char, which allows the penetration of heat into the system, and as a result

enhances flammability. Moreover, the presence of Zinc borate in the PBS matrix (PBS/ZB 97/3) was found to result in V-2 rating with a lot of dripping. According to the rheological properties, the presence of ZB was found to decrease the viscosity of the sample. A less viscous system is unable to restrain the volatiles from moving out of the system, and it easily allows the penetration heat into the sample, and as such reduced the flame resistance.

Table 4.2: UL 94 of the PBS, PBS/fly ash and PBS/fly ash_silane

Polymer composite	**UL 94**	**Dripping**
PBS	NR	Y
PBS/Fly ash (99/1)	V-0	N
PBS/Fly ash (97/3)	V-1	Y
PBS/Fly ash (95/5)	V-1	Y
PBS/Fly ash_silane (99/1)	V-0	N
PBS/Fly ash_silane (97/3)	V-0	N
PBS/Fly ash_silane (95/5)	V-1	Y
PBS/Zinc Borate (97/3)	V-2	Y
PBS/Zinc Borate (99/1)	V-2	Y
PBS/Fly ash/Zinc Borate (96/1/3)	V-2	Y
PBS/Fly ash/Zinc Borate (94/3/3)	V-1	Y
PBS/Fly ash/Zinc Borate (92/5/3)	V-0	N
PBS/Fly ash_silane/Zinc Borate (96/1/3)	V-1	Y
PBS/Fly ash_silane/Zinc Borate (94/3/3)	V-1	Y
PBS/Fly ash_silane/Zinc Borate (92/5/3)	V-2	Y

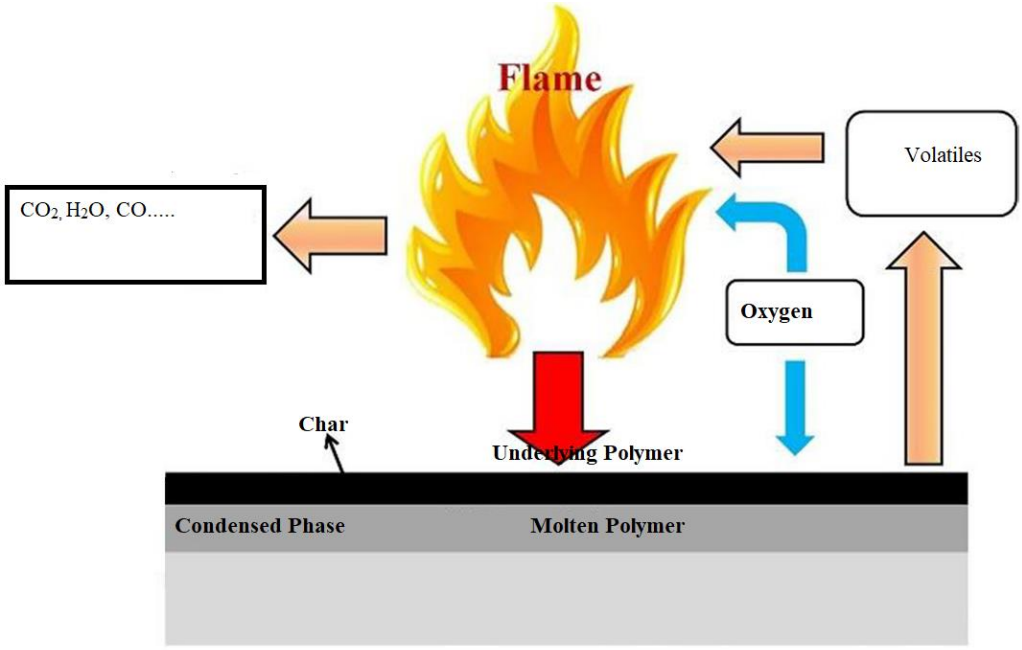

Figure 4.20 A possible mechanism for the flame retardant materials during combustion

All the synergy of fly ash with zinc borate seem to reduce the flammability of PBS, and this is denoted by UL 94 V-1 and V-2 except for PBS/Fly ash/Zinc Borate (92/5/3) with the V-0 UL 94 with no dripping. The less viscous behaviour of the Zinc borate-based composites thus reduced the flammability resistance because the less viscous system is unable to restrain the volatiles out of the system; and it is also unable to block heat from entering the system. There is also a possibility of anti-synergy between the ZB and FA at these particular systems, and thereby resulting in a less formation of an effective char layer, which can withstand the penetration heat, and which in turn reduces flammability resistance. One can however realize the formation of a synergy between the two fillers is content dependent, because at PBS/Fly ash/Zinc Borate (92/5/3) content(s), there seems to be an interaction to some extent at this composition (SEM), and as a result enhanced flame retardancy. The two fillers at these ratios seems to interact strongly enough in such a way that they formed a strong barrier against the penetration of heat into the system, and therefore an enhanced flammability resistance properties were obtained. It is well documented that a continuous, strong, compact, and thick barrier which seems to be formed at this ratio is able to prevent the decomposition of products from escaping the PBS system, and it is strong enough to block the penetration of heat into the system. Xiao *et al.* [23] reported a similar effect when investigating the anti-dripping and flame

resistance of piperazine pyrophosphate and zinc borate reinforced PBS. The researchers observed major decreases in fire growth rate index at -40%, and in peak heat release rates at -55% as well as maximum average rate of heat emission at -47% at PBS/PAPP15%/ZnB5% when examined according to the cone calorimetry testing method. The UL-94 testing method further revealed that the PBS/PAPP15%/ZnB5% specimen obtained a V-0 rating in the vertical flame test. Moreover, FTIR and solid-state nuclear magnetic resonance analyses results confirm how ZnB assisted in increasing flammability resistance by limiting energy transfer from gas and condensed phases while also forming a protective char layer.

4.7 Water absorption: PBS/fly ash composites

Figure 4.21 depicts the water absorption of PBS, PBS/fly ash and PBS/fly ash_silane treatment composites immersed for 196 hours. According to **Figure 4.21**, there is a little absorption (*viz* +/- 1%) of water by PBS matrix, which is very clear that PBS has little influence in terms of the water absorption on the PBS/fly ash system. Similar results were reported by Then *et al.* [21], and Petchwattana *et al.* [22], whereby less than 1% of water was absorbed. There was an observable decrease in water absorption percentage of the silane treated fly ash samples. Likewise, similar patterns were observed in the study conducted by Gohatre [3], whereby there was a reduction in water absorption for silane-treated FA within the recycled polyvinyl chloride (r-PVC). The main reason that there is a less absorption of water in the presence of silane is associated with a better interfacial adhesion between fly ash and PBS matrix. It is apparent that the silane treatment was able to cover the functional groups of fly ash, and as a result reduces the water absorption.

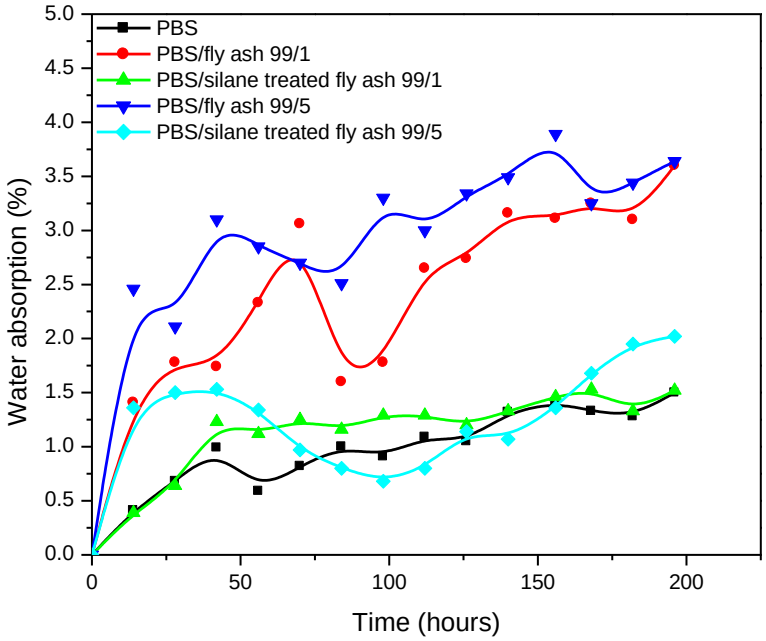

Figure 4.21 Absorption of PBS, PBS/fly ash, and PBS/fly ash_silane treatment

There is an increase in water absorption percentage with the addition of fly ash (1 and 5%) for untreated composites. According to Gohatre [3], a high-water absorption in the presence of the fly ash is associated with the hydrophilic nature of the fly ash, which in turn interact with hydrogen bonds with the water molecules. Based on **Figure 4.22**, both the PBS and ZB in the PBS/ZB composites showed little absorption on water (symbol A). The PBS/fly ash/ZB composites nonetheless showed more water absorption (symbol B) when compared with all the investigated samples. This may be associated with poor interfacial interaction between the fly ash and ZB, which might have produced voids and microcrack in the PBS composites which seems to have played a huge role in allowing more water into the system. Meanwhile, the presence of silane modified fly ash in the PBS/ZB composite showed a reduction in water uptake. This is associate with an efficient interlocking of the FA and ZB with the PBS matrix, thus increasing crosslinking, and as a result decreasing the water uptake. Based on the water absorption results and correlation with SEM, one can conclude that the PBS/fly ash has a better interaction than the PBS/fly ash/ZB composites. All the silane-based PBS/fly ash composites however showed a better interfacial interaction.

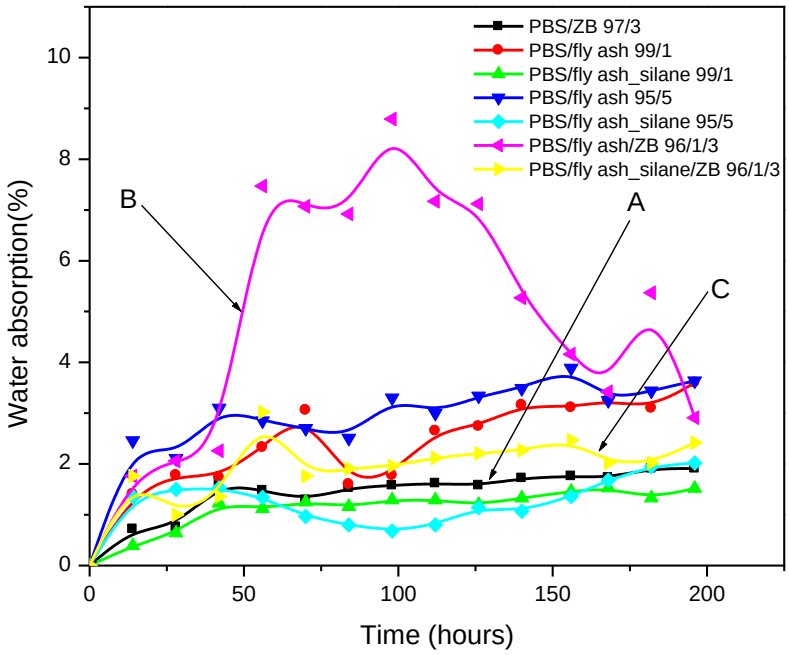

Figure 4.22 Water absorption of PBA/ZB, PBS/fly ash, PBS/fly ash_silane treatment, and PBS/fly ash/ZB composites

4.8 References

1. Subham, P., & Tiwari, S.K. 2012. Effect of unsilanized and silanized fly ash on damping properties of fly ash filled fiber reinforced epoxy composite. In *Proceedings of the international conference on advances in aeronautical and mechanical ENGINEERING-AME* (pp. 20-24).
2. Idris, A., Man, Z., Maulud, A.S., Mannan, H.A., & Shafie, A. 2019. Effect of silane coupling agents on properties and performance of polycarbonate/silica MMMs. *Polymer Testing*, 73, pp.159-170.
3. Gohatre, O.K., Biswal, M., Mohanty, S., & Nayak, S.K. 2021. Effect of silane treated fly ash on physico-mechanical, morphological, and thermal properties of recycled poly (vinyl chloride) composites. *Journal of Applied Polymer Science*, 138(19), p.50387.
4. Sim, J., Kang, Y., Kim, B.J., Park, Y.H., & Lee, Y.C. 2020. Preparation of fly ash/epoxy composites and its effects on mechanical properties. *Polymers*, 12(1), p.79.
5. Ares, A., Pardo, S.G., Abad, M.J., Cano, J., & Barral, L. 2010. Effect of aminomethoxy silane and olefin block copolymer on rheomechanical and morphological behavior of fly ash-filled polypropylene composites. *Rheologica acta*, 49(6), pp.607-618.
6. Zygmunt-Kowalska, B., Pielichowska, K., Trestka, P., Ziąbka, M., & Kuźnia, M. 2022. The Effect of Ash Silanization on the Selected Properties of Rigid Polyurethane Foam/Coal Fly Ash Composites. *Energies*, 15(6), p.2014.
7. Xie, Y., Hill, C.A., Xiao, Z., Militz, H., & Mai, C. 2010. Silane coupling agents used for natural fiber/polymer composites: A review. *Composites Part A: Applied Science and Manufacturing*, 41(7), pp.806-819.
8. Fungaro, D.A., & Silva, M.V.D. 2014. Utilization of water treatment plant sludge and coal fly ash in brick manufacturing. *Am. J. Environ. Prot*, 2(5), pp.83-88.
9. Schubert, D.M. 2019. Hydrated zinc borates and their industrial use. *Molecules*, 24(13), p.2419.
10. Qin, Q., Guo, R., Ren, E., Lai, X., Cui, C., Xiao, H., Zhou, M., Yao, G., Jiang, S., & Lan, J. 2020. Waste cotton fabric/zinc borate composite aerogel with excellent flame retardancy. *ACS Sustainable Chemistry & Engineering*, 8(28), pp.10335-10344.
11. Prusty, G., & Swain, S.K. 2012. Dispersion of expanded graphite as nanoplatelets in a copolymer matrix and its effect on thermal stability, electrical conductivity and permeability. *New Carbon Materials*, 27(4), pp.271-277.
12. Yang, J., Wang, Y., Chen, Q., Qin, G., & Liu, S. 2018. Effect of Graphite Oxide Dispersion Evaluated with Multifractal on Mechanical Properties and Thermal Stability of Poly

(3hydroxybutyrate-co-4hydroxybutyrate)/Graphite Oxide Biocomposites. *Advances in Polymer Technology*, 37(2), pp.376-383.

13. Pardo, S.G., Bernal, C., Ares, A., Abad, M.J., & Cano, J. 2010. Rheological, thermal, and mechanical characterization of fly ash-thermoplastic composites with different coupling agents. *Polymer Composites*, 31(10), pp.1722-1730.
14. Lee, J.J., Nam, I., & Kim, H. 2017. Thermal stability and physical properties of epoxy composite reinforced with silane treated basalt fiber. *Fibers and Polymers*, 18(1), pp.140-147.
15. Musapatika, E.T., Onyango, M.S., & Aoyi, O. 2010. Cobalt (II) removal from synthetic wastewater by adsorption on South African coal fly ash. *South African Journal of Science*, 106(9), pp.1-7.
16. Rahmatulloh, A., & Atmadja, L. 2021. Correlation between silane concentration and temperature operated toward conductivity of well-synthesized chitosan-fly ash composite membrane. *Journal of the Serbian Chemical Society*, (00), pp.43-43.
17. Tang, T., Zhu, J., Wang, W., & Ni, H. 2019. Morphology, thermal, and crystallization properties of poly (butylene succinate)-grafted Nanocrystalline Cellulose by polymerization in situ. *Polymer Engineering & Science*, 59(5), pp.928-934.
18. Huang, H.X., & Zhang, J.J. 2009. Effects of filler–filler and polymer–filler interactions on rheological and mechanical properties of HDPE–wood composites. *Journal of Applied Polymer Science*, 111(6), pp.2806-2812.
19. Ikuta, N., Awakura, Y., Matsui, R., Tsukano, T., & Funami, F. 2009. Effect of silane coupling agents on filling of magnetic particles in resin composites.
20. Thongsang, S., Sombatsompop, N., & Ansarifar, A. 2008. Effect of fly ash silica and precipitated silica fillers on the viscosity, cure, and viscoelastic properties of natural rubber. *Polymers for Advanced Technologies*, 19(9), pp.1296-1304.
21. Yang, Y., Haurie, L., & Wang, D.Y. 2021. Bio-based materials for fire-retardant application in construction products: a review. *Journal of Thermal Analysis and Calorimetry*, pp.1-20.
22. Wang, B., Wang, X., Tang, G., Shi, Y., Hu, W., Lu, H., Song, L., & Hu, Y. 2012. Preparation of silane precursor microencapsulated intumescent flame retardant and its enhancement on the properties of ethylene–vinyl acetate copolymer cable. *Composites Science and Technology*, 72(9), pp.1042-1048.
23. Xiao, F., Fontaine, G., & Bourbigot, S. 2022. Improvement of Flame Retardancy and Antidripping Properties of Intumescent Polybutylene Succinate Combining Piperazine Pyrophosphate and Zinc Borate. *ACS Applied Polymer Materials*, 4(3), pp.1911-1921.

24. Then, Y.Y., Ibrahim, N.A., Zainuddin, N., Ariffin, H., Chieng, B.W., & Yunus, W.M.Z.W. 2015. Influence of fiber content on properties of oil palm mesocarp fiber/poly (butylene succinate) biocomposites. *BioResources*, 10(2), pp.2949-2968.
25. Petchwattana, N., Sanetuntikul, J., Sriromreun, P., & Narupai, B. 2017. Wood plastic composites prepared from biodegradable poly (butylene succinate) and Burma Padauk sawdust (Pterocarpus macrocarpus): Water absorption kinetics and sunlight exposure investigations. *Journal of Bionic Engineering*, 14(4), pp.781-790.

Chapter 5 Conclusions and future recommendations

The study investigated the utilization of fly for as a possible filler for improving the properties of the polybutylene succinate (PBS). The current society uses coal for different purposes, but essentially for generation of electricity with fly ash being the by-product. Fly ash is regarded as a waste material globally, and it is known to consist toxic chemicals such as nickel, cadmium, arsenic, barium, and lead. The above chemical is known to cause serious diseases such premature mortality, cancer, lung, and heart ailments. The current study has added to the body of knowledge through its potential to enhance the possibility of recycling fly ash by incorporating it into a biopolymer matrix in order to improve the properties of the biopolymer for advanced applications. The investigated percentage of fly ash incorporated into the PBS matrix was 1, 3, and 5%. Generally, there was an improvement in the properties of the PBS with the addition of the fly ash. It was observed that 1% of fly ash gave better properties when compared with 3 and 5% fly ash. The reason for such an observation was associated with a better dispersion of the fly ash filler at lower content, whereas at higher content there is a possible agglomeration of the filler within the polymer matrix. For instance, the above statement is supported by an enhanced flammability, chemical resistance, and crystallinity by XRD. However, due to a poor interaction between the filler and polymer generally, fly ash in this study was modified with silane in order to further improve the properties of the PBS. As it was the case for untreated fly ash, the treated fly ash showed better properties than the polymer matrix irrespective of the content of the fly ash. Additionally, 1% of the treated fly ash however showed better properties in comparison to 3 and 5%. Notably, due to chemical and physical reactions, polymers are combustible. In this study, zinc borate was incorporated into the PBS/fly ash composites in order to enhance the flame retardancy of the system even further. Zinc borate was incorporated into the system at 3%. The incorporation of zinc borate was found to reduce the majority of the properties of the fly ash/PBS composites. For example, the addition of zinc borate was found to reduce the complex viscosity, and in turn decreased the flame retardancy of the system. It became apparent based on the reduction in properties that there was an anti-synergy between fly ash and zinc borate, which was also confirmed by SEM. For future purposes, there is a need to utilize various flame retardant fillers in order to find the best combination with fly ash as both zinc borate and fly likely formed an anti-synergy. The disadvantage of anti-synergy is primarily the formation of an inhomogeneous, weak, and discontinuous char layers, which allows ease of heat penetration into the system, and in turn

reduces the flame retardancy. Another point in terms of future recommendation is the utilization of fly ash at lower content i.e., 0.5, 1 and 2%, since it was proven in this study that the majority of the properties were improved at 1% of fly ash. One might also want to explore the possibility of using various biopolymers (i.e., poly (lactic acid) (PLA), polycaprolactone etc.) as host matrices for fly ash in order to investigate the biopolymer with high affirnity with the fly ash. Furthermore, it is essential to likewise explore the possibility of degradation kinetics of the fly ash reinforced polymer matrices as better thermal stability were reported at lower content of the fly ash (i.e., 1%). There was an interesting observation for flammability of the PBS/fly ash system, and in future, it would be necessary to utilize cone calorimetry and apply different heat flux (i.e., 35, 50, and 100 kW/m$^{2)}$. With those future recommendations guided by the results obtained in this study, it is reasonable to say that fly ash may be utilized in various applications.